



Small Molecule-Induced Cytosolic Activation of Protein Kinase Akt Rescues Ischemia-Elicited Neuronal Death

Citation

Jo, Hakryul, Subhanjan Mondal, Dewar Tan, Eiichiro Nagata, Shunya Takizawa, Alok K. Sharma, Qingming Hou, et al. 2012. "Small Molecule-Induced Cytosolic Activation of Protein Kinase Akt Rescues Ischemia-Elicited Neuronal Death." *Proceedings of the National Academy of Sciences* 106 (9): 10581–10586. doi:10.1073/pnas.1202810109.

Published Version

doi:10.1073/pnas.1202810109

Permanent link

<http://nrs.harvard.edu/urn-3:HUL.InstRepos:13338673>

Terms of Use

This article was downloaded from Harvard University's DASH repository, and is made available under the terms and conditions applicable to Other Posted Material, as set forth at <http://nrs.harvard.edu/urn-3:HUL.InstRepos:dash.current.terms-of-use#LAA>

Share Your Story

The Harvard community has made this article openly available.
Please share how this access benefits you. [Submit a story](#).

[Accessibility](#)

Small molecule-induced cytosolic activation of protein kinase Akt rescues ischemia-elicited neuronal death

Hakryul Jo^{a,b,1,2}, Subhanjan Mondal^{a,b,1}, Dewar Tan^{a,b}, Eiichiro Nagata^c, Shunya Takizawa^c, Alok K. Sharma^d, Qingming Hou^e, Kumaran Shanmugasundaram^d, Amit Prasad^{a,b}, Joe K. Tung^{a,b}, Alexander O. Tejeda^{a,b}, Hengye Man^e, Alan C. Rigby^d, and Hongbo R. Luo^{a,b,3}

^aDepartment of Pathology, Harvard Medical School, Dana–Farber/Harvard Cancer Center, Boston, MA 02115; ^bDepartment of Laboratory Medicine, Children's Hospital Boston, Boston, MA 02115; ^cDepartment of Neurology, Tokai University School of Medicine, Isehara 259-1193, Japan; ^dDivision of Molecular and Vascular Medicine, Department of Medicine, Harvard Medical School, Beth Israel Deaconess Medical Center, Boston, MA 02115; and ^eDepartment of Biology, Boston University, Boston, MA 02215

Edited by Solomon H. Snyder, The Johns Hopkins University School of Medicine, Baltimore, MD, and approved May 11, 2012 (received for review February 16, 2012)

Elevating Akt activation is an obvious clinical strategy to prevent progressive neuronal death in neurological diseases. However, this endeavor has been hindered because of the lack of specific Akt activators. Here, from a cell-based high-throughput chemical genetic screening, we identified a small molecule SC79 that inhibits Akt membrane translocation, but paradoxically activates Akt in the cytosol. SC79 specifically binds to the PH domain of Akt. SC79-bound Akt adopts a conformation favorable for phosphorylation by upstream protein kinases. In a hippocampal neuronal culture system and a mouse model for ischemic stroke, the cytosolic activation of Akt by SC79 is sufficient to recapitulate the primary cellular function of Akt signaling, resulting in augmented neuronal survival. Thus, SC79 is a unique specific Akt activator that may be used to enhance Akt activity in various physiological and pathological conditions.

drug discovery | cell signaling

Akt/PKB, a serine/threonine protein kinase with antiapoptotic activity, is one of the major downstream targets of PtdIns(3,4,5)P₃ signaling pathway. It contains a pleckstrin homology domain (PH domain) that specifically binds PtdIns(3,4,5)P₃ on the plasma membrane. Under physiological condition, the PtdIns(3,4,5)P₃-mediated membrane translocation of Akt is essential for its phosphorylation at Thr308 and Ser473 and the subsequent activation. Activated Akt, in turn, phosphorylates a variety of proteins, including several associated with cell survival/death pathways such as BAD and FoxOs (1, 2). Akt is a crucial mediator of cell survival and its deactivation is implicated in various stress-induced pathological cell death and degenerative diseases. For example, Akt was shown to be important in mediating the survival of a range of neuronal cell types. Deactivation of Akt was implicated in pathogenesis of numerous neurological diseases (3–7). In addition, Akt signaling is critically important for myelination of axons (8, 9). Activation of Akt in myelin-forming cells will be beneficial for various neuropathies, such as multiple sclerosis, caused by demyelination of axons. The acute activation of Akt is also beneficial to prevent apoptosis of cardiomyocytes upon ischemic injury (6).

Elevating Akt signaling can be achieved by activating upstream components by using certain growth factors or growth factor receptor agonists. Akt phosphorylation and activation are directly determined by the level of PtdIns(3,4,5)P₃ on the plasma membrane, which is regulated by phosphatidylinositol 3'-kinases (PI3-kinase or PI3K), the tumor suppressor PTEN, SHIP, and 5ptase IV (a phosphoinositide-specific inositol polyphosphate 5-phosphatase IV). It was reported that two inositol phosphates, InsP₇ and Ins(1,3,4,5)P₄, compete for Akt-PH domain binding with PtdIns(3,4,5)P₃ both in vitro and in vivo, providing another level of regulation for Akt membrane translocation and activation (10–13). Thus, activation of Akt can also be achieved by manipulating these related cellular factors. However, none of

these approaches are specific because multiple signaling pathways are activated downstream of the receptors or PtdIns(3,4,5)P₃.

Despite the great need of Akt activator for a variety of therapeutic applications, the effort of identifying genuine activator of Akt was ultimately unsuccessful. In this study, we setup a cell-based high-throughput chemical genetic screening system aiming to identifying novel Akt inhibitors that specifically target PtdIns(3,4,5)P₃-mediated Akt membrane translocation. However, paradoxically, from this screening, we discovered a genuine activator of Akt that suppressed PH_{Akt}-GFP plasma membrane translocation but enhanced Akt phosphorylation. It enables cytosolic activation of Akt independent of PtdIns(3,4,5)P₃-mediated Akt membrane translocation. In addition, this activator-induced Akt activation recapitulates the primary function of Akt signaling because it efficiently prevented excitotoxicity-induced neuronal death.

Results

High-Throughput Screening for Inhibitors of Akt Plasma Membrane Translocation. To visualize Akt translocation, we used the PH domain of Akt (PH_{Akt}) fused with green fluorescent protein (PH_{Akt}-GFP) as a marker. When serum-starved cells were stimulated with insulin-like growth factor (IGF), the membrane translocation of PH_{Akt}-GFP occurred within 5 min. As a control, IGF-elicited membrane translocation was significantly suppressed in cells treated with LY294002, which inhibits PI3K activity and, therefore, reduces the level of PtdIns(3,4,5)P₃ on the plasma membrane (*SI Appendix, Fig. S1*). Using a stable HeLa cell line expressing PH_{Akt}-GFP fusion protein (*SI Appendix, Fig. S2*), we performed a cell-based chemical genetic screening for compounds that suppress IGF-induced PH_{Akt}-GFP membrane translocation (*SI Appendix, Fig. S3*). The pilot screening identified 21 positive hits from a library containing 480 bioactive compounds. Several chemicals known to be able to inhibit PtdIns(3,4,5)P₃ signaling, including Wortmannin, Celastrol, Quercetin, and LY294002, were among the identified compounds (*SI Appendix, Fig. S4 and Table S1*). The subsequent high-throughput screening (HTS) of more than 60,000 synthetic chemical compounds (*SI Appendix, Table S2*) identified 125 positive hits (Fig. 1A and *SI Appendix, Table S3 and Fig. S5*).

Author contributions: H.J., S.M., H.M., A.C.R., and H.R.L. designed research; H.J., S.M., D.T., E.N., S.T., A.K.S., Q.H., K.S., A.P., J.K.T., and A.O.T. performed research; H.J., S.M., and H.R.L. contributed new reagents/analytic tools; H.J., S.M., and H.R.L. analyzed data; and H.J., S.M., and H.R.L. wrote the paper.

The authors declare no conflict of interest.

This article is a PNAS Direct Submission.

¹H.J. and S.M. contributed equally to this work.

²Present address: Environmental Health Sciences Program, Yale University School of Public Health, New Haven, CT 06520.

³To whom correspondence should be addressed. E-mail: hongbo.luo@childrens.harvard.edu.

This article contains supporting information online at www.pnas.org/lookup/suppl/doi:10.1073/pnas.1202810109/-DCSupplemental.

To confirm the inhibitory effect of the positive hit compounds on PH_{Akt}-GFP membrane translocation, we examined PH-Akt translocation by using time-lapse fluorescent imaging. We found that 25 of the positive compounds generated autofluorescence and their effect on PH-Akt membrane translocation was, in fact, the result of greatly enhanced background fluorescence (*SI Appendix, Table S3*). Fifty-four of the initial 125 positive compounds could inhibit IGF-induced Akt membrane translocation at the concentration of 8 $\mu\text{g/mL}$ (*SI Appendix, Figs. S6 and S7*). However, these compounds may have a general translocation inhibitory effect and, thus, prevent any protein from translocating to the plasma membrane. In addition, some “positive hits” may affect PtdIns(3,4,5)P₃ level via modulating cellular levels of phosphoinositides. To eliminate these possibilities, we examined PtdIns(4,5)P₂-mediated protein translocation. We used a cell line stably expressing GFP-PLC-delta1-PH domain, which specifically binds to PtdIns(4,5)P₂, but not PtdIns(3,4,5)P₃ (14, 15). It appeared that none of the positive hit compounds suppressed the membrane localization of GFP-PLC-delta1-PH (*SI Appendix, Fig. S8*). Another general issue in cell-based HTS is the indirect effects of compounds on the assay readout (e.g., via inducing cell death or affecting transcription or translation). None of the positive hit compounds caused morphological changes in this short period, suggesting that the inhibited PH_{Akt}-GFP plasma membrane translocation was not the result of cell death (*SI Appendix, Fig. S9*). However, many positive compounds turned out to be toxic when cells were incubated with them for longer time (*SI Appendix, Fig. S9 and Table S4*), indicating that these chemicals may target cellular components other than Akt.

Synthetic Compound SC79 Suppresses PH_{Akt}-GFP Plasma Membrane Translocation but Enhances Akt Phosphorylation and Activation in the Cytosol. To investigate the effect of each positive hit compound on Akt activity, we next assessed IGF-elicited Akt

phosphorylation, a commonly used reporter for Akt activation. To our surprise, we unexpectedly found that one of the positive hits, SC79, could suppress PH_{Akt}-GFP plasma membrane translocation but enhance Akt phosphorylation (Fig. 1*B*). Upon PtdIns(3,4,5)P₃-mediated recruitment to the plasma membrane, Akt is phosphorylated at two different regulatory sites, T308 and S473, respectively. Both phosphorylations were augmented by SC79 treatment (Fig. 1*C*). In addition, SC79 not only enhanced IGF1-induced Akt phosphorylation in serum-starved cells, but also elevated the level of Akt phosphorylation in cells grown in serum-rich medium (Fig. 1*D*). The kinetic studies revealed that Akt phosphorylation could be increased within a minute of SC79 treatment (*SI Appendix, Fig. S10*).

Various chemicals targeting the ATP binding pocket of Akt and inhibiting its kinase activity paradoxically lead to hyperphosphorylation of Akt (16, 17) (*SI Appendix, Fig. S11*). Importantly, once the drug is removed, such phosphorylated Akt was shown to be fully active (18). One explanation for SC79-induced Akt phosphorylation might be that SC79 transiently binds to the ATP binding pocket, leading to Akt phosphorylation, and then readily dissociates from the activated Akt. To rule out this possibility, we first determined whether SC79 could inhibit the Akt kinase activity in intact cells. At a comparable concentration, SC79 failed to demonstrate any inhibition toward Akt kinase activity. Instead, phosphorylation of several downstream effectors of Akt, including and FOXO, was much enhanced in SC79-treated cells, suggesting that SC79-induced augmentation of Akt phosphorylation led to enhanced Akt kinase activity (Fig. 1*D*). A compound that shares structure similarity with SC79, HA14-1, showed the same effect (*SI Appendix, Fig. S11*).

SC79 enhanced Akt phosphorylation but inhibited PtdIns(3,4,5)P₃-mediated Akt membrane translocation, indicating that the binding between Akt and PtdIns(3,4,5)P₃ may not be

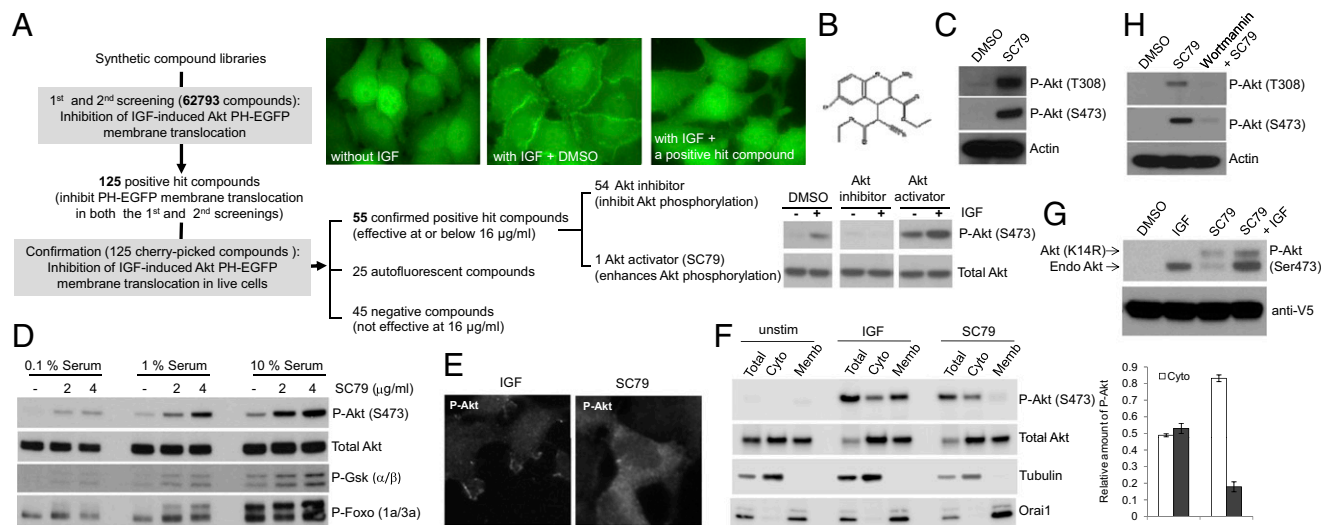


Fig. 1. High-throughput screening identifies a synthetic compound SC79 that suppresses PH_{Akt}-GFP plasma membrane translocation but enhances Akt phosphorylation and activation in the cytosol. (A) High-throughput screening identified SC79 as an inhibitor of Akt-PH domain translocation and an enhancer of Akt phosphorylation. (B) Chemical structure of SC79. (C) SC79 augmented Akt phosphorylation at both the Thr308 and S473 sites. (D) SC79 enhanced Akt phosphorylation and its kinase activity. Phosphorylation of downstream targets, GSK-3 β and Foxo, was detected by using specific Phospho-GSK3 β and Phospho-Foxo antibodies. (E) The representative images of SC79-induced cytosolic phosphorylation of Akt. Cells were serum-starved for overnight and then treated with IGF or SC79 for 15 min. The fixed cells were immunostained with the phospho-Akt (S473) antibody. (F) SC79-induced cytosolic phosphorylation of Akt analyzed by Western blotting. HeLa cells were serum starved for 1 h and treated with IGF (100 ng/mL) or SC79 (4 $\mu\text{g/mL}$) for 30 min. Total cell lysate, cytosolic, and membrane fractions were resolved by SDS/PAGE and analyzed for phospho-Akt (S473), Total Akt, Tubulin (cytosolic marker), and Orai1 (membrane marker) by Western blotting. (G) SC79 treatment led to phosphorylation of Akt (K14R) mutant, a PH domain mutant incapable of binding to PtdIns(3,4,5)P₃. Serum-starved cells stably expressing the V5-tagged Akt (K14R) were treated with IGF, SC79, or in combination before analysis for Akt phosphorylation. The phosphorylated forms of endogenous and mutant Akt (K14R) were indicated by arrows. A mouse monoclonal V5 antibody was used to detect Akt (K14R) mutant and to serve as the loading control. (H) Pretreatment with PI3K inhibitor wortmannin abolished SC79-induced Akt activation.

converts Akt from an inactive conformation to an active conformation, leading to hyperactivation of Akt. To determine whether SC79 directly interacts with the Akt-PH domain, we performed an *in vitro* binding assay with PtdIns(3,4,5)P₃-coated beads. In the presence of increasing amounts of SC79, Akt-PH-EGFP brought down by PtdIns(3,4,5)P₃ beads was found to be reduced, indicating that SC79 could directly bind to PH domain and compete with PtdIns(3,4,5)P₃ for such binding (Fig. 3*A* and *B*). In contrast to Akt PH domain, the *in vitro* PtdIns(3,4,5)P₃ binding capacity of Itk PH domain was unaffected by SC79, although Itk PH domain manifested a relatively higher affinity toward PtdIns(3,4,5)P₃ compared with Akt-PH domain (Fig. 3*C*).

The structure of Akt PH domain has been reported (21). PtdIns(3,4,5)P₃ binds to a shallow pocket in the Akt PH domain largely mediated through several salt bridges between the phosphate groups and basic residues in the protein. Molecular docking of Akt-PH domain with SC79 revealed that SC79 binds to the same PtdIns(3,4,5)P₃ binding pocket (Fig. 3*D*). By performing circular dichroism (CD) spectroscopy, we further examined whether the binding of SC79 to the PH domain can alter the overall structure of Akt. Far-UV CD spectra were recorded for full-length human Akt1 in the presence or absence of SC79 (Fig. 3*E*). The overall secondary structural content of Akt1 was decreased by 4.3% because of ligand binding at both 25 μ M and 50 μ M concentrations (Fig. 3*E* and *SI Appendix, Table S5*). At 25 μ M, SC79 binding resulted in a decrease in α -helical content by 17% and an increase in β -strand content by 19% compared with Akt1 alone (Fig. 3*E* and *SI Appendix, Table S5*). These results indicate that SC79 can physically interact with and modulate the structure of Akt.

SC79 significantly increased the level of Akt phosphorylation. One possibility is that, in the presence of SC79, the phosphorylated Akt could be more resistant to dephosphorylation by cellular phosphatases. To test this possibility, we examined whether SC79 affects Akt dephosphorylation by using an *in vitro* assay. When the cytosolic extract of HEK293 cells was incubated at

37 °C, a dramatic dephosphorylation of T308 ensued, whereas that of S473 was progressed in a relatively slower kinetics. Under this condition, neither the cytosolic extract from SC79 pretreated cells nor addition of SC79 to the cell lysate attenuated dephosphorylation of either T308 or S473 site (Fig. 3*F*).

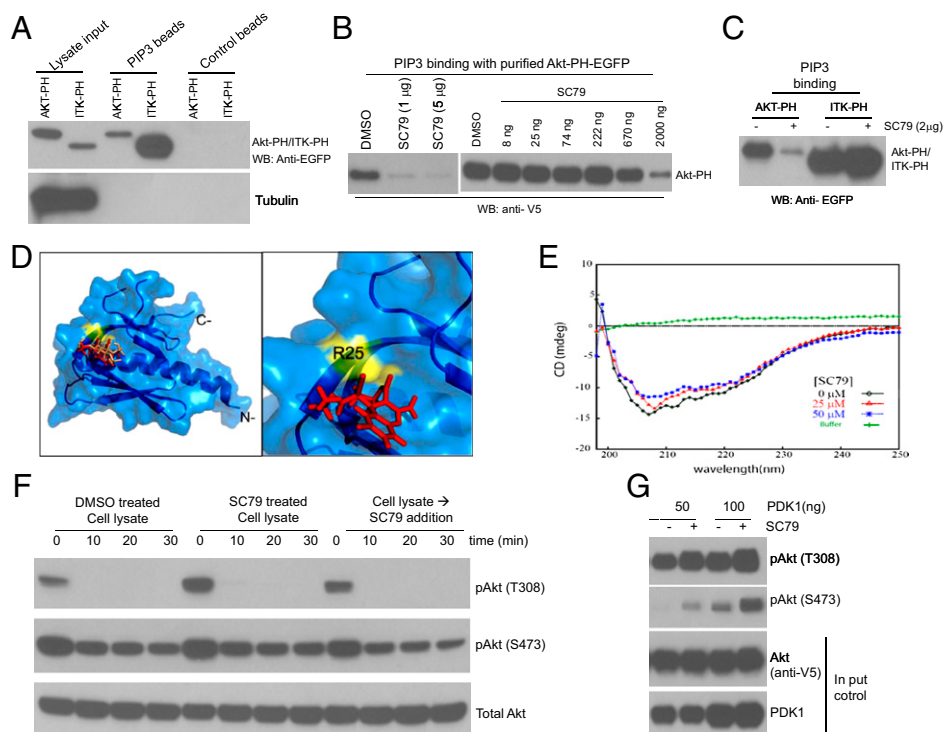
To provide direct evidence that SC79-bound Akt adopts a conformation more amenable to be phosphorylated by upstream kinases, we explored the effect of SC79 on Akt phosphorylation by using a cell-free assay. Unphosphorylated Akt was immunoprecipitated from the lysate of serum-starved cells. *In vitro* phosphorylation by purified PDK1 was conducted in the presence or absence of SC79. This assay revealed that SC79 could enhance Akt phosphorylation at T308 site by PDK1. Interestingly, when T308 site was highly phosphorylated, the phosphorylation at S473 site was also dramatically increased in the absence of any PDK2 kinases (Fig. 3*G*). The *in vitro* autophosphorylation at S473 site, which depends on T308 phosphorylation, has been reported (22). Thus, our finding is consistent with this report and supports a positive role for SC79 in T308 phosphorylation by PDK1.

SC79 Reduces Neuronal Excitotoxicity and Prevents Stroke-Induced Neuronal Death.

Next, we determined whether SC79-induced Akt activation could recapitulate the physiological function of Akt signaling. Because Akt deactivation is a causal mediator of neuronal death in various neurological diseases, we investigated whether SC79 can suppress such pathological neuronal death by preventing Akt deactivation. We first examined the effect of SC79 on neuronal death elicited by glutamate excitotoxicity. Excitotoxicity-induced neuronal death is a unique type of cell death that is mainly mediated by *N*-methyl-D-aspartate (NMDA) receptors (3, 23–25). Akt deactivation is a causal mediator of excitotoxicity-induced neuronal death (26). Treatment of cultured cortical neurons with Akt activator SC79 markedly enhanced Akt phosphorylation without altering total Akt levels (Fig. 4*A*). Similarly, SC79 treatment substantially reduced the death of

Fig. 3. SC79 directly binds to Akt and converts it from an inactive conformation to an active conformation, leading to hyperactivation of Akt.

(*A*) Both Akt-PH domain and Itk-PH domain could bind to PtdIns(3,4,5)P₃. (*B*) SC79 inhibited PtdIns(3,4,5)P₃ binding function of Akt PH domain. (*C*) SC79 did not affect the PtdIns(3,4,5)P₃ binding function of Itk PH domain. (*D*) *In silico* docking of SC79 ligand onto the Akt PH domain structure. (*Left*) Docked SC79 ligand (rendered red) onto crystal structure of Akt PH domain (PDB ID code: 1UNR, rendered marine). Shown in “wheat” color is the IP4 ligand that docks at the site almost similar to the SC79 binding site. Highlighted in yellow is the residue surface located adjacent to the SC79 binding site that exhibits significant interaction with ligand SC79. (*Right*) Zoomed region, as in *Left*, shows docked SC79 ligand and interaction residue R25. (*E*) CD spectra of human Akt1 (shown in black) alone and in the presence of SC79 of 25 μ M (shown in red) or 50 μ M (shown in blue) collected at 25 °C is shown. Baseline was corrected for buffer contribution. (*F*) SC79 did not affect Akt dephosphorylation *in vitro*. HEK293 cells grown in serum-rich medium were treated with DMSO or SC79 (4 μ g/mL) for 20 min. Cells were lysed on ice in a control buffer devoid of phosphatase inhibitors or supplemented with SC79 (4 μ g/mL). After centrifugation at 4 °C, the lysates were kept on ice (time 0 min) or incubated at 37 °C for indicated time points. The kinetics of Akt dephosphorylation at T308 and S473 was determined by Western blot. (*G*) SC79 directly enhanced Akt phosphorylation by purified recombinant PDK1 *in vitro*.



constraint, thus making it a more favorable conformation. Given that SC79 acts as a PtdIns(3,4,5)P₃ mimetic and induces an Akt conformational change (Fig. 1 *D* and *E*), our results also support such possibility. We further demonstrated that SC79-induced Akt activation could recapitulate the primary function of Akt signaling because it efficiently prevented the excitotoxicity-induced neuronal death both in vitro and in vivo. Although the activation of Akt signaling plays significant roles in protecting the ischemic-injury induced neuronal death, other cellular pathways and components are also important. Nevertheless, the SC79-induced Akt activation alone manifested a significant protection. Identifying other cellular pathways leading to synergistic protection in combination with SC79 would be important.

Deactivation of Akt contributes to pathogenesis of numerous neurological diseases (3–5) and, thus, elevating Akt activity becomes an obvious clinical strategy to suppress progressive neuronal death under these pathological conditions. However, this endeavor has been hindered because of the lack of specific Akt activators. Our results suggest that chemical mimetics of PtdIns(3,4,5)P₃, such as SC79, could be explored to develop legitimate Akt activators. SC79 is relatively unstable in aqueous environment (*SI Appendix*, Fig. S13*A*). Intriguingly, however, after the removal of SC79, the sustained level of phosphorylated Akt was observed both in cell culture and in vivo (*SI Appendix*, Fig. S13 *B* and *C*), indicating that SC79 may act irreversibly. SC79 contains the chemical moieties (i.e., nitrile group) that could be modified and/or reacts with amino acids. Nevertheless, SC79 appeared to be a relatively safe drug. SC79 treatment, even at much high dose (0.4 mg/g of body weight), did not induce any detectable changes in body weight, survival rate, appearance, and behavior in mice (*SI Appendix*, Fig. S14). The fact that neuronal protective effect was achieved by i.p. injection suggests that SC79 also has a good penetration of blood–brain barrier. Therefore,

SC79 can be used as a chemical platform to develop novel drugs for neurological and other complications (*SI Appendix*).

Materials and Methods

In this study, infarct volume was used to evaluate MCAO-induced brain damage. For histological examination of infarcted area, mice were deeply anesthetized either 24 h or 1 wk after permanent MCAO by excess pentobarbital sodium (100 mg/kg). Upon removal, brains were sectioned coronally into five slices of 1 mm thickness starting from the frontal pole by using a mouse brain matrix (ASI Instruments). Slices were stained with 2% (wt/vol) 2,3,5-triphenyltetrazolium chloride (TTC; Sigma) for 30 min at room temperature. Areas ipsilateral to the occlusion, which were not stained, were recorded as infarcted. After fixation with 4% paraformaldehyde/PBS, the unstained area of infarction was measured on the posterior surface of each coronal section by using an Image J system (Wayne Rasband, National Institutes of Health). Because of substantial hemispheric swelling after ischemia, the corrected infarct volume was calculated by using an indirect method to compensate for the effect of brain edema. The infarcted area of the ipsilateral (ischemic) hemisphere (II) was determined by subtracting the noninfarcted area of the ipsilateral hemisphere (IN) from the total area of the contralateral (uninfarcted) hemisphere (CT): $II = CT - IN$. Total infarct volume was then determined by multiplying the area of infarct for each slice by the slice thickness (1 mm) and summing for the seven brain slices.

Other materials and methods are presented in *SI Appendix*. Analysis of statistical significance for indicated datasets was performed by using the Student *t* test capability on Microsoft Excel.

ACKNOWLEDGMENTS. The authors thank Solomon H. Snyder, Sangwon Kim, and Lewis C. Cantley for very helpful comments and suggestions on the manuscript; Leslie Silberstein, John Manis, and Li Chai for helpful discussions; Natsuko Fujii, Yusuke Moriya, Yoko Takahara for help with middle cerebral artery occlusion model; and Bo Chen and Kai Yao for intraocular injections. H.L. is supported by National Institutes of Health Grants HL085100, AI076471, HL092020, and GM076084.

- Woodgett JR (2005) Recent advances in the protein kinase B signaling pathway. *Curr Opin Cell Biol* 17:150–157.
- Brazil DP, Hemmings BA (2001) Ten years of protein kinase B signalling: A hard Akt to follow. *Trends Biochem Sci* 26:657–664.
- Yuan J, Yankner BA (2000) Apoptosis in the nervous system. *Nature* 407:802–809.
- Brunet A, Datta SR, Greenberg ME (2001) Transcription-dependent and -independent control of neuronal survival by the PI3K-Akt signaling pathway. *Curr Opin Neurobiol* 11:297–305.
- Dudek H, et al. (1997) Regulation of neuronal survival by the serine-threonine protein kinase Akt. *Science* 275:661–665.
- Harvey PA, Leinwand LA (2011) The cell biology of disease: Cellular mechanisms of cardiomyopathy. *J Cell Biol* 194:355–365.
- Russo R, et al. (2009) Identification of novel pharmacological targets to minimize excitotoxic retinal damage. *Int Rev Neurobiol* 85:407–423.
- Zhu D, et al. (2006) Deactivation of phosphatidylinositol 3,4,5-trisphosphate/Akt signaling mediates neutrophil spontaneous death. *Proc Natl Acad Sci USA* 103:14836–14841.
- Cotter L, et al. (2010) Dlg1-PTEN interaction regulates myelin thickness to prevent damaging peripheral nerve overmyelination. *Science* 328:1415–1418.
- Luo HR, et al. (2003) Inositol pyrophosphates mediate chemotaxis in Dictyostelium via pleckstrin homology domain-PtdIns(3,4,5)P₃ interactions. *Cell* 114:559–572.
- Jia Y, et al. (2007) Inositol 1,3,4,5-tetrakisphosphate negatively regulates PtdIns(3,4,5)P₃ signaling in neutrophils. *Immunity* 27:453–467.
- Prasad A, et al. (2011) Inositol hexakisphosphate kinase 1 regulates neutrophil function in innate immunity by inhibiting phosphatidylinositol-(3,4,5)-trisphosphate signaling. *Nat Immunol* 12:752–760.
- Chakraborty A, et al. (2010) Inositol pyrophosphates inhibit Akt signaling, thereby regulating insulin sensitivity and weight gain. *Cell* 143:897–910.
- Razzini G, Brancaccio A, Lemmon MA, Guarnieri S, Falasca M (2000) The role of the pleckstrin homology domain in membrane targeting and activation of phospholipase C β (1). *J Biol Chem* 275:14873–14881.
- Stauffer TP, Ahn S, Meyer T (1998) Receptor-induced transient reduction in plasma membrane PtdIns(4,5)P₂ concentration monitored in living cells. *Curr Biol* 8:343–346.
- Levy DS, Kahana JA, Kumar R (2009) AKT inhibitor, GSK690693, induces growth inhibition and apoptosis in acute lymphoblastic leukemia cell lines. *Blood* 113:1723–1729.
- Han EK, et al. (2007) Akt inhibitor A-443654 induces rapid Akt Ser-473 phosphorylation independent of mTORC1 inhibition. *Oncogene* 26:5655–5661.
- Okuzumi T, et al. (2009) Inhibitor hijacking of Akt activation. *Nat Chem Biol* 5:484–493.
- Chen J, Tang H, Hay N, Xu J, Ye RD (2010) Akt isoforms differentially regulate neutrophil functions. *Blood* 115:4237–4246.
- Park WS, et al. (2008) Comprehensive identification of PIP₃-regulated PH domains from *C. elegans* to *H. sapiens* by model prediction and live imaging. *Mol Cell* 30:381–392.
- Thomas CC, Deak M, Alessi DR, van Aalten DM (2002) High-resolution structure of the pleckstrin homology domain of protein kinase b/akt bound to phosphatidylinositol (3,4,5)-trisphosphate. *Curr Biol* 12:1256–1262.
- Toker A, Newton AC (2000) Akt/protein kinase B is regulated by autophosphorylation at the hypothetical PDK-2 site. *J Biol Chem* 275:8271–8274.
- Yu SW, et al. (2002) Mediation of poly(ADP-ribose) polymerase-1-dependent cell death by apoptosis-inducing factor. *Science* 297:259–263.
- Choi DW (1992) Excitotoxic cell death. *J Neurobiol* 23:1261–1276.
- Olney JW (2003) Excitotoxicity, apoptosis and neuropsychiatric disorders. *Curr Opin Pharmacol* 3:101–109.
- Luo HR, et al. (2003) Akt as a mediator of cell death. *Proc Natl Acad Sci USA* 100:11712–11717.
- Choi DW (1996) Ischemia-induced neuronal apoptosis. *Curr Opin Neurobiol* 6:667–672.
- Coyle JT, Puttfarcken P (1993) Oxidative stress, glutamate, and neurodegenerative disorders. *Science* 262:689–695.
- Zhao H, Sapolsky RM, Steinberg GK (2006) Phosphoinositide-3-kinase/akt survival signal pathways are implicated in neuronal survival after stroke. *Mol Neurobiol* 34:249–270.
- Hillion JA, et al. (2006) Involvement of Akt in preconditioning-induced tolerance to ischemia in PC12 cells. *J Cereb Blood Flow Metab* 26:1323–1331.
- Miyawaki T, et al. (2009) The endogenous inhibitor of Akt, CTMP, is critical to ischemia-induced neuronal death. *Nat Neurosci* 12:618–626.
- Yano S, et al. (2001) Activation of Akt/protein kinase B contributes to induction of ischemic tolerance in the CA1 subfield of gerbil hippocampus. *J Cereb Blood Flow Metab* 21:351–360.
- Andjelković M, et al. (1997) Role of translocation in the activation and function of protein kinase B. *J Biol Chem* 272:31515–31524.
- Stokoe D, et al. (1997) Dual role of phosphatidylinositol-3,4,5-trisphosphate in the activation of protein kinase B. *Science* 277:567–570.
- Calleja V, Laguerre M, Parker PJ, Larijani B (2009) Role of a novel PH-kinase domain interface in PKB/Akt regulation: Structural mechanism for allosteric inhibition. *PLoS Biol* 7:e17.

Supplementary Information

Supplementary Discussion

One caveat of using Akt activator as a drug for neurological disorders is that hyperactivation of Akt signaling may induce cancer. Nevertheless, induction of cancer by elevating PtdIns(3,4,5)P3/Akt signaling is a progressive process and usually takes several months or even years. For example, in myeloid-specific PTEN knockout mice, we could not find any tumor until 3 months after the birth. When used as a suppressor of neuronal death caused by glutamate-excitotoxicity, Akt activator will only be given for several days, even several hours; thus it is unlikely that this type of treatment will lead to tumorigenesis. Interestingly, it was recently reported that activation of Akt1 decreases mammary epithelial cell migration, and Akt1 prevents an epithelial-to-mesenchymal transition that resembles events required for metastasis (1, 2). Another report showed that in some acute myeloid leukemia (AML), activation of Akt surprisingly reduced leukemic cell growth by inhibiting FOXO (3), suggesting that Akt activator can even potentially be used to treat certain cancers.

Akt is also a key enzyme involved in other processes such as cell migration, immune cell activation, embryonic development, hematopoietic and mesenchymal differentiation, and glucose homeostasis, thus SC79 may potentially be used to modulate cell function in other physiological and pathological situations such as wound healing, host defense, and blood glucose control in diabetes. For example, SC79 may have a potential benefit in regulating glucoregulatory responses and insulin sensitivity in type 1 and 2 diabetes. Phosphorylation and deactivation of GSK3b promotes glycogen synthesis resulting in decreased blood glucose. Akt-mediated GLUT4 translocation mediates glucose transport. GSK3b and FOXO also play a role in expression of genes in gluconeogenesis like G6Pase and PEPCK(4). In innate immunity, activating neutrophil functions by elevating PI3K/Akt pathway using PTEN inhibitor has been previously reported (5). SC79 may also offer similar effect by directly activating Akt. In addition, SC79 may also be effective in preventing myocardial infarction in heart attack, in which the acquired resistance to apoptosis is mediated at least in part by the sustained activation of Akt. Use of SC79 could exert a wide range of cardio-protective effects in myocardial ischemia/reperfusion-induced injury, myocardial hypertrophy, hypertension and vascular diseases by suppressing cell death and inducing angiogenesis by regulating eNOS.

Supplementary Methods

A cell-based screening system for detection of Akt plasma membrane translocation.

Activation of PtdIns(3,4,5)P3/Akt pathway relies on PtdIns(3,4,5)P3-mediated plasma membrane translocation of Akt. To visualize the Akt membrane translocation in intact cells, we used the PH-domain of Akt (PH_{Akt}) fused with green fluorescent protein (PH_{Akt}-GFP) as a marker for this event. The 120 amino acids PH domain is from human Akt1 and specifically bind to PtdIns(3,4,5)P3. Overnight starvation in serum-free medium abolished PH_{Akt}-GFP membrane localization in unstimulated cells (Figure S1). Subsequent PH_{Akt}-GFP membrane translocation was triggered by the addition of insulin growth factor (IGF) (100 ng/ml). In the experiment described in Figure S1, we utilized transient transfection to deliver PH_{Akt}-GFP construct. Although we were able to detect robust membrane translocation of PH_{Akt}-GFP, variable transfection efficiency and levels of recombinant protein expression could be problematic for high-throughput screening. To circumvent this problem, we generated a stable cell line expressing PH_{Akt}-GFP fusion protein. These cells were healthy and IGF-elicited PH_{Akt}-GFP membrane translocation could be easily detected as described in Figure S1 (Figure S2). More

importantly, the expression level of PH_{Akt}-GFP fusion protein was almost the same in each individual cell, thus making the automatic imaging analysis feasible.

Screening for inhibitors of Akt plasma membrane translocation.

To validate our cell based assay for high throughput screening, we first conducted a pilot screening using a bioactive compound library (approximately 3000 compounds). The screening was performed at the Institute for Chemistry and Cell Biology (ICCB) at Harvard Medical School. Every step of the experiment was handled in a high throughput mode (Figure S3). Based on our preliminary data, we incubated cells which have been serum-starved (0.1% serum) for overnight with chemical compounds for 30 min before inducing PH_{Akt}-GFP membrane translocation with IGF. Our goal is to identify compounds which directly inhibit PtdIns(3,4,5)P3/Akt signaling pathway. Thus, we chose to use short incubation time to exclude compounds which indirectly block GFP-PH membrane translocation (e.g. via affecting transcription or translation). From the pilot screening, we identified 21 positive hit compounds (Figure S4 and Table S1). As expected, several known PI3 kinase inhibitors and compounds that nonspecifically inhibit PI3 kinase activity were identified as positive hit compounds, validating our strategy and method for high throughput screening.

We then carried out the high throughput screening using several synthetic compound libraries. The ICCB compounds are from a variety of sources including commercial libraries from ChemBridge, ChemDiv, Bionet, Maybridge, Peakdale, and CEREP, NIH-NCI collections, libraries that result from diversity-oriented organic synthesis (DOS), known bioactive compounds, and historic collections of compounds resulting from different synthetic strategies. When ICCB purchased compound libraries, they selected collections that are enriched for complex heterocyclic compounds and compounds of higher molecular weight (an average mw of ~350-400 Daltons) because these types of compounds are more likely to provide interesting hits in high throughput screens. In addition, they sought to minimize the number of potentially “bad” compounds, those with groups that might make them unstable or toxic. In particular, they eliminated unstable imines, compounds with free carboxyl groups, and compounds with building block elements that might chelate metals. Table S2 is a list of libraries used for current screening, which include more than 60,000 synthetic compounds.

The high throughput screening was performed twice to minimize the number of false positive hit compounds. From the first screening, we identified about 446 positive hit compounds and 125 of them were confirmed in the second screening (Table S3 and Figure S5). We later found that 25 of the positive compounds could generate auto-florescence and their effect on PH-Akt membrane translocation was in fact of the result of the greatly enhanced background florescence (Table S3).

Confirmation of the positive hits by time-lapse fluorescent imaging.

In this study, more than 60,000 chemical compounds were screened and it is difficult to titrate the optimal concentration of each compound. The compound stocks were stored at 5 mg/ml in DMSO. In our screen, 100 nl of compound stock was transferred into a 50 μ l assay volume, resulting in a final concentration of 20 μ M for a compound of 500 Daltons. This is a generally utilized concentration at ICCB. One potential problem of our screening assay is that the transferred compounds may not be able to diffuse evenly in each well due to the relatively short incubation time. Thus, the effect of some positive hit compounds on PH-Akt membrane translocation could be result of very high local concentration. In order to select the most potent compounds for further characterization, we conducted dose-ranging experiments using live cells cultured in 35-mm plate.

The initial 125 positive hit compounds identified after the second screening (**Figure S5**) were purchased from ChemBridge, ChemDiv, or Maybridge. The fresh stock solution was freshly prepared in DMSO (5 mg/ml). This stock solution was directly added to culture medium to yield three different final concentrations (4, 8, 16 μ g/ml). For time-lapse live cell imaging, HeLa-PH-EGFP cells were plated into a 35-mm glass-bottom dish (MatTek) and cultured for 24 to 48 hours. Cells were serum-starved in 2 mL Leibovitz L15 medium for 1 to 2 h and the medium was replaced with 1 mL of fresh serum-free Leibovitz

L15 medium containing a desired concentration of each compound. After 30 min pre-incubation, IGF1 (5 ng/mL) was added and images were taken every 5 to 10 min under a 40× oil objective lens. The relative fluorescent intensity at the membrane versus adjacent cytoplasm was determined. The compounds that led to a greater than 75% inhibition of PH-EGFP membrane translocation at or below 16 µg/ml were identified and designated as the confirmed hits. The representative live images and structure of 55 confirmed hit compounds were shown in **Figure S6** and **Figure S7**.

SC79-induced cytosolic phosphorylation of Akt analyzed by western blotting.

Hela cells were serum starved for 1 hr and treated with IGF (100ng/ml) or SC79 (4 µg/ml) for 30 minutes. Cells were lysed in Lysis buffer containing 250 mM Sucrose, 20 mM HEPES, 10 mM KCl, 1.5 mM MgCl₂, 1 mM EDTA, 1 mM EGTA supplemented with protease inhibitors. Cells were passed through 25G needle several times and kept on ice for 20 minutes. Total cell lysate was taken at this point. Cell lysates were centrifuged at 100,000g for 30 minutes. Supernatant was collected as the cytosolic fraction. Pellet was washed with lysis buffer and represents the membrane fraction. Total cell lysate, cytosolic and membrane fractions were resolved by SDS-PAGE and analyzed for phospho-Akt (S473), Total Akt, Tubulin (cytosolic marker) and Orai1 (membrane marker) by western blotting.

MTT (3-(4,5-Dimethylthiazol-2-yl)-2,5-diphenyltetrazolium bromide) assay for cell viability.

HsSultan or NB4 cells (2.5×10^5) were plated in a 24-well plate in 500 µL of phenol red-free RPMI medium supplemented with 10% FBS. After incubation for 24 hours, each compound (8 µg/ml) was added and cultured for overnight (16–20 h). Fifty microliters of MTT solution (5 mg/mL in PBS) were added to each well. Following 2 hrs incubation, the purple formazan crystals were dissolved by directly adding in 500 µL of isopropanol with 0.1 M HCl to each well. After clearing the cell debris by centrifugation, the absorbance was measured at a wavelength of 570 nm.

***In silico* docking**

In silico docking calculations were carried out using AutoDock Vina (6) as described elsewhere (7). Three dimensional crystal structures of Protein Kinase B/Akt PH domain unbound form (RCSB PDB ID: 1UNR) and inositol-(1,3,4,5)-tetrakisphosphate (IP4) bound form (RCSB PDB ID: 1UNQ) were retrieved from Protein Data Bank corrected for bond order and orientation with application of proper protonation states used in docking experiments using MGLTools (v1.5.4) (8). Structural coordinates of ligand SC79 were generated using Sybyl sketcher module (9) and energy minimized using a standard Tripos forcefield (TRIPOS, St. Louis, MI) that employs Powell minimization and simplex optimization with the distance dielectric function and an energy gradient of 0.05 Kcal/Mol Å with application of Gasteiger charges. Docking of SC79 onto proteins 1UNR and 1UNQ was carried out with similar grid dimension of 100 Å × 100 Å × 100 Å. A local optimization and exhaustive search was carried out by docking algorithm to find and cluster best docked poses of SC79 onto protein structures. Similar docking parameters were applied in both the cases. The best 9 lowest-energy docked poses were identified and analyzed. Ligand IP4 was also docked onto ligand free Akt PH domain structure. As a validation to the applied parameters, native ligand IP4 was redocked onto bound PH domain structure that resulted in binding to similar pocket with a RMSD of 0.9581 Å. Figures were generated using program PyMOL (DeLano Scientific, LLC, San Carlos, CA, USA).

A flexible grid-based SC79-PH domain docking protocol defined 9 clustered poses for the PH domain bound to SC79. Figure 3D illustrates best docked pose of SC79 onto unbound PH domain that possessed ΔG of -5.6 kcal/mol. This pose identified residue Arg25 within binding site which exhibits numerous interactions with the ligand SC79 including hydrogen bond interaction. Results demonstrate that SC79 binds to the similar pocket in unbound PH domain structure as was reported a IP4 binding site in bound PH domain structure. This prompted us to investigate about the IP4 binding pocket in unbound PH domain. Interestingly, IP4 binding site resembles the SC79 binding site in unbound PH domain (Figure 3D, *left panel*). The SC79 and IP4 ligands compete with each other to occupy a similar binding

site onto PH domain. SC79 docking onto IP4 bound PH domain resulted in yielding alternate binding pockets of SC79 other than noted above (Figure 3D). Taken together, these docking analyses suggest that SC79 binds to PH domain. SC79 binding to IP4 bound PH domain may result in a weaker affinity complex.

Circular Dichroism (CD)

Far-UV CD (260-195 nm) was carried out at 25 °C on a Jasco-810 spectropolarimeter (Jasco, Easton, MD) purged with nitrogen gas. Data were acquired in 1-mm quartz cuvette with 1-nm bandwidth, 2-s response time, 10 nm/min scan speed, and four scans. Pure N-terminal 6His-tagged recombinant full length Human Akt1 was purchased from Millipore (www.millipore.com/catalogue/item/14-279). Chemically synthesized and purified SC79 was purchased from ChemBridge. Protein and ligand samples were prepared in 50 mM Tris pH 7.5, 150 mM NaCl. Akt1 was incubated with SC79 at 37 °C for 30 min. Data sets were acquired in duplicate. Percent secondary structure was determined using programs K2D (<http://www.embl.de/~andrade/k2d.html>) and K2D2 (<http://www.ogic.ca/projects/k2d2/>).

Neuronal cell cultures and Cytotoxicity Primary cortical or hippocampal neuronal cultures were prepared as previously described (10). To induce excitotoxicity, the cells were prewashed with Tris-buffered control salt (CSS) solution (120 mM NaCl, 5.4 mM KCl, 1.8 mM CaCl₂, 25 mM Tris-HCl, pH 7.4, and 15 mM glucose) and treated with CSS containing 50 µM glutamate for 40 min, followed by 4 hr recovery in regular culture medium. SC79 (4 µg/ml) was given 15 min before and during glutamate treatment. Toxicity was assayed 4 h after glutamate exposure by microscopic examination with computer-assisted cell counting. Total and dead cells were determined by nuclei staining with Hoechst (0.5 ng/ml) and propidium iodide (1 µg/ml), respectively. After 20 min incubation, the cells were examined under a fluorescence microscope with excitation at 360 nm. Cell death was determined as the ratio of dead-to-total cell number and quantified by counting 1,000 cells.

Permanent focal cerebral ischemia model

This study was conducted in accordance with the Animal Welfare Guidelines of Tokai University School of Medicine, Japan. The permanent focal cerebral ischemia was induced by middle cerebral artery occlusion (MCAO) essentially as described previously (11). Briefly, mice (C57 Black/6) weighing 17–25 g were anesthetized with 4% isoflurane/66% N₂O/30% O₂ and maintained with 1.5% isoflurane. Permanent focal ischemia was achieved as follows: a 2-mm hole was drilled at a site superior and lateral to the left foramen ovale to expose the left middle cerebral artery. The proximal portion of the left middle cerebral artery (MCA) was permanently occluded over a 1-mm segment distal to the origin of the lenticulostriate branches through the use of a bipolar coagulator (12). SC79 was injected intraperitoneally (0.04 mg/g mouse body weight) 5 min before permanent MCAO (Figure 4E). In another experiment, extra SC79 was injected (0.04 mg/g mouse body weight, once per hour for 6 hours) (Figure 4F).

Akt activation in the brain assessed by immunohistochemistry

The mouse brains were perfused from the apex of the heart with PBS and perfusion-fixed with 4% paraformaldehyde in PBS. They were then immersion-fixed overnight at 4°C in 4% paraformaldehyde with rocking and subsequently cryoprotected in 10% (2 hours), 15% (2 hours), 20% (2 hours), and 25% (overnight) sucrose in PBS at 4°C. The slices were then embedded in OCT compound (Miles Scientific) and quickly frozen in isopentane. Coronal frozen sections (10-µm) were prepared on a cryostat and stored at -80 °C until use. The frozen sections were thawed, washed three times in PBS, permeabilized with 0.1% Triton X-100/PBS at room temperature for 5 min, and then blocked in 5% skim milk/3% BSA/PBS for 60 min. Total and phosphorylated Akt/PKB were detected using anti-Akt and anti-Phospho-Akt (Ser473) antibodies (Cell Signaling), respectively. The slides were incubated with primary antibodies (1:200) at 4 °C overnight, and with the secondary antibodies at room temperature for 2 h, and immunoreactivity visualized by the ABC method (10).

References

1. Yoeli-Lerner M, *et al.* (2005) Akt blocks breast cancer cell motility and invasion through the transcription factor NFAT. *Mol Cell* 20(4):539-550.
2. Manning BD, *et al.* (2005) Feedback inhibition of Akt signaling limits the growth of tumors lacking Tsc2. *Genes Dev* 19(15):1773-1778.
3. Sykes SM, *et al.* (2011) AKT/FOXO Signaling Enforces Reversible Differentiation Blockade in Myeloid Leukemias. *Cell* 146(5):697-708.
4. Wymann MP & Schneider R (2008) Lipid signalling in disease. *Nat Rev Mol Cell Biol* 9(2):162-176.
5. Li Y, *et al.* (2011) Pretreatment with phosphatase and tensin homolog deleted on chromosome 10 (PTEN) inhibitor SF1670 augments the efficacy of granulocyte transfusion in a clinically relevant mouse model. *Blood* 117(24):6702-6713.
6. Trott O & Olson AJ (AutoDock Vina: improving the speed and accuracy of docking with a new scoring function, efficient optimization, and multithreading. *J Comput Chem* 31(2):455-461.
7. Sharma AK, *et al.* (Solution structure of the guanine nucleotide-binding STAS domain of SLC26-related SulP protein Rv1739c from Mycobacterium tuberculosis. *J Biol Chem* 286(10):8534-8544.
8. Sanner MF (1999) Python: a programming language for software integration and development. *J Mol Graph Model* 17(1):57-61.
9. SYBYL 8.0 TI, 1699 South Hanley Rd., St. Louis, Missouri, 63144, USA. (SYBYL 8.0, Tripos International, 1699 South Hanley Rd., St. Louis, Missouri, 63144, USA.
10. Luo HR, *et al.* (2003) Akt as a mediator of cell death. *Proc Natl Acad Sci U S A* 100(20):11712-11717.
11. Kawada H, *et al.* (2006) Administration of hematopoietic cytokines in the subacute phase after cerebral infarction is effective for functional recovery facilitating proliferation of intrinsic neural stem/progenitor cells and transition of bone marrow-derived neuronal cells. *Circulation* 113(5):701-710.
12. Zhang F & Iadecola C (1992) Stimulation of the fastigial nucleus enhances EEG recovery and reduces tissue damage after focal cerebral ischemia. *J Cereb Blood Flow Metab* 12(6):962-970.

Table S1. Positive hit bioactive compounds identified from the pilot screening.

Plate #	Well #	Name	Target or biological activity	Molecular formula	Molar weight	Source
500	E17	Ciprofloxacin hydrochloride	Antibiotics; Inhibit bacterial DNA rewind	C17N3O3F	312.99234	NINDS
500	F15	Econazole nitrate	Antifungal drug; Inhibit fungal cell membranes	C18H15N2OCl3	380.02496	NINDS
500	H18	Miconazole nitrate	Antifungal drug; Inhibit fungal cell membranes	C18H14N2OCl4	413.98596	NINDS
500	I15	Gossypol	Polyphenols; Inhibitor of dehydrogenases	C30H30O8	518.1939	NINDS
500	M20	Tamoxifen citrate	Competitive antagonist of estrogen receptor	C26H29NO	371.2248	NINDS
500	B13	Gentian violet	Antifungal and bactericidal agent	C25H30N3I+	372.2439	NINDS
500	K11	Centrimonium bromide	Antiseptic agent; Cationic surfactants	C19H42N1+	284.33173	NINDS
500	O8	Phenylmercuric acetate	Fungicide; Herbicide	C8H8O2Hg	338.023	NINDS
1362	I17	NSC-95397	Inhibitor of Cdc25 dual specificity phosphatases	C14H14O4S2	310.03336	BIOMOL
1362	K19	BAY 11-7082	Inhibitor of NF kappa B activation	C10H9NO2S	207.0354	BIOMOL
1362	N13	Wortmannin	Inhibitor of phosphoinositide 3 kinases	C23H24O8	428.1471	BIOMOL
501	E17	Merbromin	Antiseptic agent	C20O6Br2Hg2-	695.77686	NINDS
500	E16	Hexylresorcinol	Antiseptic and antihelmintic agent	C12H18O2	194.13069	NINDS
501	B08	Cetylpyridinium chloride	Antiseptic and antibacterial agent	C21H38N1+	304.3004	NINDS
1362	E19	Ro 31-8220	Selective PKC inhibitor	C25H23N5O2S	457.15714	BIOMOL
1362	J07	Staurosporine	ATP-competitive protein kinase inhibitor	C28H26N4O3	466.53	BIOMOL
503	G17	Harmalol hydrochloride	Alkaloids from plants	C12H12N2O	200.09496	NINDS
502	D20	Celastrol	Antioxidant and anti-inflammatory agent	C28H36O4	436.2613	NINDS
1569	L10	Ellipticine	Anticancer agent; Binds to topoisomerase II	C17H14N2	246.11569	Prestwick
1362	F09	Quercetin dihydrate	Antioxidant flavonoid; Inhibitor of cAMP-phosphodiesterases	C15O7	291.9644	BIOMOL
1362	M5	LY294002	Inhibitor of phosphoinositide 3 kinases	C19H17NO3	307.343	BIOMOL

Table S2. Compound libraries used for primary and secondary screenings.

	Library name	# of Compounds	Plate Numbers	# of Plates
Bioactive Compounds	Biomol ICCB Known Bioactives	480	1361-1362	2
	NINDS Custom Collection	1,040	500-503	4
	Prestwick 1 Collection	1,120	1568-1571	4
Synthetic Compounds	ChemBridge 3	19,560	1577-1606	30
	ChemDiv 4	14,677	1607-1648	42
	Maybridge 5	3,212	1661-1670	10
	ChemDiv 3	16,544	1473-1519	47
	Maybridge 1	8,800	542-563	22
	Total number of chemicals	65433		

Table S3. Positive hit compounds identified from the primary and secondary screenings.

ID	Plate/Well #	Source	Reagent Source ID	Mol. Formula	Mol. Weight	PubChem CID	Autofluorescence	Toxicity	ID
SC1	545	H12	Maybridge	Maybridge BTB 06587	C ₉ NO ₄	191	2799766		SC1
SC2	550	I05	Maybridge	Maybridge CD 08589	C ₉ H ₄ N ₅ O ₄ SF ₃	335	2805154		SC2
SC3	550	O05	Maybridge	Maybridge CD 08635	C ₁₆ H ₂₂ N ₂ O ₂ S ₂	338	2805164		SC3
SC4	554	P07	Maybridge	Maybridge KM 02595	C ₈ H ₁₃ NO ₂ S ₃	251	2778657		SC4
SC5	554	P22	Maybridge	Maybridge KM 03776	C ₁₂ H ₁₃ NO ₃ S ₂	283	2820297	*	SC5
SC6	558	H11	Maybridge	Maybridge RDR 03078	C ₆ H ₁₂ N ₂ S ₂	176	167013; 167304; 123256; 105062; 522634; 313; 10313041		SC6
SC7	561	H02	Maybridge	Maybridge S 02113	C ₁₄ H ₁₅ NO ₂	229	300890		SC7
SC8	561	K13	Maybridge	Maybridge RJC 03273	C ₇ H ₅ O ₂ Br	200	2729629		SC8
SC9	1476	B07	ChemDiv	ChemDiv 2548-0771	C ₁₈ H ₁₉ NO ₆	329	4606022		SC9
SC10	1477	C02	ChemDiv	ChemDiv 3182-0185	C ₁₃ H ₂₁ N ₂ S ₂ ¹⁺	269	5475033; 5749630; 102370; 7015549	*	SC10
SC11	1478	C16	ChemDiv	ChemDiv 3448-1880	C ₁₈ H ₁₄ N ₂ O ₅	338	1917689; 703540; 1917688	*	SC11
SC12	1479	N21	ChemDiv	ChemDiv 3888-0510	C ₁₇ H ₁₃ NO ₃ S	311	5724532; 6740709; 5398661		SC12
SC13	1481	H17	ChemDiv	ChemDiv 4340-1702	C ₂₁ H ₁₇ N ₂ O ₃ SBr	456	1337448; 1337447	*	SC13
SC14	1481	H22	ChemDiv	ChemDiv 4379-0593	C ₁₆ H ₁₂ N ₂ O ₂ S ₄	388	2194030	*	SC14
SC15	1483	O06	ChemDiv	ChemDiv 4663-0305	C ₁₂ H ₇ O ₂ Br	262	749613		SC15
SC16	1490	I04	ChemDiv	ChemDiv 6234-0158	C ₁₇ H ₁₇ N ₄ S ₂ F	360	7045555; 3357152; 7127443		SC16
SC17	1491	N08	ChemDiv	ChemDiv 6658-0003	C ₂₃ H ₂₈ N ₂ O	348	2952775; 961714; 961713	*	SC17
SC18	1491	N15	ChemDiv	ChemDiv 6623-0252	C ₁₅ H ₁₇ NO	227	781226; 2063512; 781227	*	SC18
SC19	1498	A09	ChemDiv	ChemDiv C301-2030	C ₁₄ N ₂ OC ₂	282	584802	*	SC19
SC20	1498	G02	ChemDiv	ChemDiv C301-3578	C ₁₄ NO ₂ Cl	249	768385		SC20
SC21	1498	I18	ChemDiv	ChemDiv C306-0545	C ₂₅ HN ₃ O ₂ S	407	6621759		SC21
SC22	1511	J19	ChemDiv	ChemDiv K788-0502	C ₂₆ N ₂ O ₂ S	404	4058887		SC22
SC23	1515	D07	ChemDiv	ChemDiv 7286-2245	C ₁₅ H ₁₄ N ₄ O ₃ S	326	970664		SC23
SC24	1515	M03	ChemDiv	ChemDiv E746-0124	C ₁₈ H ₁₉ N ₃ O ₂ S	337	6624952		SC24
SC25	1517	D06	ChemDiv	ChemDiv D053-0021	C ₁₃ H ₁₁ N ₃ O ₄ SCl ₂	375	2987701	*	SC25
SC26	1577	C20	ChemBridge	5106399	C ₁₃ H ₉ NO ₄	243	2192517		SC26
SC27	1577	D22	ChemBridge	5193093	C ₁₀ H ₇ NOS	189	1626686; 2832913	*	SC27
SC28	1578	B03	ChemBridge	5140994	C ₈ H ₈ N ₄	160	6787450; 6863956; 5544086	*	SC28
SC29	1578	B09	ChemBridge	5214970	C ₁₅ H ₁₇ NO	227	781226; 2063512; 781227	*	SC29
SC30	1578	B15	ChemBridge	5216515	C ₁₀ H ₁₃ O ₂ Br	244	787529		SC30
SC31	1578	F19	ChemBridge	5260273	C ₁₆ H ₂₃ NO ₂	261	792319; 792320; 2838039		SC31
SC32	1578	I07	ChemBridge	5115555	C ₂₇ H ₃₅ N ₅ S	461	6759337; 1377982; 5717379; 2828280	*	SC32
SC33	1578	N08	ChemBridge	5169046	C ₁₁ H ₁₂ N ₂ O ₂	204	5569250; 6611042; 5718022		SC33
SC34	1579	C19	ChemBridge	5264570	C ₁₆ H ₁₃ NO	235	2177126; 2838279; 2177244		SC34
SC35	1579	E22	ChemBridge	5176963	C ₈ H ₅ NS ₃	187	2832072	*	SC35
SC36	1579	F18	ChemBridge	5240810	C ₁₀ H ₈ N ₂ O ₄	220	747593; 1911041; 1911042	*	SC36
SC37	1579	N16	ChemBridge	5240765	C ₁₈ H ₁₄ N ₂ O ₄	322	6746064; 5417561; 5596031		SC37
SC38	1580	B08	ChemBridge	5317697	C ₉ HN ₂ OS	185	794582		SC38
SC39	1581	A12	ChemBridge	5431041	C ₁₇ H ₁₈ NOF ₃	309	783606		SC39
SC40	1582	E17	ChemBridge	5710104	C ₈ H ₇ NO ₃	165	869076; 96000; 11897671		SC40
SC41	1582	L14	ChemBridge	5459675	C ₁₇ H ₂₁ NO ₂	271	11921442; 6456397; 11921441	*	SC41
SC42	1582	M19	ChemBridge	5718756	C ₁₆ H ₁₃ N ₅ O ₂ S	339	6745067; 5336479		SC42
SC43	1583	F15	ChemBridge	5735144	C ₁₆ H ₁₂ N ₂ O ₂	264	869358; 869359; 2865647		SC43

SC44	1584	A21	ChemBridge	5787636	C ₂₂ H ₂₇ NO ₄	369	5508822; 6758018; 5726290	*	SC44
SC45	1585	D07	ChemBridge	5809904	C ₁₇ H ₁₂ N ₂ O ₄	308	1916528; 873244		SC45
SC46	1585	I05	ChemBridge	5943536	C ₁₈ H ₁₂ N ₂ O ₃ S ₂	368	9586234; 2235899		SC46
SC47	1586	G16	ChemBridge	6274843	C ₁₉ H ₁₄ N ₃ O ₄ S ₂ Cl	447	1348278; 1348277; 2274928	*	SC47
SC48	1587	F16	ChemBridge	6598710	C ₁₀ NOSCl ₂	252	759209		SC48
SC49	1588	G16	ChemBridge	6888464	C ₁₈ H ₁₁ N ₃ O ₆	365	1323123		SC49
SC50	1590	I16	ChemBridge	7564073	C ₁₄ H ₂₃ NO ₃ S	285	623015		SC50
SC51	1593	E15	ChemBridge	7693384	C ₁₅ H ₁₆ NOCl	261	2948191; 828623; 828622		SC51
SC52	1593	O07	ChemBridge	7772407	C ₁₇ H ₂₀ N ₂ O ₃ S	328	2953048	*	SC52
SC53	1600	N13	ChemBridge	7992444	C ₁₂ H ₁₆ N ₂ O ₂	220	2985018		SC53
SC54	1607	B19	ChemDiv	ChemDiv 0455-0021	C ₁₃ H ₂₁ N ₂ O ₂ ¹⁺	237	4597466; 6160337	*	SC54
SC55	1607	K10	ChemDiv	ChemDiv 0149-0135	C ₂₁ H ₂₈ O ₃	328	5239155		SC55
SC56	1607	M10	ChemDiv	ChemDiv 0157-0001	C ₉ O ₂ Cl	175	87326	*	SC56
SC57	1607	O08	ChemDiv	ChemDiv 0139-0206	C ₇ H ₃ NO ₂ Cl ₄	273	676444		SC57
SC58	1614	A09	ChemDiv	ChemDiv 4767-1305	C ₂₄ H ₂₆ N ₂ O ₆ S	470	1009503; 1809094	*	SC58
SC59	1614	K07	ChemDiv	ChemDiv 4762-1092	C ₂₀ H ₂₀ N ₃ O ₂ SF	385	No ID		SC59
SC60	1617	H15	ChemDiv	ChemDiv 6383-0891	C ₁₇ H ₁₈ N ₃ Cl	299	975900	*	SC60
SC61	1617	K01	ChemDiv	ChemDiv 6177-0034	C ₂₀ H ₂₀ N ₂ O ₂	320	7114457; 675011; 7114459; 5291898; 7114458; 2973216		SC61
SC62	1618	N08	ChemDiv	ChemDiv 7202-2080	C ₂₀ H ₁₆ N ₄ O ₄ S ₂	436	22525620; 3318217; 5791770		SC62
SC63	1618	N18	ChemDiv	ChemDiv 7218-1489	C ₁₃ H ₁₂ N ₂ O ₂ S ₂	292	22332416		SC63
SC64	1618	P08	ChemDiv	ChemDiv 7202-2246	C ₁₆ H ₉ N ₄ O ₃ S ₃	401	24283764; 7728365		SC64
SC66	1621	D01	ChemDiv	ChemDiv C151-0032	C ₁₈ H ₁₆ N ₂ O	276	4137609; 6018993		SC66
SC67	1621	P05	ChemDiv	ChemDiv C151-0517	C ₁₈ H ₁₇ N ₃ O	291	702066; 2265242; 2265240		SC67
SC68	1621	P07	ChemDiv	ChemDiv C151-0796	C ₁₅ H ₁₇ NO	227	5050194		SC68
SC69	1622	C10	ChemDiv	ChemDiv C201-0114	C ₁₁ N ₂ O ₃	208	No ID		SC69
SC70	1628	N07	ChemDiv	ChemDiv C700-1471	C ₂₀ N ₃ O ₃ S	362	20876818		SC70
SC71	1648	C05	ChemDiv	ChemDiv K906-4279	C ₁₀ H ₁₂ N ₂ O	176	20969907		SC71
SC72	1648	C13	ChemDiv	ChemDiv K939-0016	C ₁₄ H ₁₀ N ₂ O	222	5398228; 260652; 16039283		SC72
SC73	1648	M09	ChemDiv	ChemDiv K915-1566	C ₂₄ H ₂₈ N ₃ O ₃ Cl	441	3241960		SC73
SC74	1661	C05	Maybridge	Maybridge AW 00693	C ₁₅ H ₁₄ N ₄ OCIF ₃	358	2795918		SC74
SC75	1661	J01	Maybridge	Maybridge BTB 08680	C ₁₇ H ₁₂ N ₂ O ₃ F ₂	330	2801021		SC75
SC76	1662	F06	Maybridge	Maybridge GK 03531	C ₁₄ H ₁₁ N ₅ OF ₃	336	2809005; 9583713; 5714465		SC76
SC77	1662	J21	Maybridge	Maybridge GK 02921	C ₁₄ H ₁₂ N ₃ O ₂ F ₃	311	2808617		SC77
SC78	1662	P03	Maybridge	Maybridge FM 00024	C ₁₁ H ₁₅ NO ₂	193	11859264; 16100370; 2807445		SC78
SC79	1663	O19	Maybridge	Maybridge HTS 02701	C ₁₇ H ₁₇ N ₂ O ₅ Cl	364	6975756; 6975759; 6975757; 2810830; 6975758		SC79
SC80	1664	P13	Maybridge	Maybridge HTS 12963	C ₈ HN ₂ OS	173	173760		SC80
SC81	1668	B19	Maybridge	Maybridge SEW 03790	C ₁₂ H ₁₂ O ₄ S	252	591564		SC81
SC82	1668	D19	Maybridge	Maybridge SEW 03825	C ₈ H ₃ N ₂ SCI	194	2740505		SC82
SC83	1668	E07	Maybridge	Maybridge S 15443	C ₁₁ N ₂ O ₂	192	2738086		SC83
SC84	1668	K16	Maybridge	Maybridge SEW 00543	C ₁₀ H ₉ OSCl	212	6925757; 6925758; 2739084		SC84
SC85	1669	D06	Maybridge	Maybridge SPB 05266	C ₁₅ H ₉ N ₄ O ₂ Cl ₂	346	628891		SC85
SC86	1585	E12	ChemBridge	6082181	C ₁₈ H ₁₆ N ₄ O ₂ S ₂	384	No ID		SC86
E1	1481	E10	ChemDiv	ChemDiv 4286-0237	C ₁₈ H ₁₆ N ₂ O ₂	292	6620710; 5334000		E1
E2	1484	N01	ChemDiv	ChemDiv 4999-0666	C ₁₈ H ₁₆ N ₂ O ₄ S	356	16193244; 6620788	*	E2
E3	1607	N06	ChemDiv	ChemDiv 0645-0166	C ₁₈ N ₂ O ₂	276	202512	*	E3
E4	1473	D13	ChemDiv	ChemDiv 0388-0143	C ₁₈ H ₁₅ NO ₂	277	67273		E4

E5	1476	C14	ChemDiv	ChemDiv 2374-0075	C ₂₁ H ₂₃ NO ₂	321	4533882; 11878901; 11878907; 11878905; 11878903	*	E5
E6	1487	A14	ChemDiv	ChemDiv 5701-0577	C ₂₂ H ₂₅ NO ₄	367	4602281; 1854370	*	E6
E7	1624	O09	ChemDiv	ChemDiv C301-5476	C ₉ N ₅ O	236	3163523		E7
E8	1669	K04	Maybridge	Maybridge SPB 00784	C ₂₀ H ₂₃ N ₃ OS	353	2743318		E8
E9	1476	A20	ChemDiv	ChemDiv 2422-1298	C ₁₈ NOS	278	1730434; 744351	*	E9
E10	1477	M05	ChemDiv	ChemDiv 3062-0036	C ₁₈ H ₂₃ NO ₂ S ₂	349	1514885; 1514884; 3071511		E10
E11	1481	I10	ChemDiv	ChemDiv 4286-0239	C ₁₇ H ₁₄ N ₂ O ₂	278	14741964; 6620717	*	E11
E12	1580	H11	ChemBridge	5279826	C ₁₁ O ₂	164	765984		E12
E13	1608	P13	ChemDiv	ChemDiv 1683-1038	C ₁₇ N ₂ O ₃ S	312	668008; 668009	*	E13
E14	1612	P06	ChemDiv	ChemDiv 4286-0232	C ₁₆ H ₁₄ N ₂ O	250	5339421; 5416091; 6801758	*	E14
E15	1639	B02	ChemDiv	ChemDiv E781-0267	C ₁₇ H ₂₁ N ₅ OCi	360	16456505		E15
E16	1669	O21	Maybridge	Maybridge SPB 00465	C ₁₂ H ₉ N ₂ O ₂ SClF ₂	318	2743188		E16
E17	544	K16	Maybridge	Maybridge BTB 04176	C ₁₅ H ₁₁ NOSCl ₃ F	377	2798260		E17
E18	545	J10	Maybridge	Maybridge BTB 06548	C ₁₇ H ₁₃ N ₅ O	303	2799743		E18
E19	545	L09	Maybridge	Maybridge BTB 06196	C ₁₃ H ₉ NOCiF	249	705916	*	E19
E20	550	M11	Maybridge	Maybridge CD 09133	C ₁₀ H ₁₁ O ₆ S ₃ F ₃	380	2805283		E20
E21	554	A04	Maybridge	Maybridge KM 01302	C ₉ N ₄ O	180	2735244		E21
E22	1474	D07	ChemDiv	ChemDiv 1326-0389	C ₁₇ H ₁₂ NO ₂ Cl	297	598489		E22
E23	1502	O11	ChemDiv	ChemDiv C620-0170	C ₁₉ H ₁₅ N ₂ O ₂ Br	382	6622833		E23
E24	1517	D20	ChemDiv	ChemDiv D090-0079	C ₁₄ H ₁₇ N ₂ Cl	248	846381; 3138840; 846380		E24
E25	1577	A04	ChemBridge	5108485	C ₁₇ H ₁₇ NO ₂	267	744328; 744324	*	E25
E26	1581	M02	ChemBridge	5406375	C ₁₁ H ₉ NO ₃	203	5397103		E26
E27	1582	L05	ChemBridge	5402066	C ₁₆ H ₁₁ NO ₃	265	5403890; 768328		E27
E28	1586	L12	ChemBridge	6717002	C ₁₄ H ₁₄ NO ₄ S ₂ Br	403	5733354; 2911684	*	E28
E29	1610	A10	ChemDiv	ChemDiv 3178-0151	C ₁₇ H ₁₄ O ₅	298	743982		E29
E30	1624	B02	ChemDiv	ChemDiv C355-1313	C ₂₁ N ₄ O ₇ S ₂ Cl	519	No ID	*	E30
E31	1639	J17	ChemDiv	ChemDiv E771-0423	C ₁₉ H ₂₃ N ₃ O	309	20916544	*	E31
E32	1641	F12	ChemDiv	ChemDiv G017-4142	C ₁₆ H ₂₂ N ₂ O ₃ S ₃	382	20937318		E32
E33	1642	I06	ChemDiv	ChemDiv G125-0751	C ₂₅ H ₃₀ N ₄ O ₂ S	450	20940800		E33
E34	1643	O03	ChemDiv	ChemDiv G278-0048	C ₁₇ H ₂₁ N ₃ O ₂ S	331	20947619		E34
E35	1645	D06	ChemDiv	ChemDiv K405-2825	C ₁₆ H ₁₆ N ₅ Cl	313	17017244		E35
E36	1647	M07	ChemDiv	ChemDiv K786-8481	C ₂₅ N ₅ O ₂ Cl ₂	472	15994483		E36
E37	1663	E03	Maybridge	Maybridge HTS 01393	C ₁₈ H ₁₉ N ₃ OF ₄	369	2810103; 7189247; 7189249		E37
E38	1669	A20	Maybridge	Maybridge SPB 02768	C ₁₄ H ₁₅ N ₂ O ₂ SBr	354	2744343		E38
E39	1669	K02	Maybridge	Maybridge SPB 00548	C ₁₆ H ₁₄ N ₃ OSCl	331	2743236		E39
E40	1669	P15	Maybridge	Maybridge SPB 04530	C ₁₆ H ₁₅ N ₃ O ₃ S	329	2745327		E40
E41	1670	C01	Maybridge	Maybridge SPB 07631	C ₁₈ H ₁₉ NO	265	2746994		E41

Table S4. Characterization of the confirmed positive hit compounds. ^a ‘+’ indicates inhibition of membrane translocation greater than 75% of control.

^b For morphological observation of adherent cells, HeLa cells were plated in 24-well culture dish and grown overnight in serum rich condition. Following chemical addition (8 µg/ml), the bright field images of live cells were taken at 30 min and 6 hr. ‘+’ indicates chemicals that lead to morphological changes and/or detachment. For MTT-based cell viability assay for suspension cells, the readings (absorbance 570 nm) from triplicates were averaged and normalized against DMSO-treated group. The relative inhibitory activity was presented as following: +/- (0.9-1.16); + (0.75-0.90); ++ (0.60-0.75); +++ (0.45-0.60); ++++ (0.30-0.45); +++++ (0.15-0.30); ++++++ (<0.15).

ID	Membrane translocation assay ^a			Drug toxicity ^b						Effect on Akt phosphorylation (-, no effect; +, inhibited)				
	PH _{AM} -GFP		PH _{PLCδ} -GFP	Cell morphology		MTT assay				IGF-induced			GPCR-mediated	
	High throughput screening	Live cell imaging	Live cell imaging	0.5 hr	6 hr	(16 hr treatment)				(4 µg/ml)			(HL60 cells)	
	First	Second				HsSultan cells	NB4 cells			HeLa	NB4	HsSultan	8 mg/ml	4 mg/ml
SC2	+	+	+	-	-	0.13	+++++	0.19	+++++	+	+	+	+	-
SC3	+	+	+	-	-	0.76	+	0.79	+	-	+	+	-	+
SC4	+	+	+	-	-	0.25	+++++	0.28	+++++	+	+	+	+	+
SC5	+	+	+	-	-	0.12	+++++	0.20	+++++	+	+	+	+	+
SC7	+	+	+	-	-	0.13	+++++	0.32	+++++	+	+	+	+	+
SC16	+	+	+	-	-	0.20	+++++	0.45	+++++	+	+	+	+	+
SC17	+	+	+	-	-	0.12	+++++	0.19	+++++	+	+	+	-	-
SC25	+	+	+	-	-	0.13	+++++	0.20	+++++	+	+	+	+	-
SC26	+	+	+	-	-	0.13	+++++	0.84	+	+	+	-	+	-
SC30	+	+	+	-	-	0.73	++	0.69	++	-	+	-	+	-
SC31	+	+	+	-	-	1.05	+/-	1.02	+/-	+	-	-	+	+
SC33	+	+	+	-	-	0.89	+	1.16	+/-	-	-	-	-	-
SC35	+	+	+	-	-	0.14	+++++	0.33	+++++	+	+	-	-	-
SC36	+	+	+	-	-	0.82	+	0.83	+	+	+	+	+	+
SC38	+	+	+	-	-	0.71	++	0.90	+/-	+	+	+	+	+
SC39	+	+	+	-	-	0.69	++	0.84	+	+	-	-	+	+
SC43	+	+	+	-	-	0.89	+	0.75	+	+	+	+	+	+
SC44	+	+	+	-	-	0.83	+	1.02	+/-	+	+	+	-	-
SC45	+	+	+	-	-	0.85	+	1.00	+/-	+	+	+	+	+
SC46	+	+	+	-	-	0.51	+++	0.37	+++++	-	+	-	-	-
SC51	+	+	+	-	-	1.02	+/-	0.68	++	+	+	+	-	-
SC55	+	+	+	-	-	0.80	+	0.62	++	+	+	+	+	+
SC57	+	+	+	-	-	0.20	+++++	0.70	++	+	+	-	+	+
SC59	+	+	+	-	-	0.27	+++++	0.38	+++++	-	-	-	+	-
SC62	+	+	+	-	-	0.32	+++++	0.27	+++++	+	-	-	+	-
SC64	+	+	+	-	-	0.27	+++++	0.25	+++++	+	-	-	-	-
SC69	+	+	+	-	-	0.90	+/-	0.96	+/-	+	+	+	-	-
SC74	+	+	+	-	-	0.74	++	0.26	+++++	+	+	+	-	-
SC75	+	+	+	-	-	0.97	+/-	0.99	+/-	+	+	+	-	-
SC79	+	+	+	-	-	0.90	+/-	0.83	+	increase	increase	increase	increase	increase
SC80	+	+	+	-	-	0.91	+/-	0.98	+/-	-	+	+	-	-
SC83	+	+	+	-	-	0.76	+	0.82	+	+	+	+	+	+
SC84	+	+	+	-	-	0.89	+	0.88	+	+	+	+	+	+
E7	+	+	+	-	-	1.02	+/-	0.96	+/-	+	+	-	+	+
E8	+	+	+	-	-	0.84	+	0.69	++	+	+	-	+	+
E10	+	+	+	-	-	0.61	++	0.44	+++++	+	+	+	+	-
E12	+	+	+	-	-	0.36	+++++	0.18	+++++	+	+	+	+	+
E17	+	+	+	-	-	0.80	+	0.74	++	+	+	+	+	+
E19	+	+	+	-	-	0.83	+	0.66	++	+	-	+	+	+
E20	+	+	+	-	-	0.57	+++	0.51	+++	-	-	-	+	+
E29	+	+	+	-	-	0.44	+++++	0.35	+++++	+	-	-	+	+
E40	+	+	+	-	-	1.05	+/-	0.94	+/-	+	+	+	+	+
SC1	+	+	+	-	-	0.13	+++++	0.27	+++++	-	+	+	+	+
SC11	+	+	+	-	-	0.27	+++++	0.41	+++	+	+	-	+	+
SC13	+	+	+	-	-	0.19	+++++	0.21	+++++	+	+	+	+	+
SC19	+	+	+	-	-	0.12	+++++	0.19	+++++	+/-	+	-	+	-
SC23	+	+	+	-	-	0.21	+++++	0.38	+++++	+	+	-	+	-
SC27	+	+	+	-	-	0.14	+++++	0.35	+++++	+	+	+	+	-
SC49	+	+	+	-	-	0.58	+++	1.08	+/-	+	+	+	+	+
SC63	+	+	+	-	-	0.69	++	0.83	+	+	+	+	+	+
SC66	+	+	+	-	-	0.15	+++++	0.40	+++++	+/-	+	-	+	+
SC67	+	+	+	-	-	0.21	+++++	0.57	+++	-	-	-	+	+
SC86	+	+	+	-	-	0.55	+++	1.05	+/-	+/-	-	-	+	+
E26	+	+	+	-	-	0.88	+	0.92	+/-	+/-	-	+	+	+
WTM (100 nM)	+	+	+	-	-	0.94	+/-	0.84	+	+	+	+	+	+
DMSO	-	-	-	-	-	1	+/-	1	+/-	-	-	-	-	+

Table S5. The secondary structures of human Akt1 and its complex with SC79 were analyzed using circular dichroism (CD) spectroscopy.

	Akt1 (5mM)	Akt1+ SC79 (25 mM)	Akt1+ SC79 (50 mM)
% alpha-helix	30	25	26
% beta-sheets	16	19	18
% random coil	54	56	56
Sum (sec. structural content)	46	44	44
Random coil	54	56	56
% Loss in sec. structure upon SC79 binding		4.3	4.3

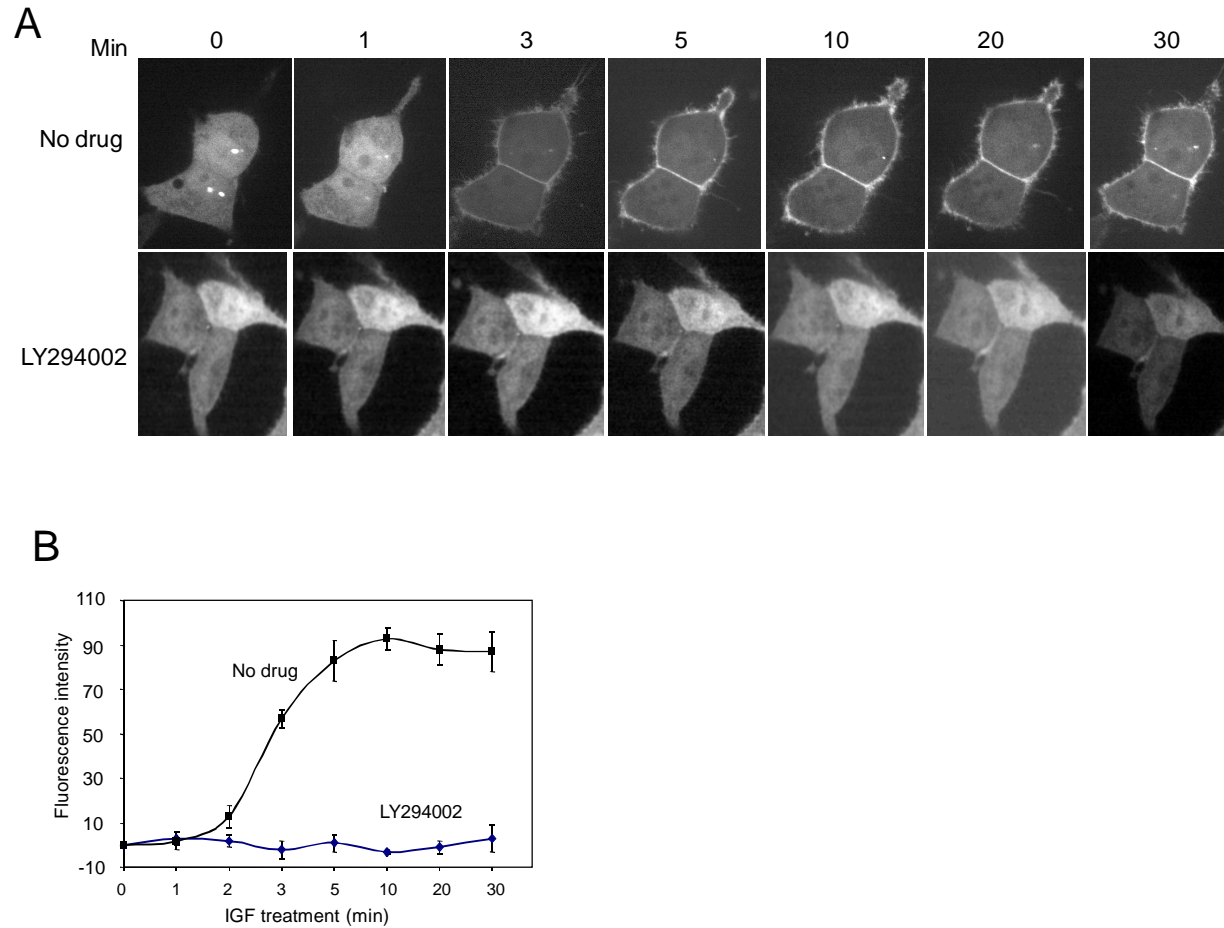


Figure S1. Insulin-like growth factor 1 -induced Akt plasma membrane translocation. HeLa cells were transfected with a construct expressing the PH-domain of Akt fused with enhance green fluorescent protein (PH-EGFP). Using Lipofectamine 2000 reagent (Invitrogen), transfection efficiencies of >80% were routinely obtained. Cells were starved in serum free medium overnight and the Akt membrane translocation was triggered by IGF1 (final concentration 100 ng/ml). For LY294002 treatment, the drug (20 μ M) was added to the culture medium 60 min before the IGF1 stimulation. **(A)** Confocal fluorescent images of PH-EGFP were captured at each of the indicated time points. Each experiment was repeated at least three times and virtually the same results were obtained each time. The figure shows the results of a representative experiment. **(B)** Quantitative analysis of the IGF1-elicited translocation of PH-EGFP. The average membrane fluorescence intensities in (A) were measured with IPLab software as previously described. The arbitrary number of the membrane fluorescence intensity in each individual cell was normalized to the total fluorescence intensity of the cell. Intensities from “0 min” frame was subtracted from each of the other frames and plotted as a function of time after IGF1 stimulation. The results are the means (\pm SD) of 20 transfected cells in three independent experiments.

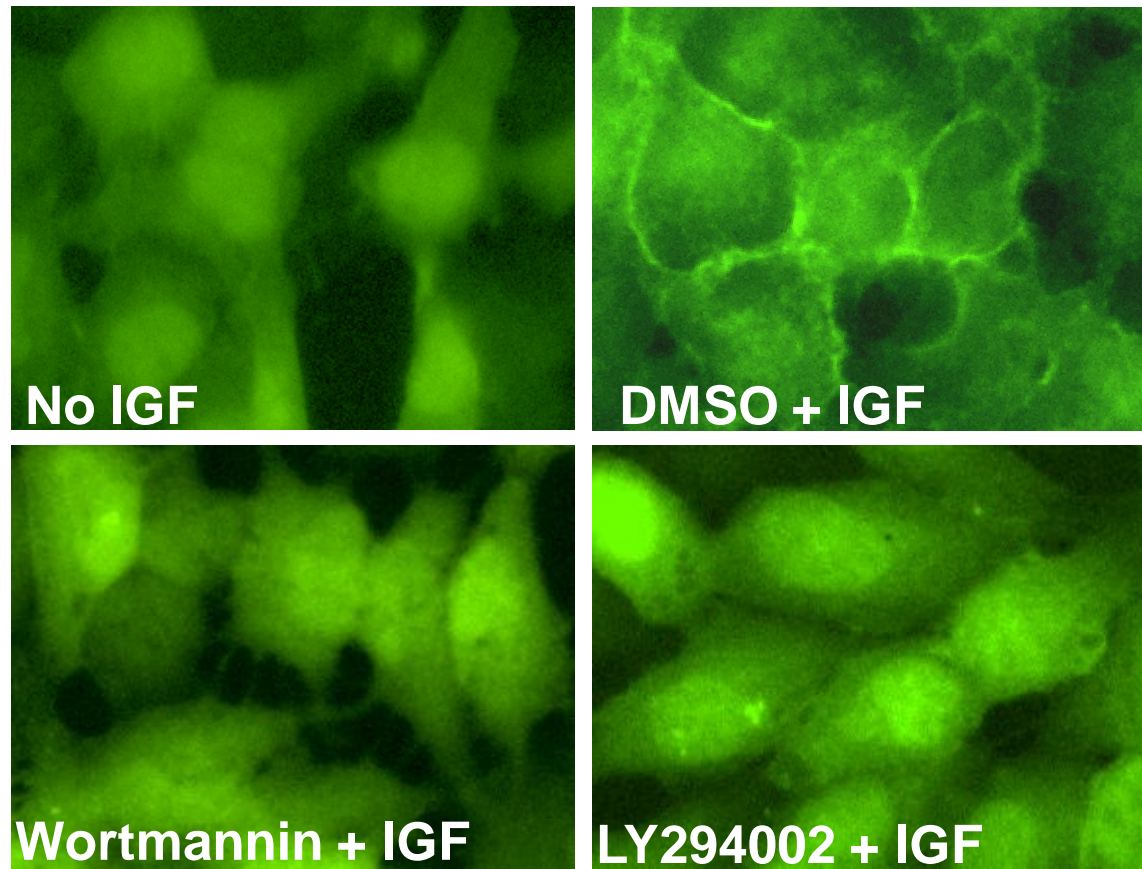


Figure S2. Generation of a stable HeLa cell line expressing Akt-PH-EGFP fusion protein. To generate a stable HeLa cell line, the plasmid containing PH-EGFP driven by chicken beta-globin promoter was co-transfected with pcDNA3.1. The transfected cells were selected in the presence of G418 (2 mg/ml) for two weeks, and the stable PH-EGFP expressing clones were isolated and maintained in the medium containing G418 (200 mg/ml). The membrane translocation of PH-EFP, as described in Figure S1, was conducted in 384-well plate. Serum-starved cells were fixed in 3 % PFA (no IGF) or pre-treated with DMSO or PI3K inhibitors; wortmannin (200 nM) and LY294002 (20 mM) for 30 min and stimulated with IGF1 (100 ng/ml) for additional 15-30 min before fixation. Images were taken using a fully automated fluorescent microscope, Image Xpress Micro (Molecular Dynamics).

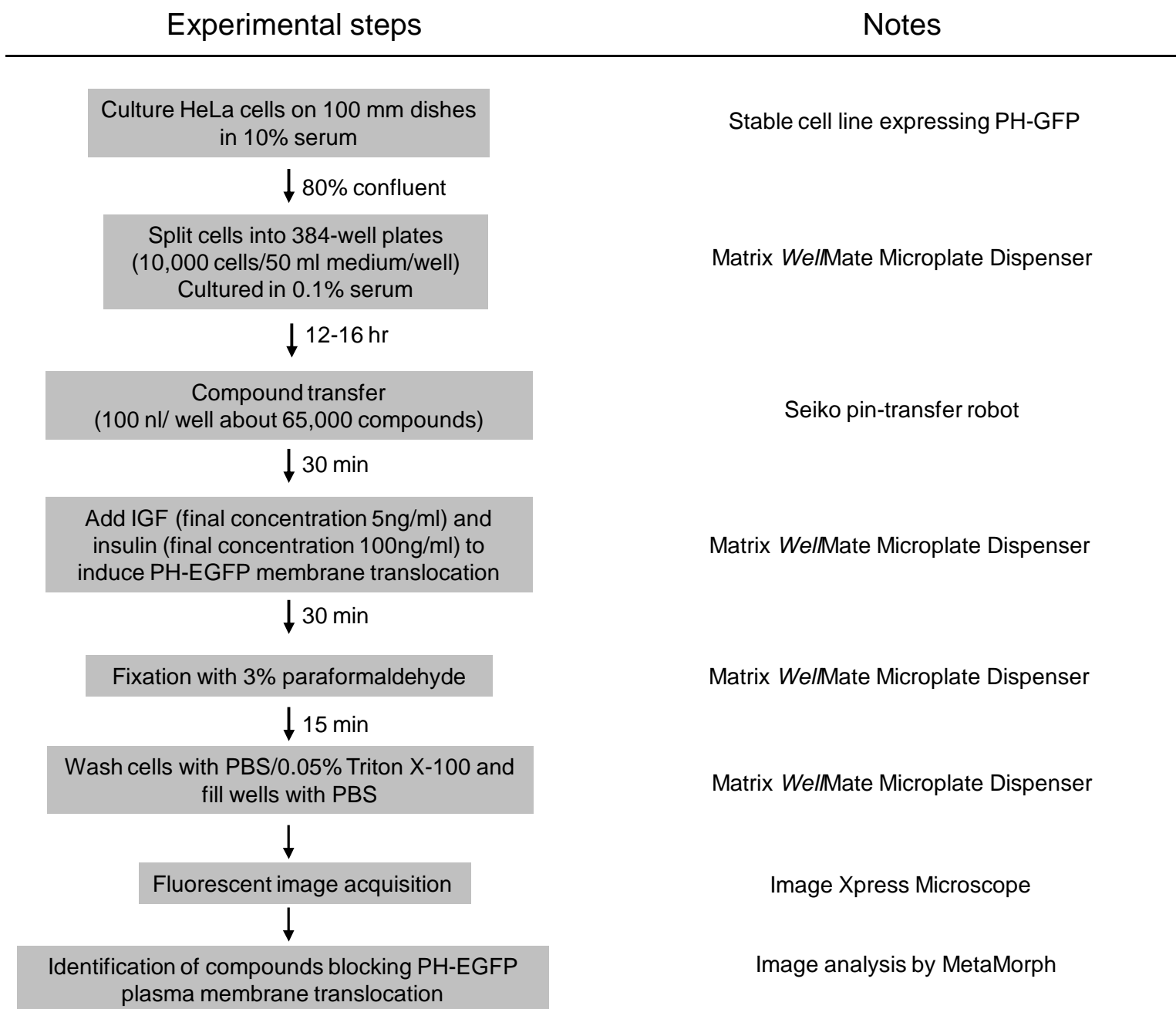
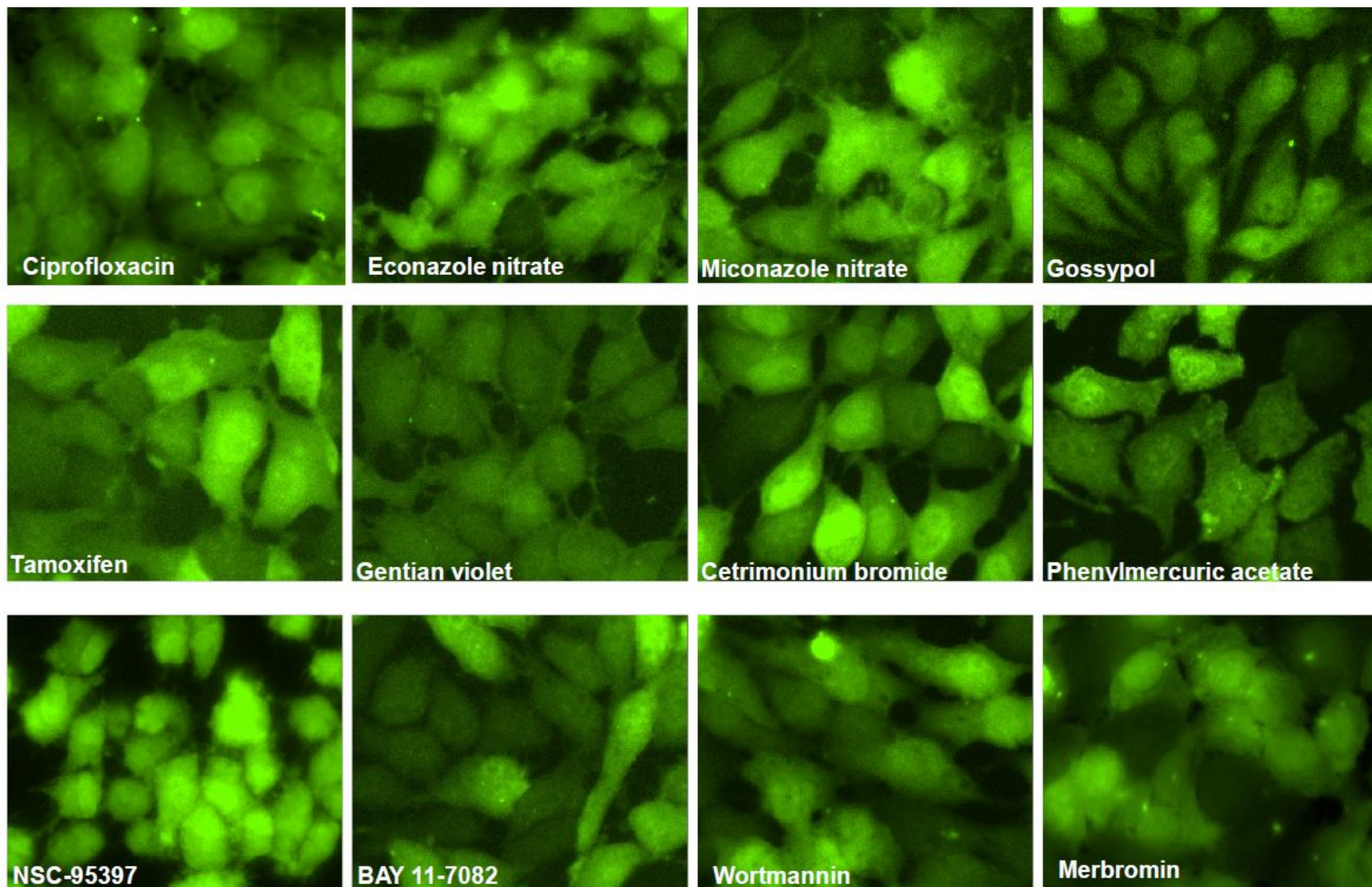


Figure S3. The flowchart of the cell-based high throughput screening for inhibitors of Akt plasma membrane translocation.



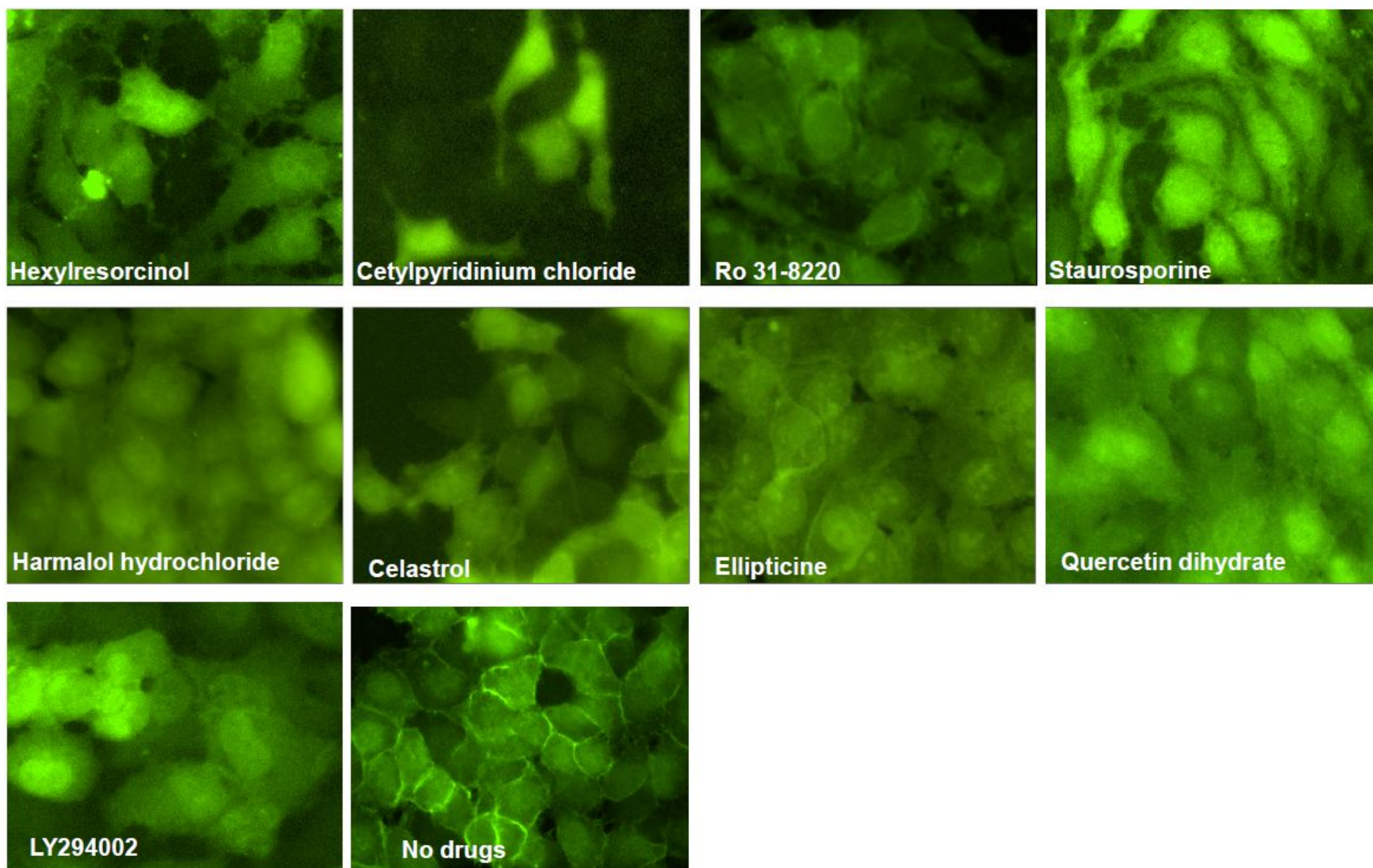
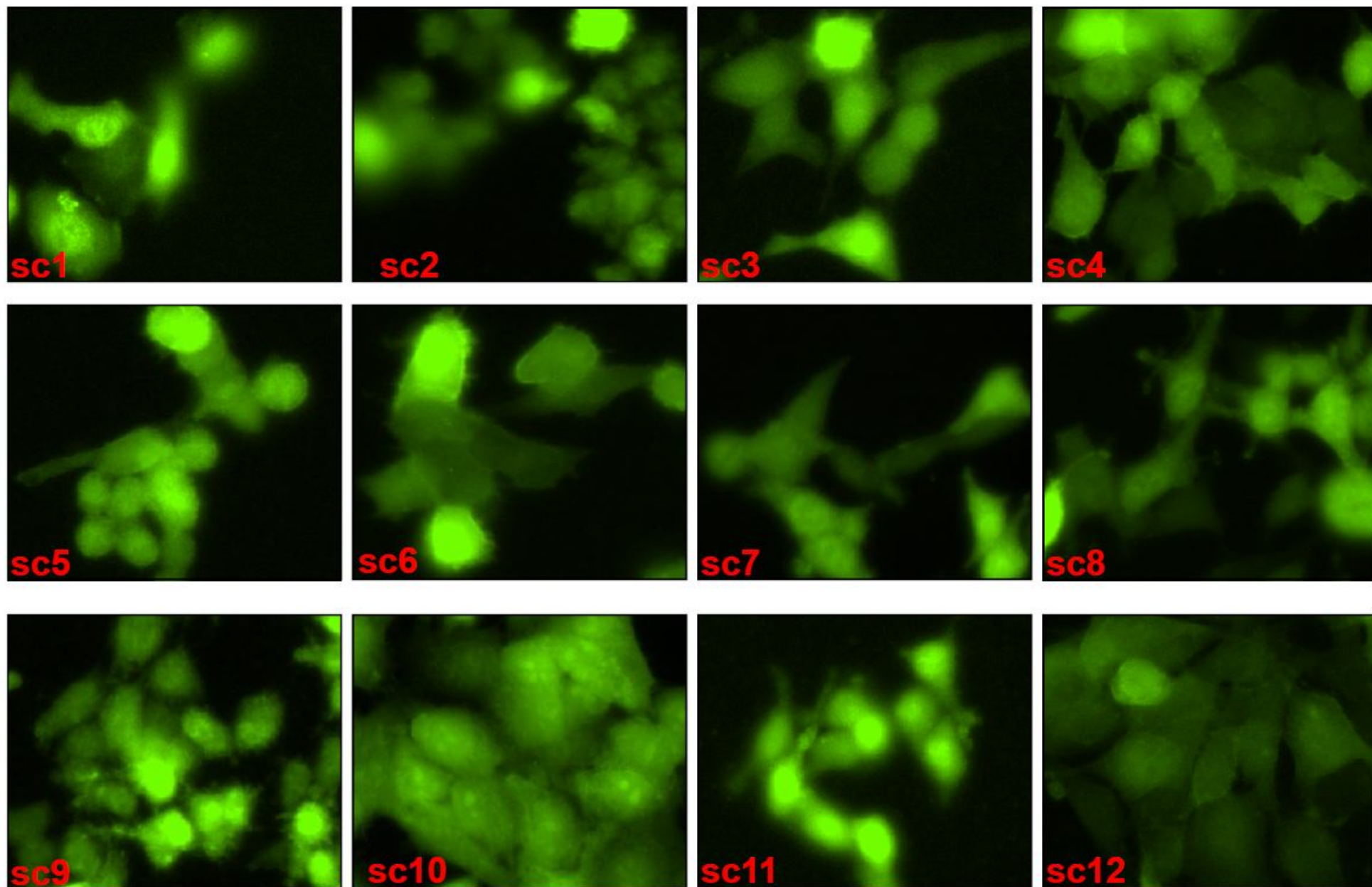
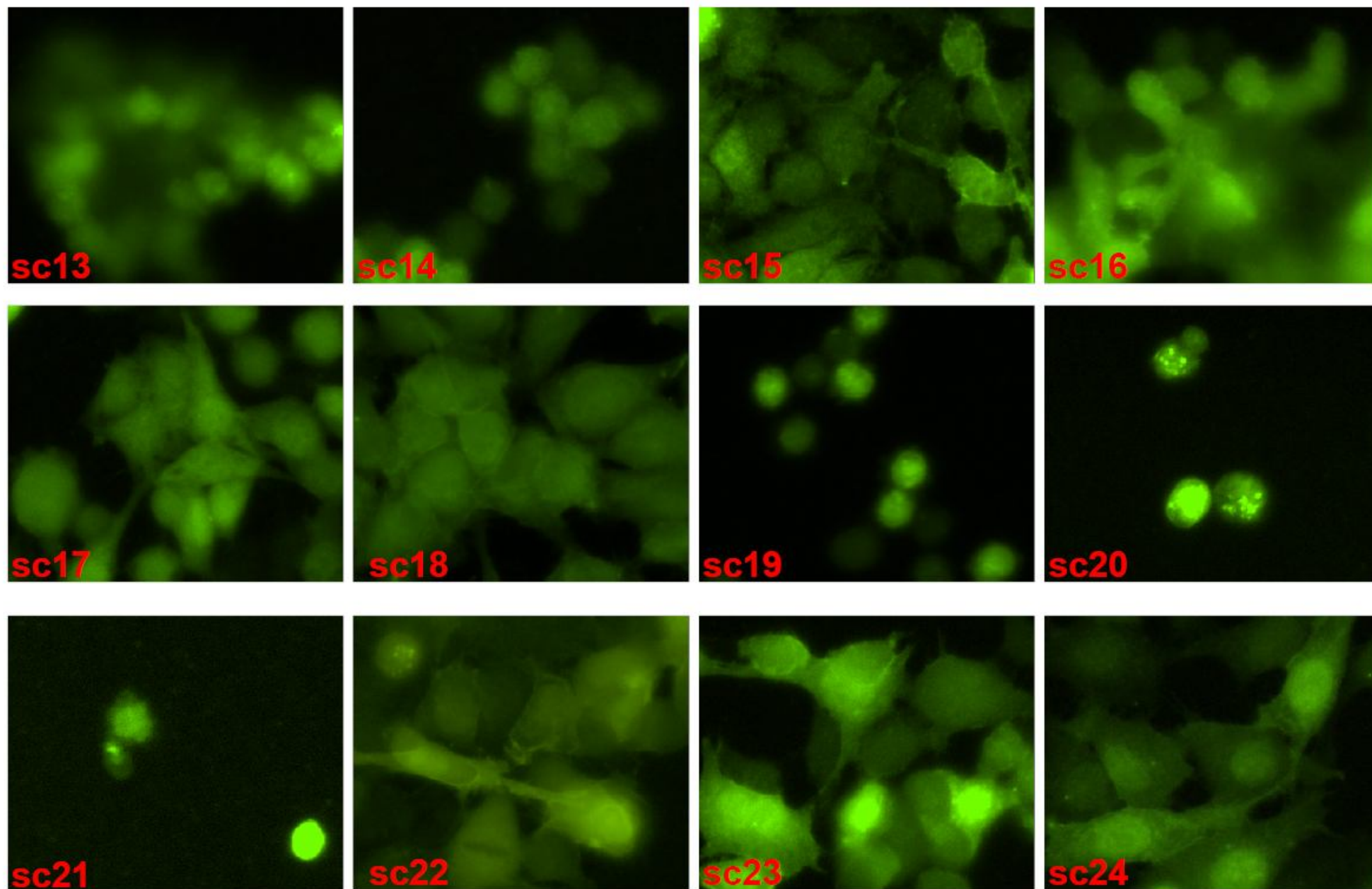
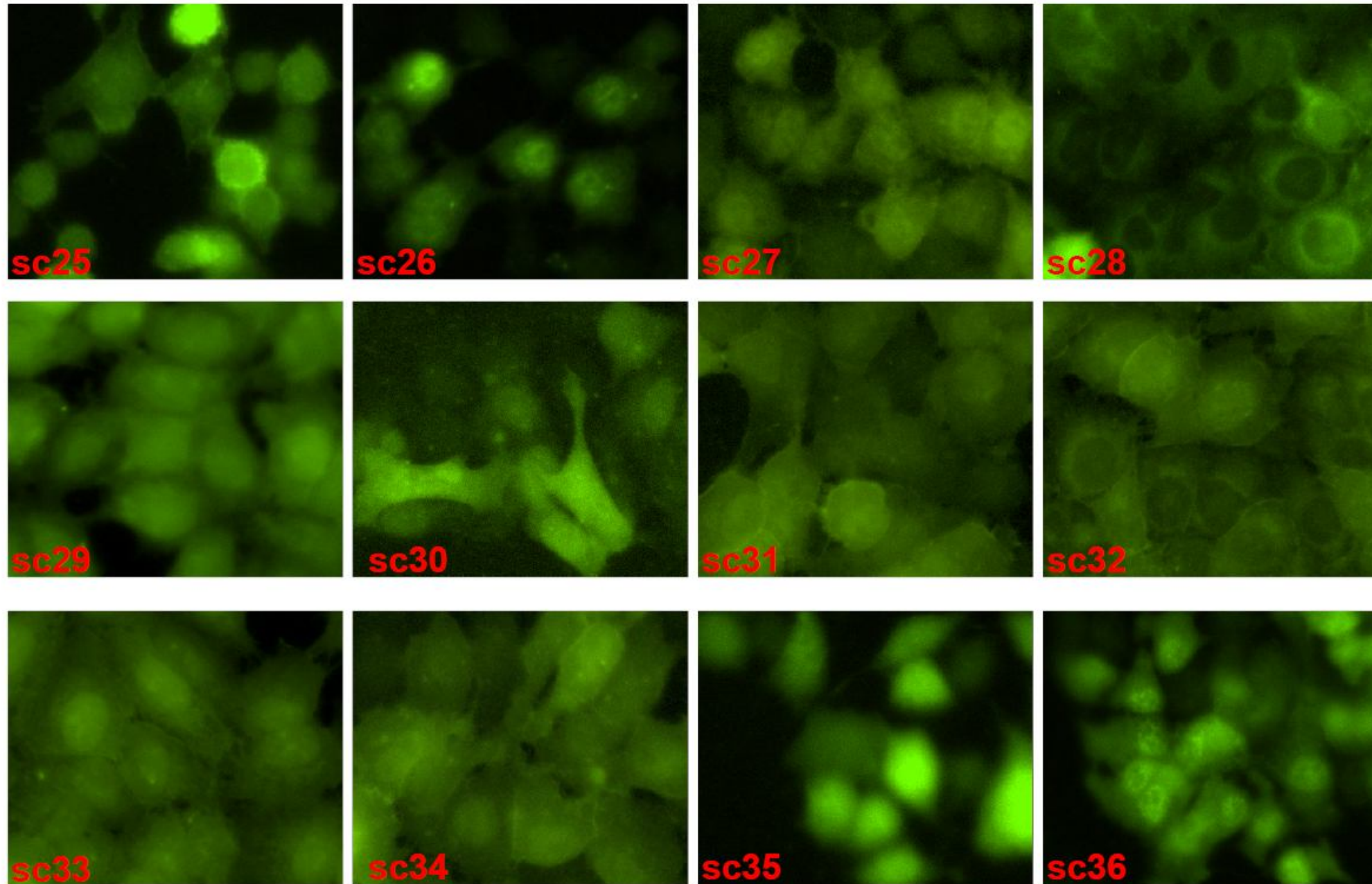
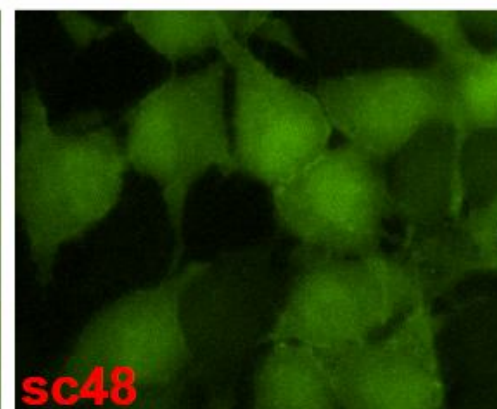
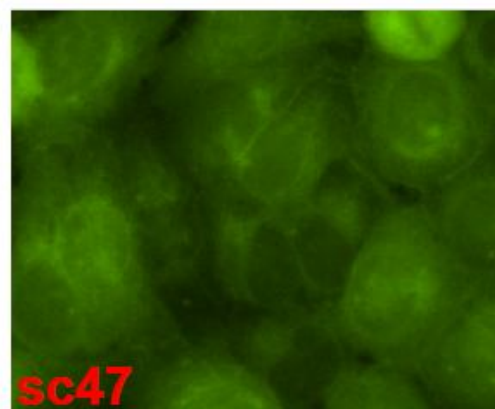
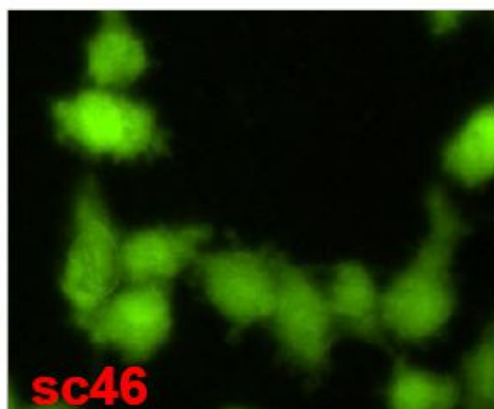
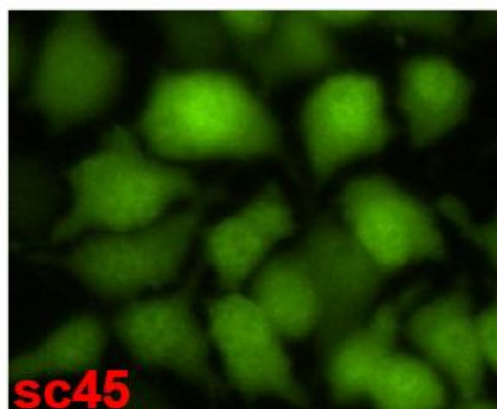
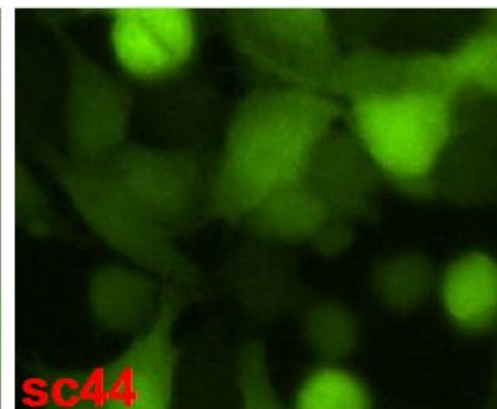
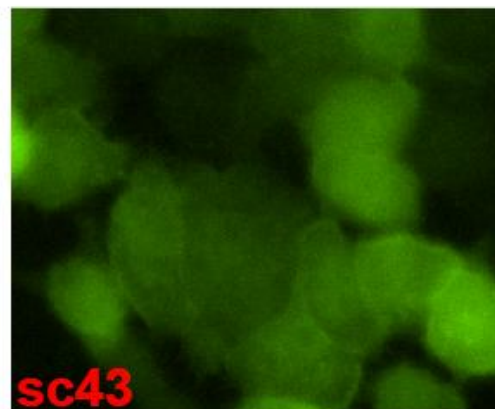
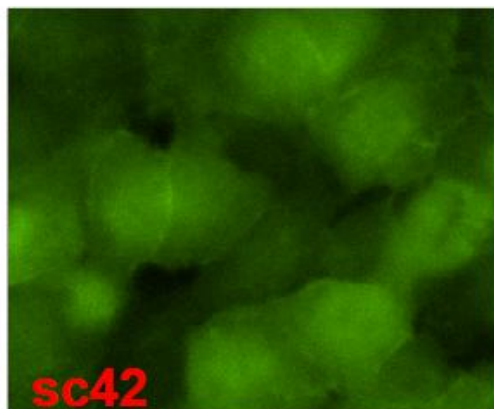
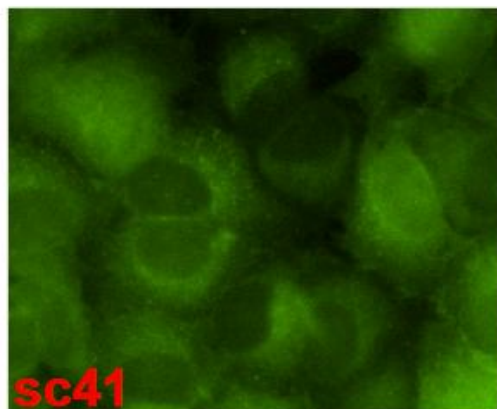
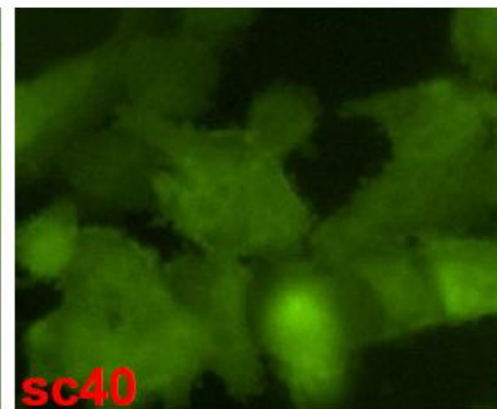
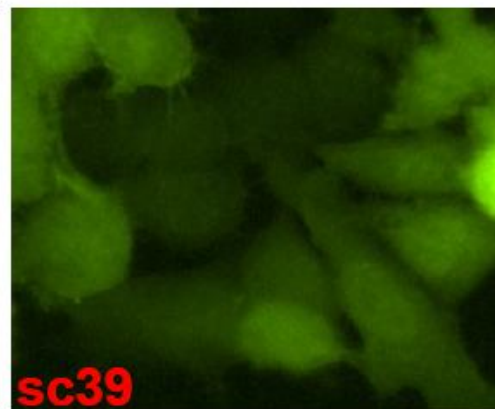
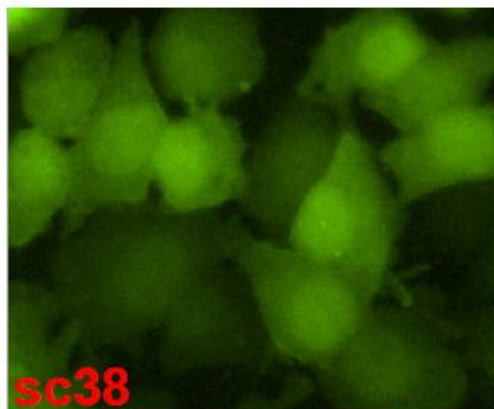
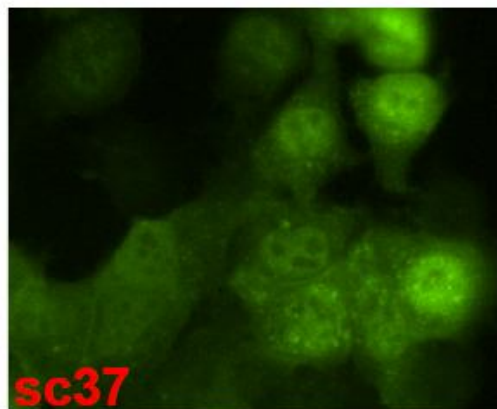


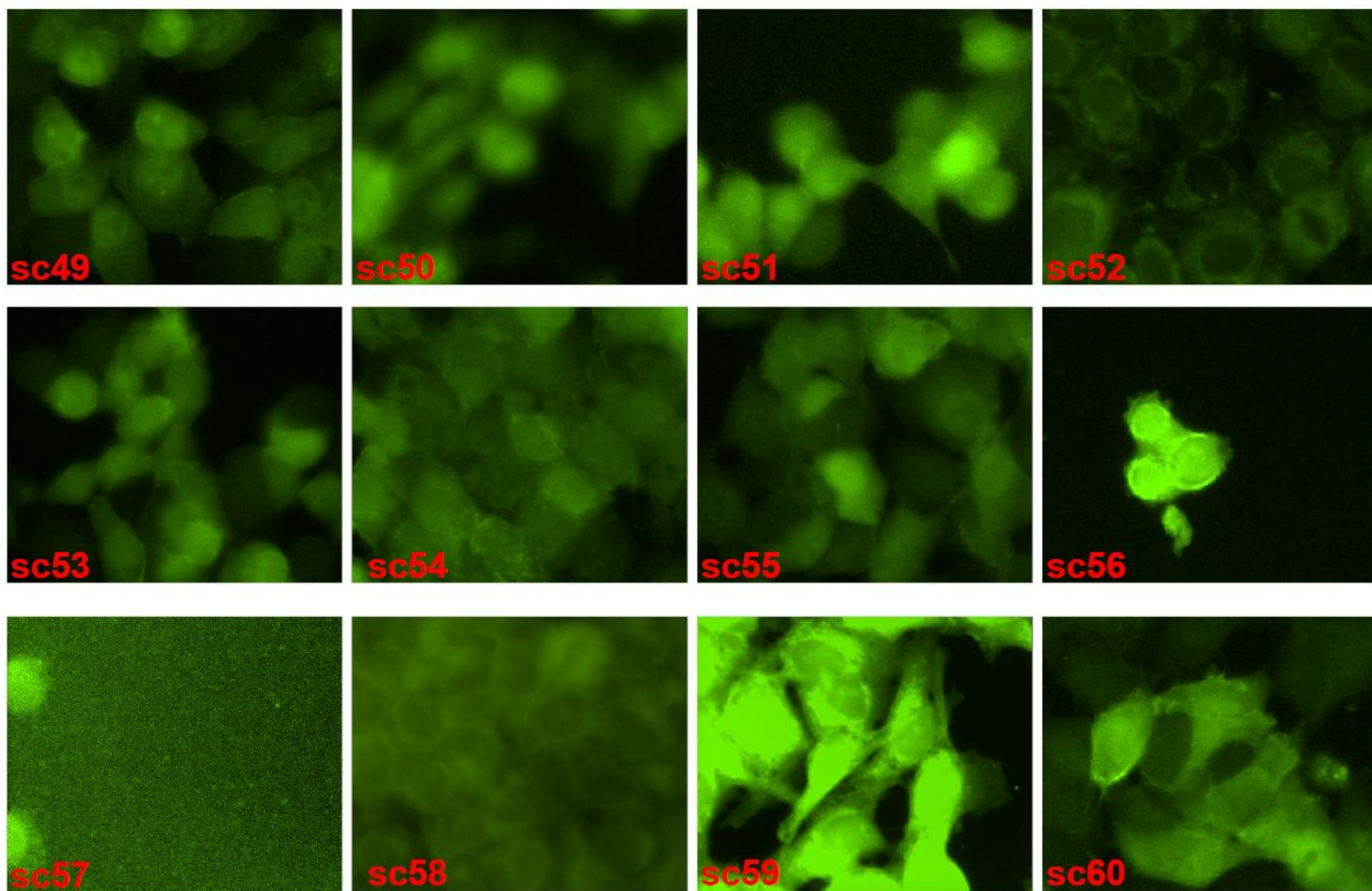
Figure S4. Pilot screening identified 21 bioactive compounds that inhibit IGF1-induced Akt-PH-EGFP membrane translocation.

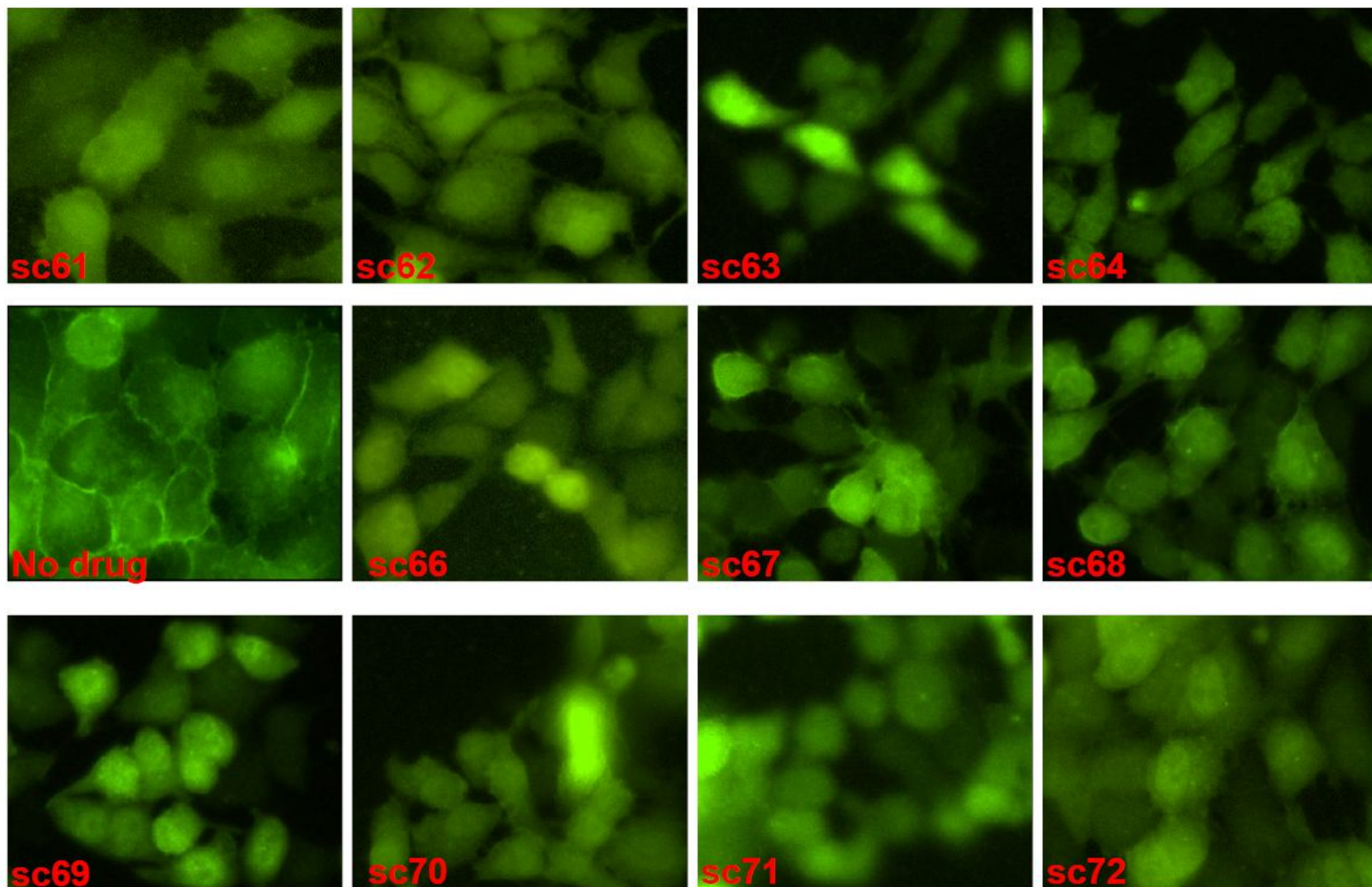


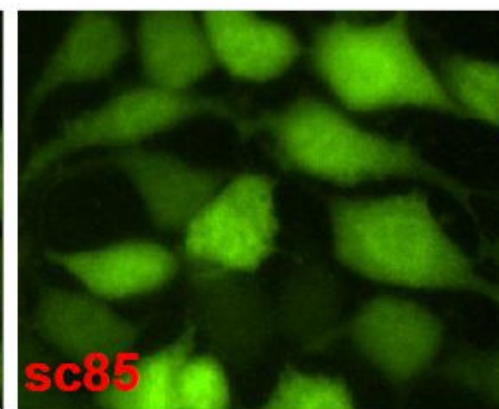
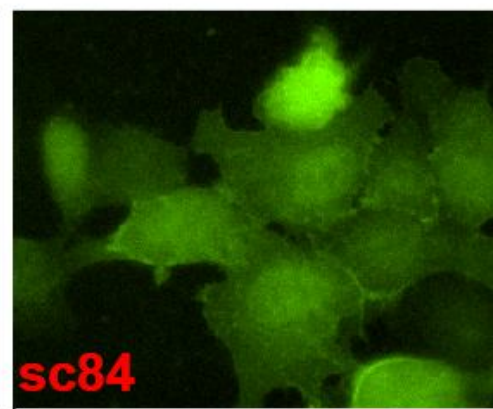
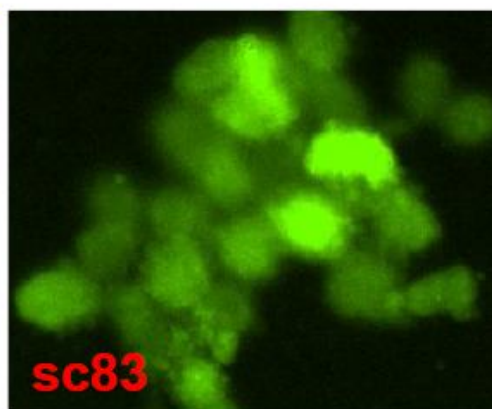
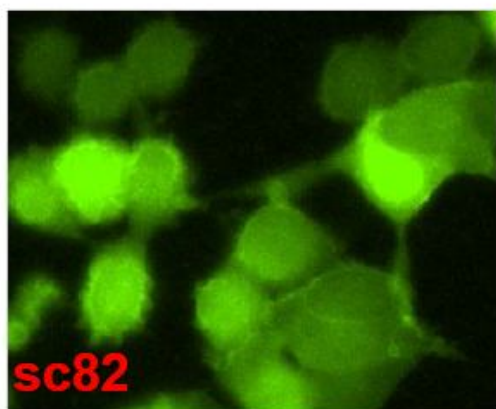
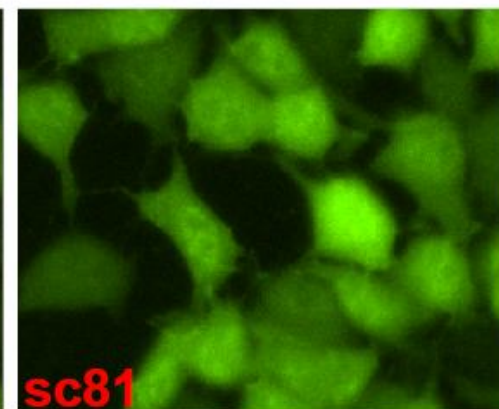
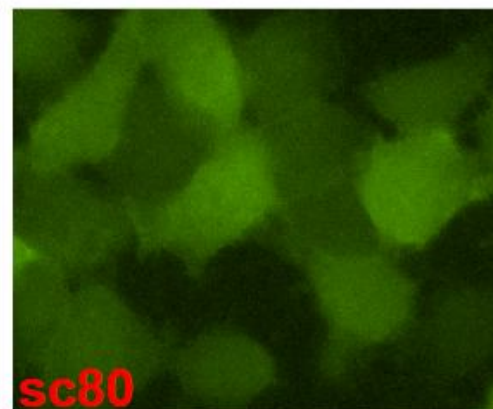
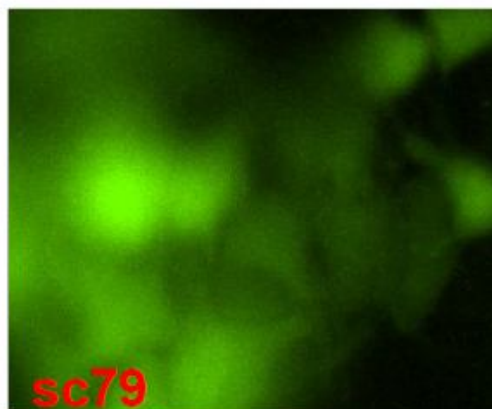
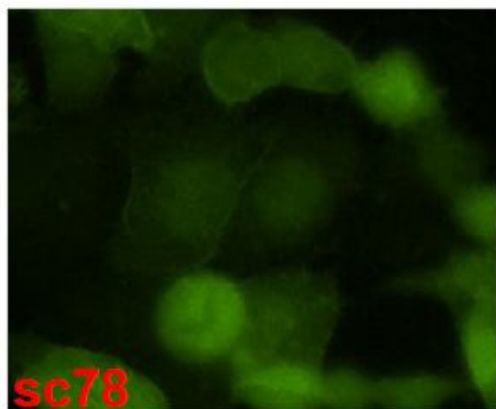
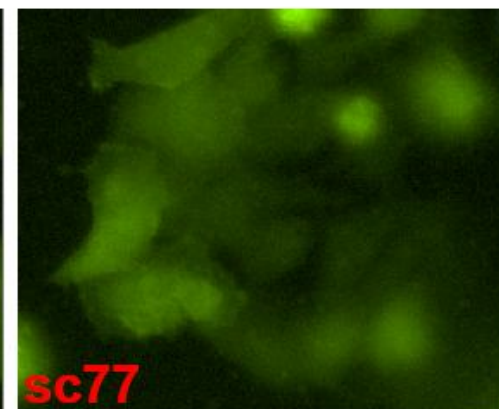
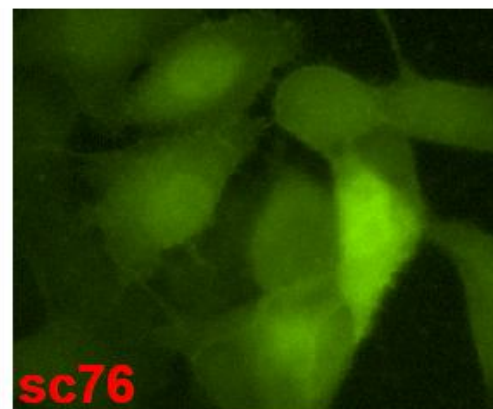
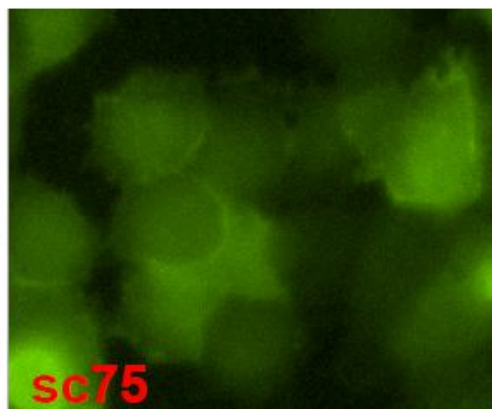
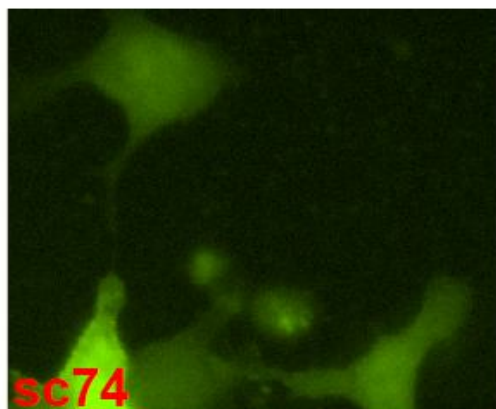


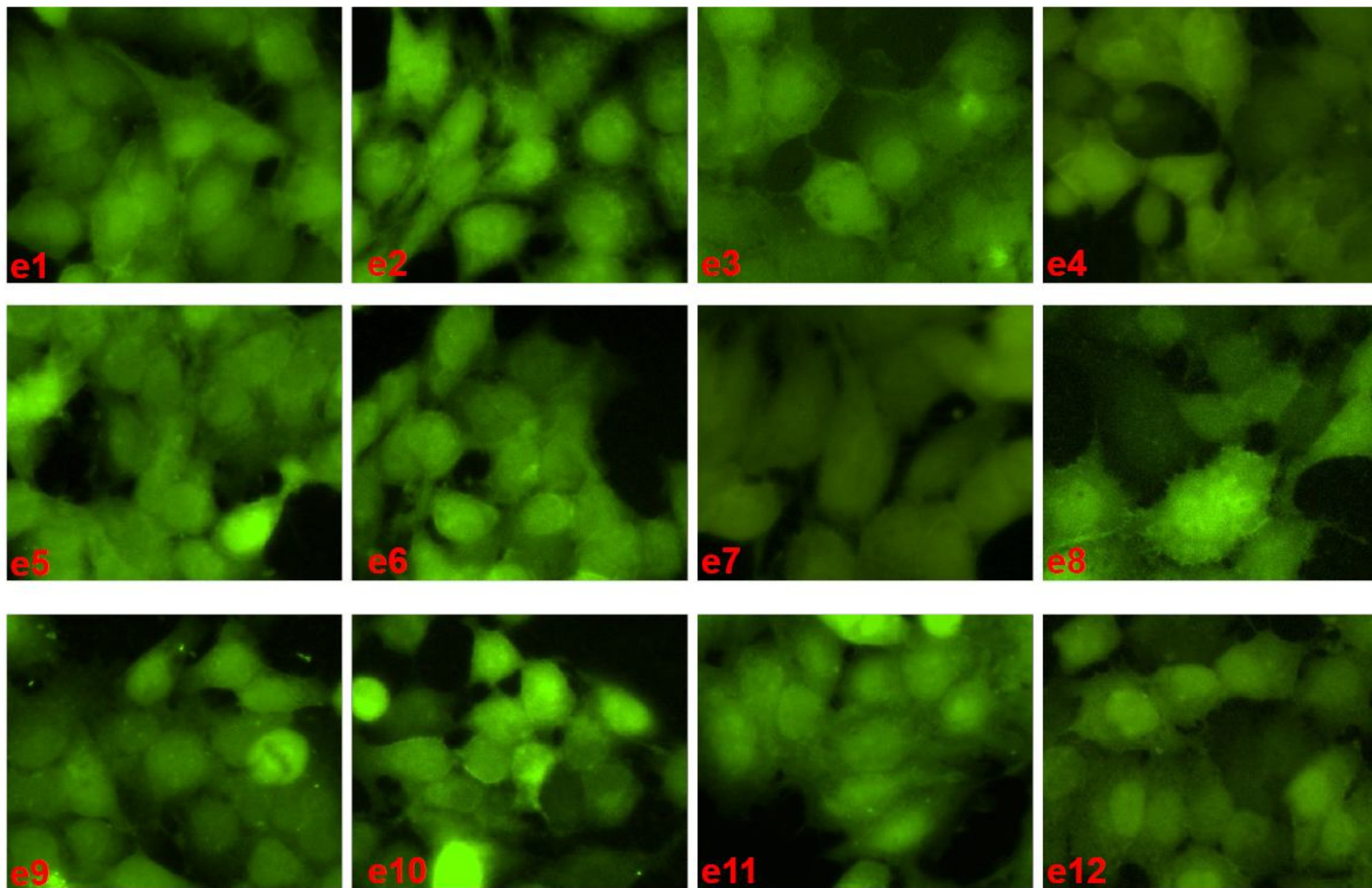


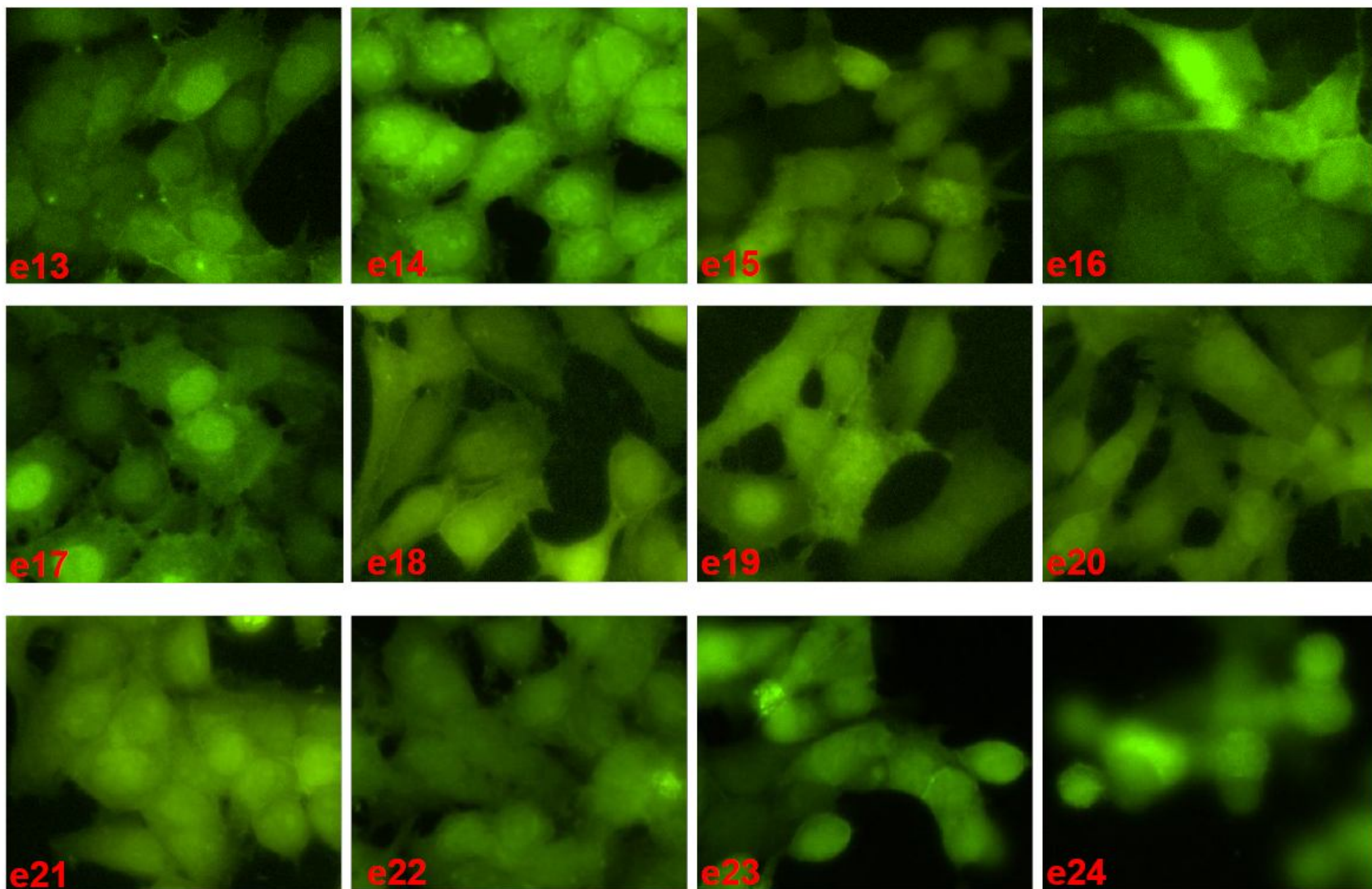


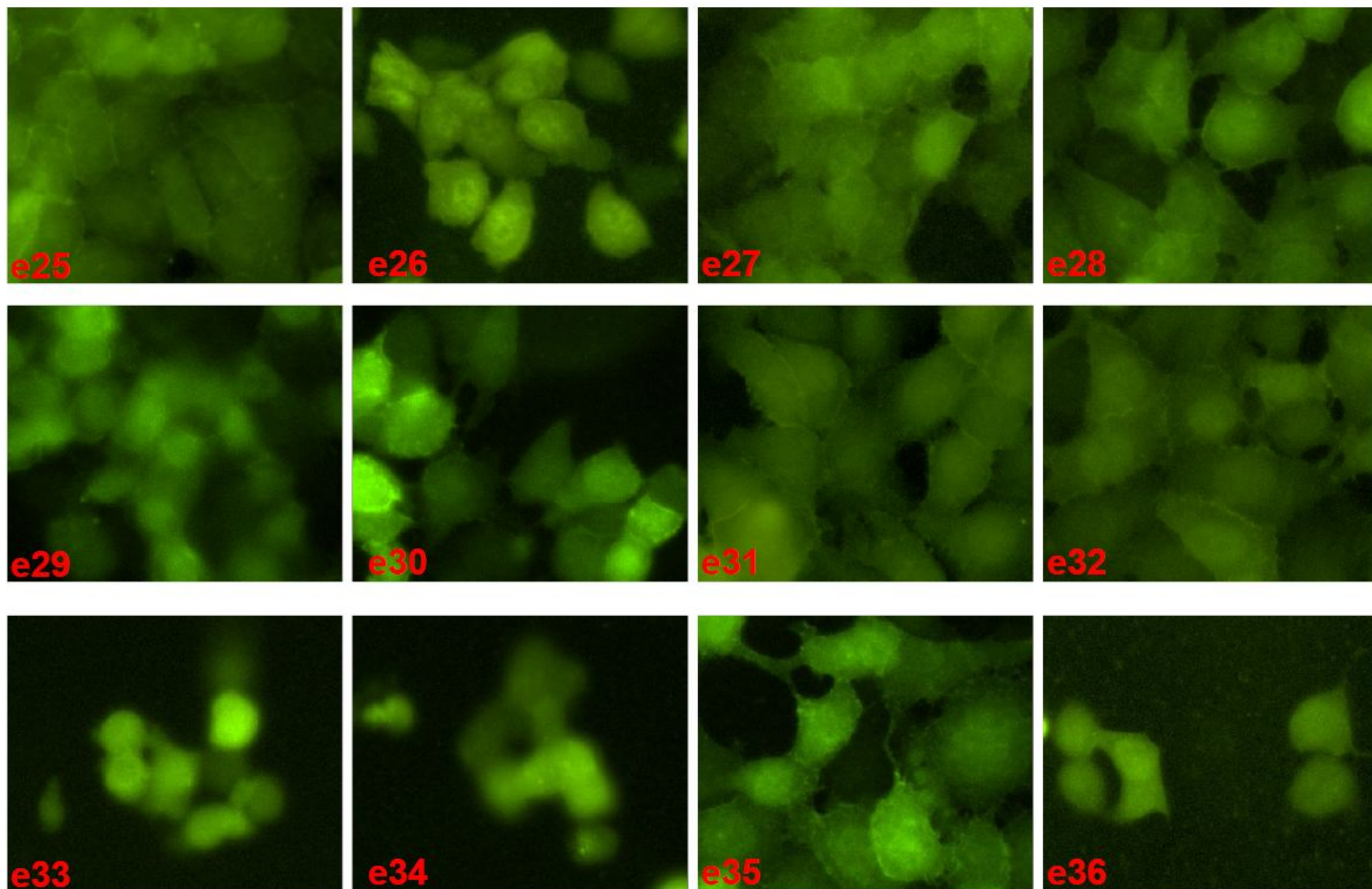












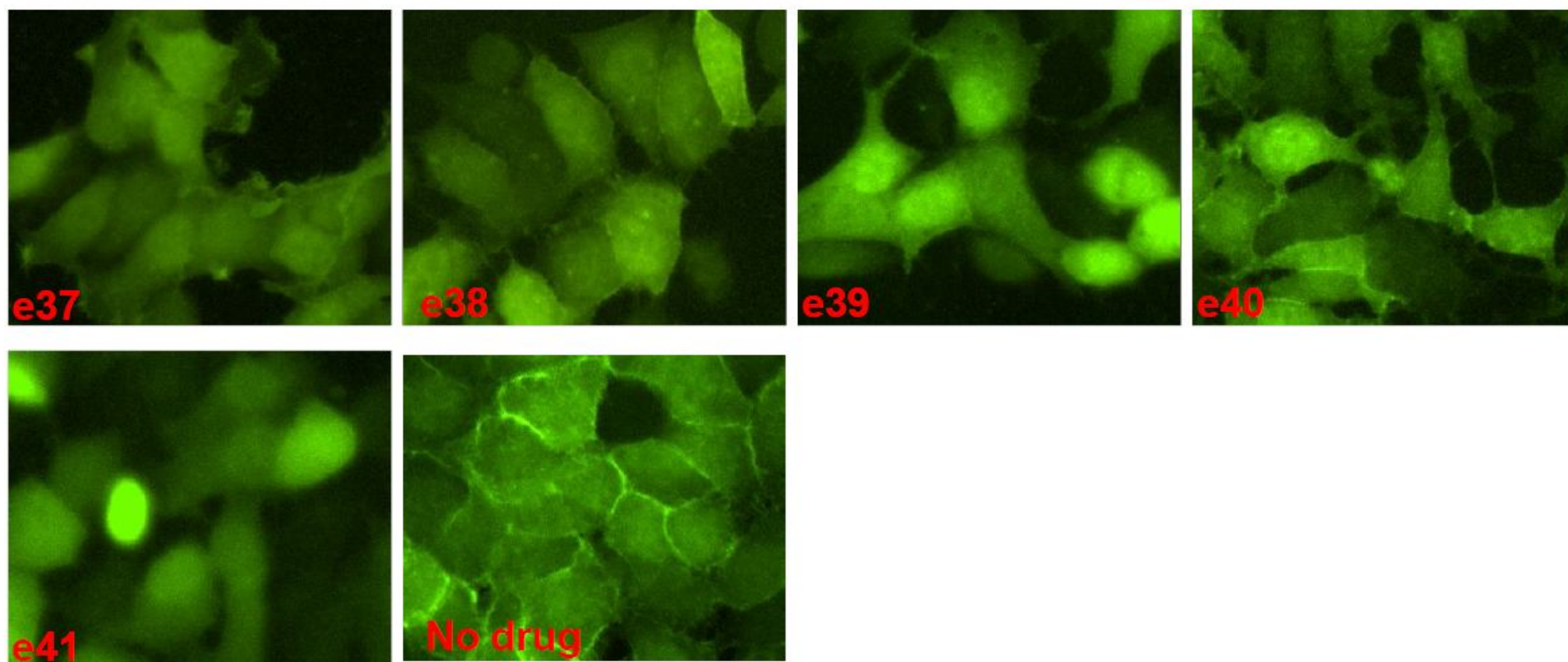
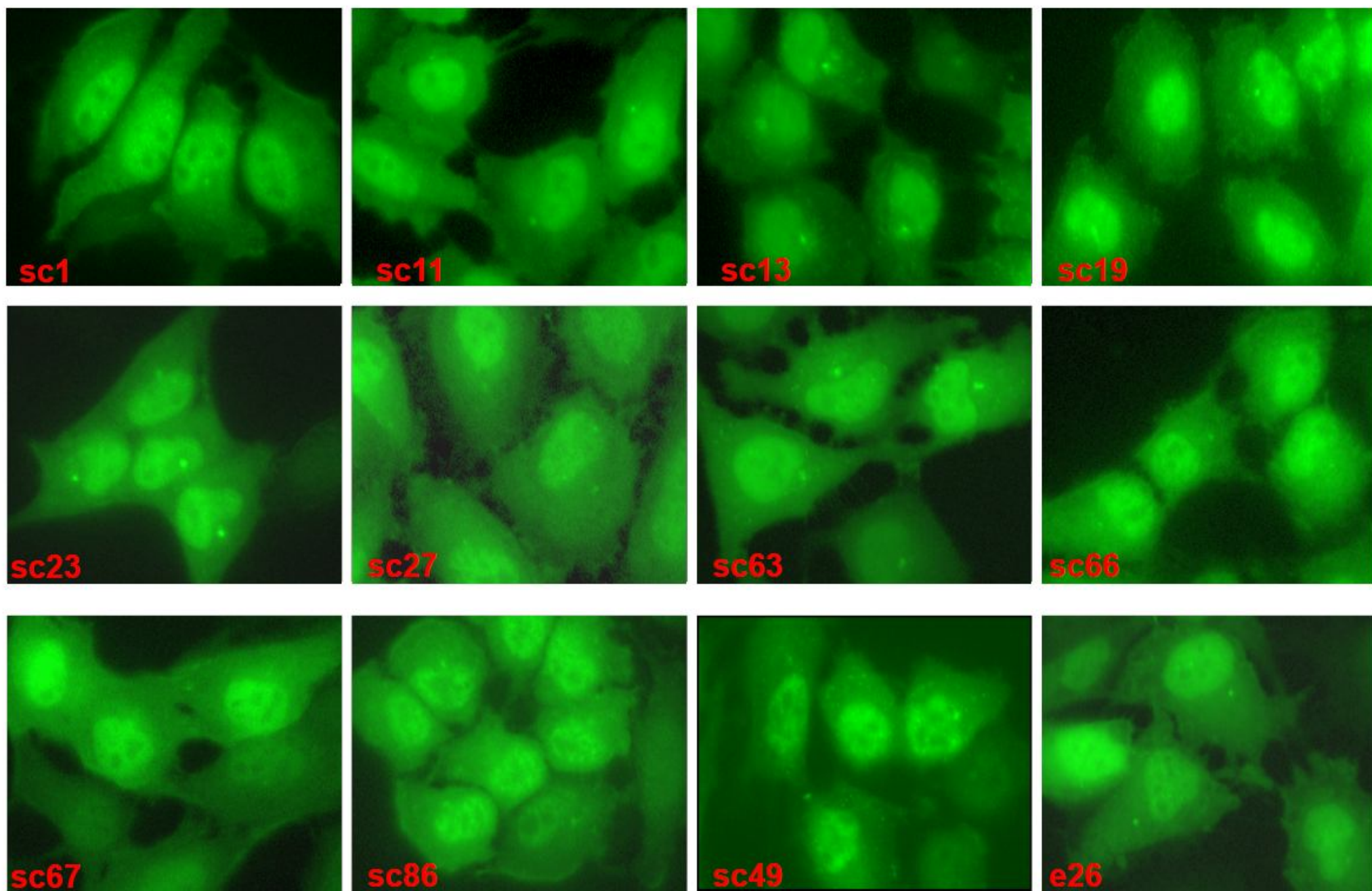
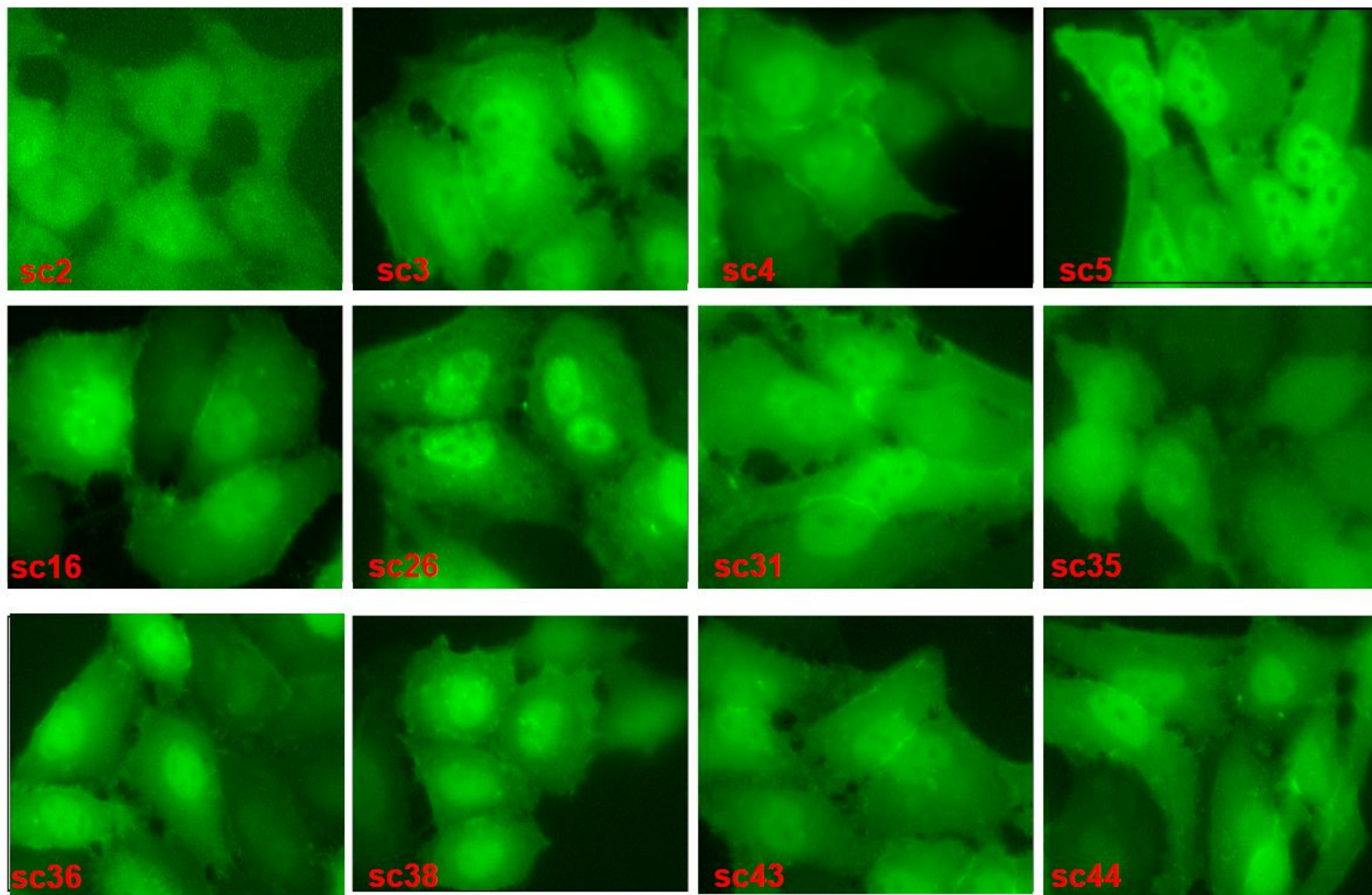
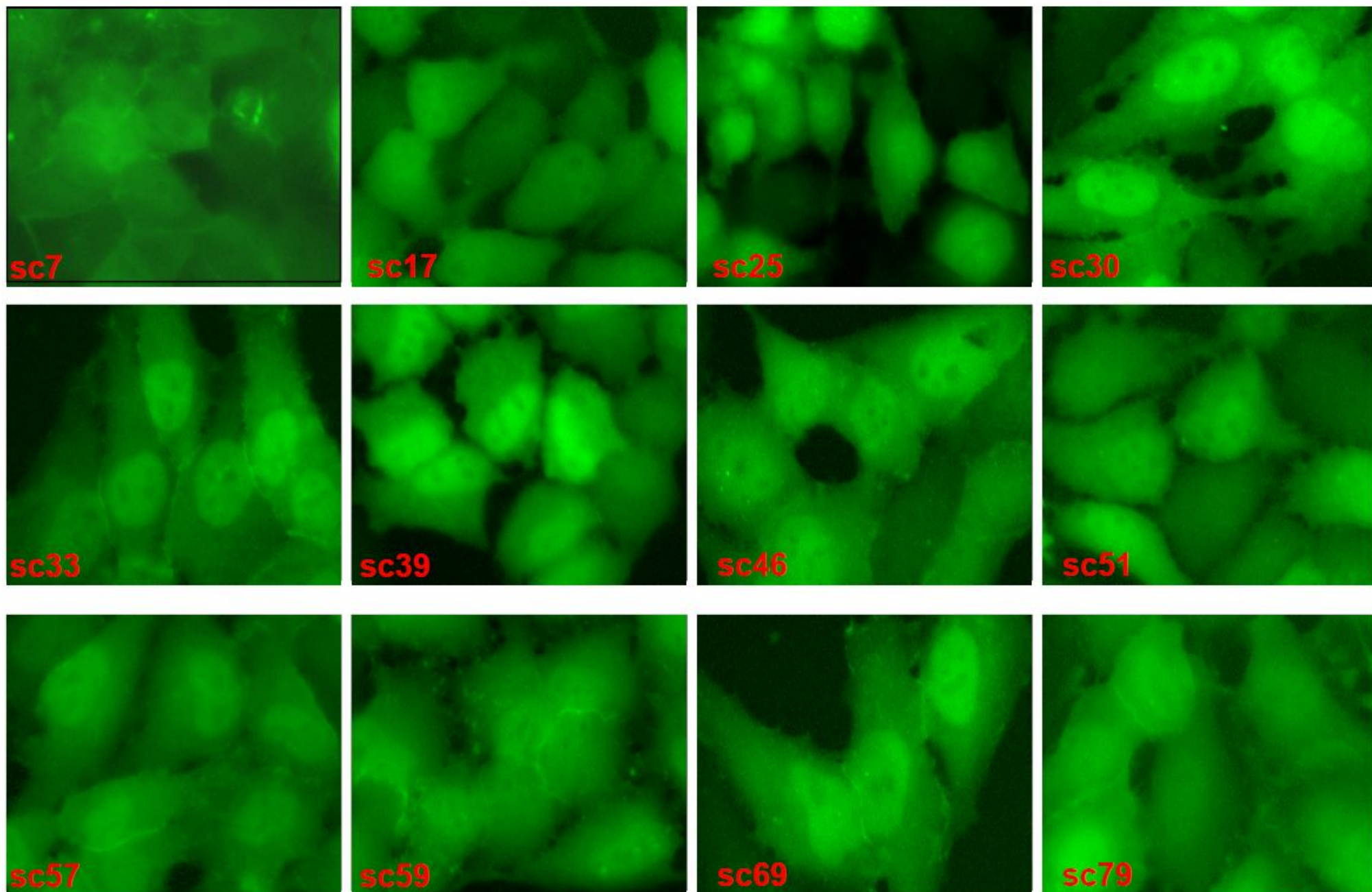
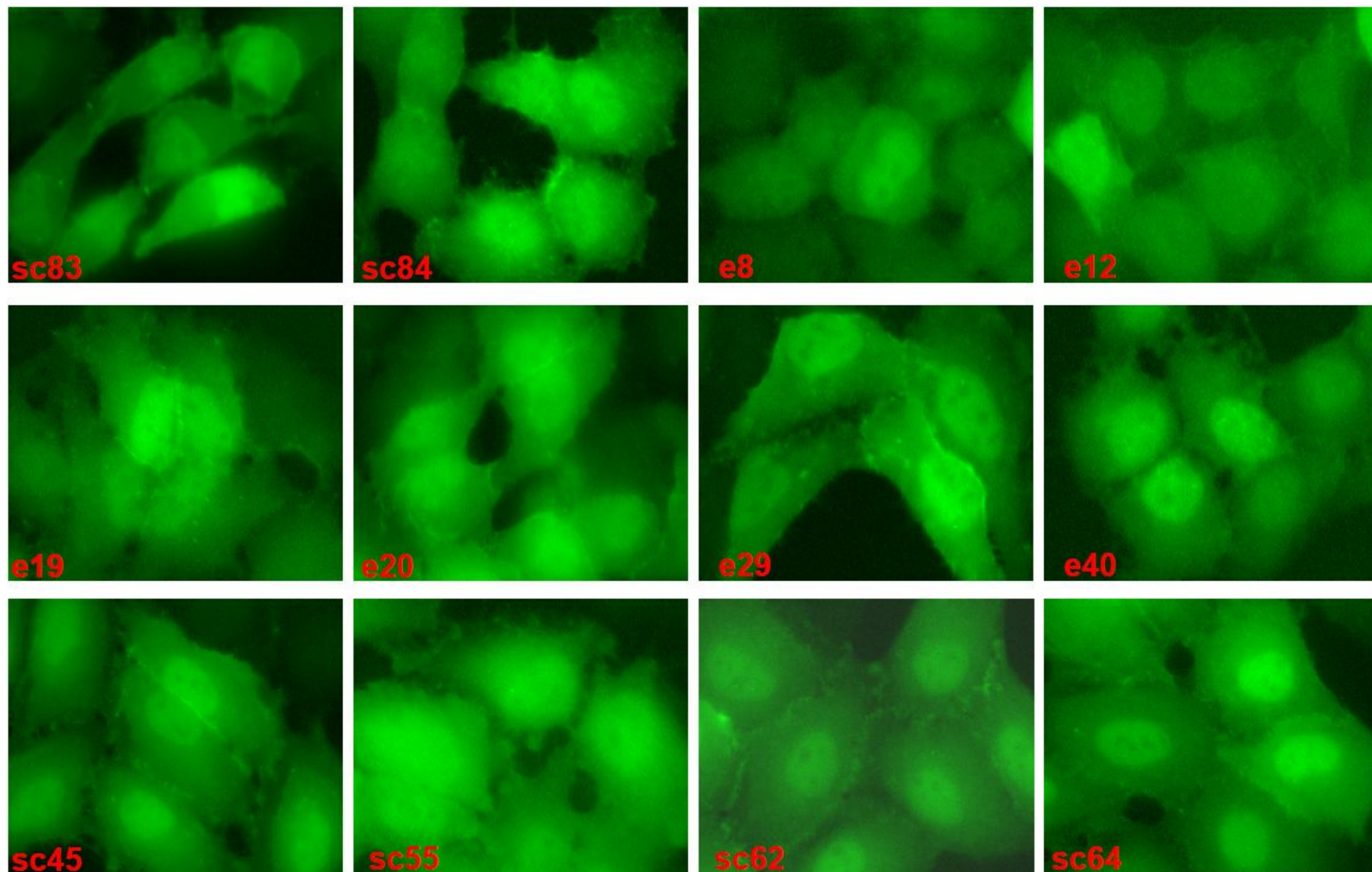


Figure S5. Positive hit compounds identified from the primary and secondary high throughput screenings.









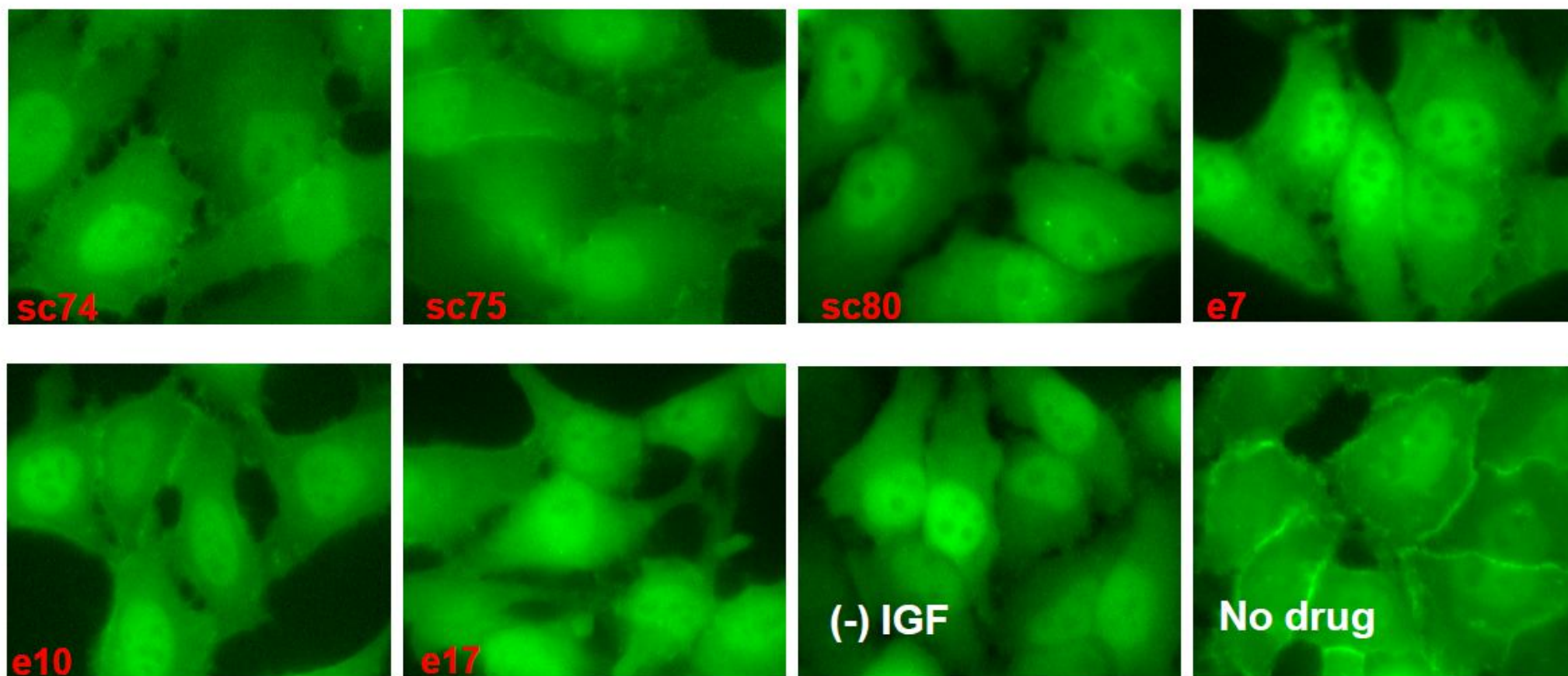
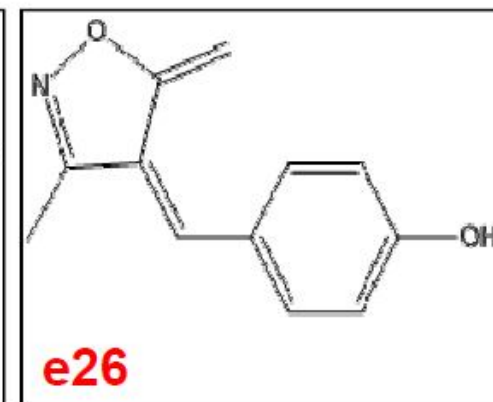
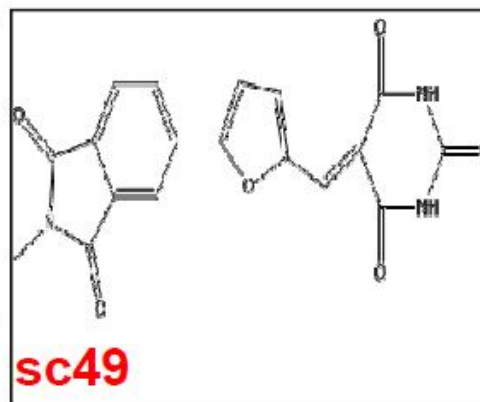
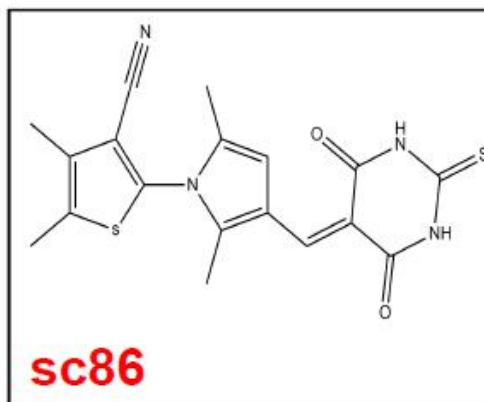
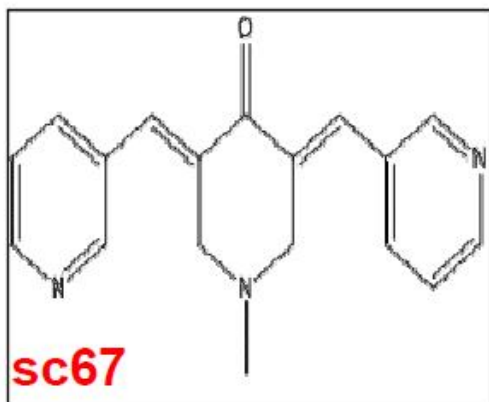
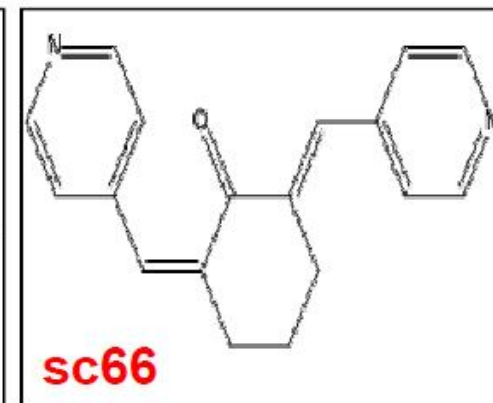
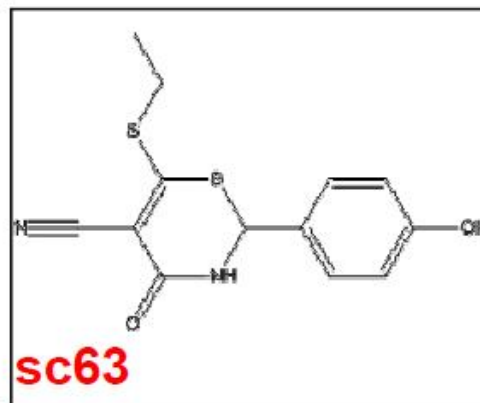
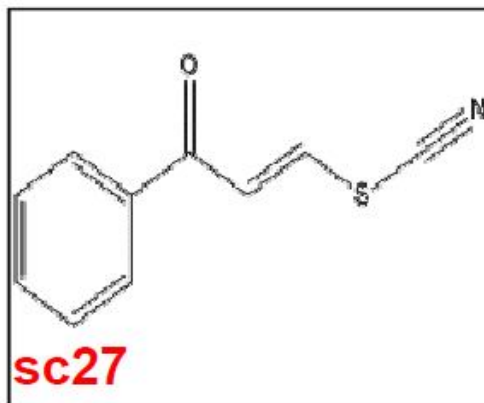
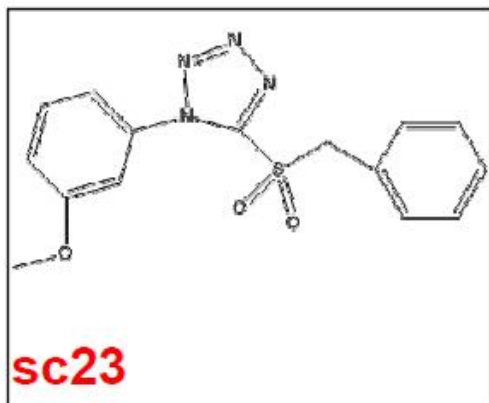
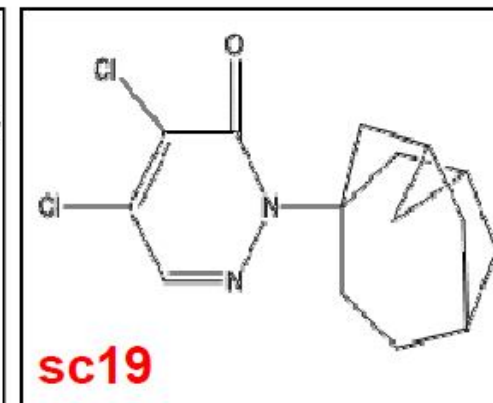
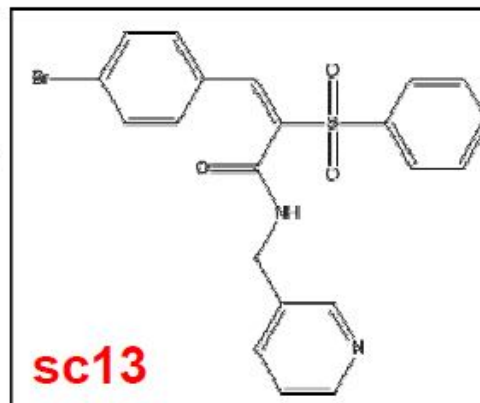
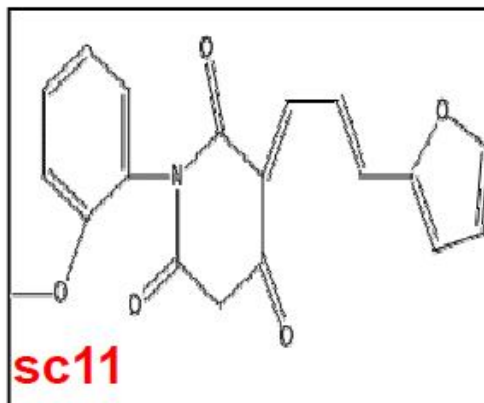
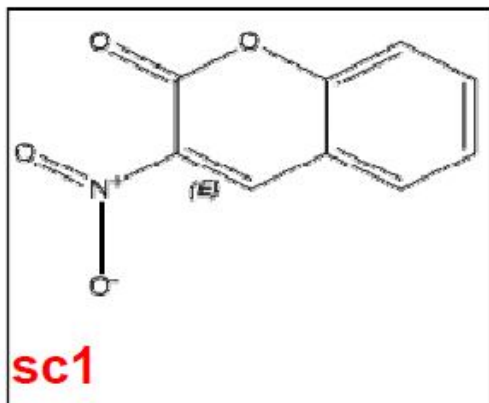
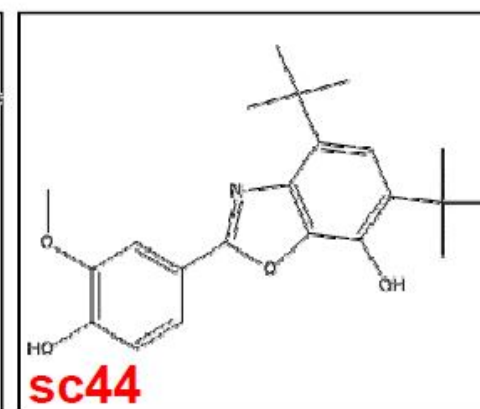
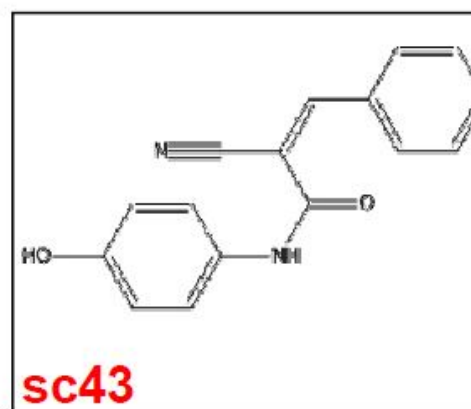
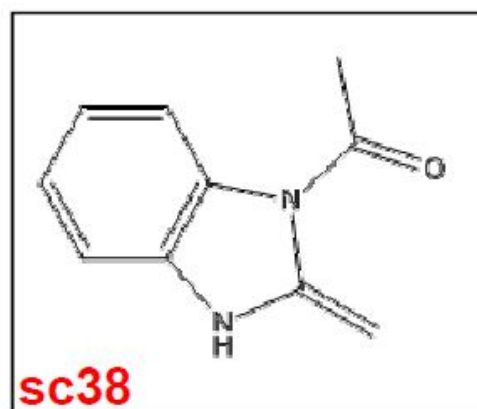
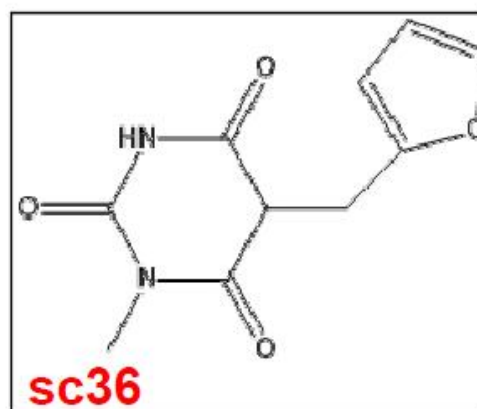
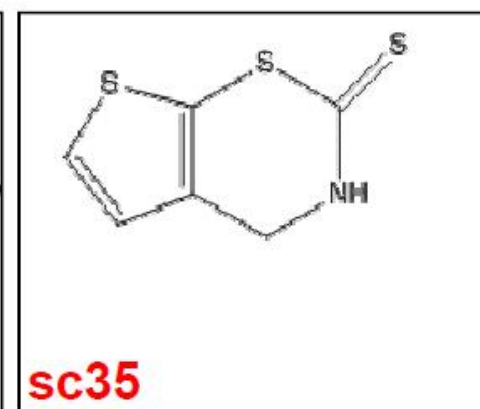
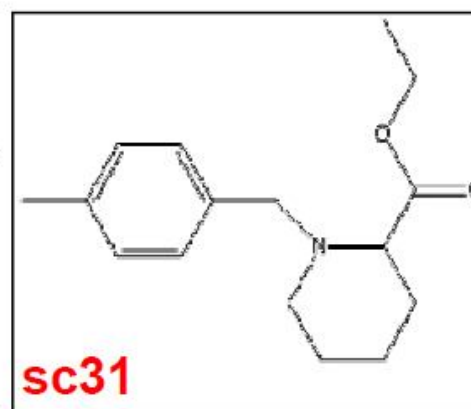
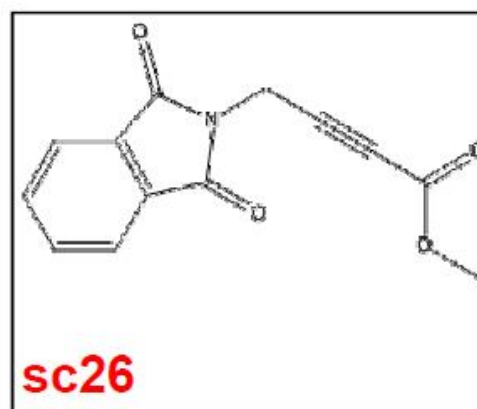
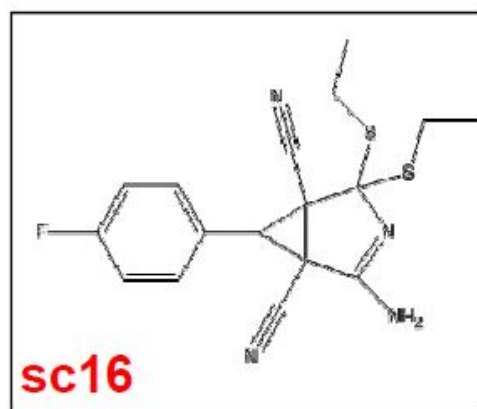
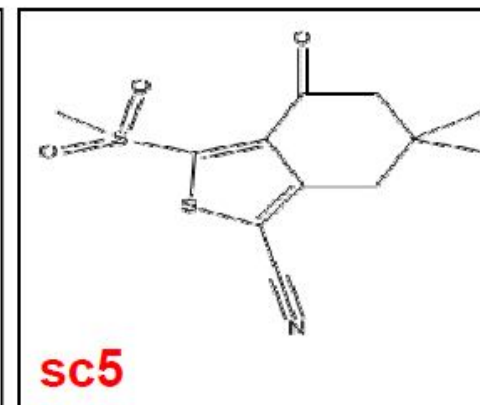
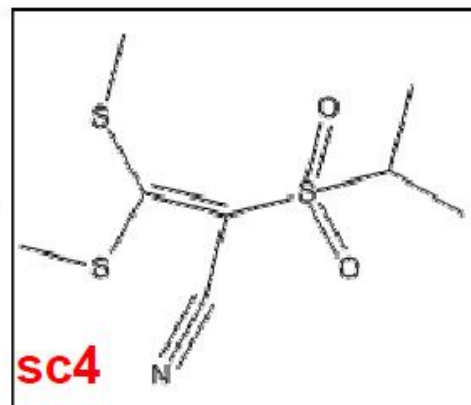
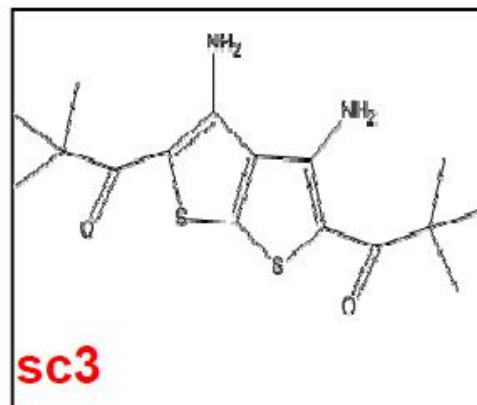
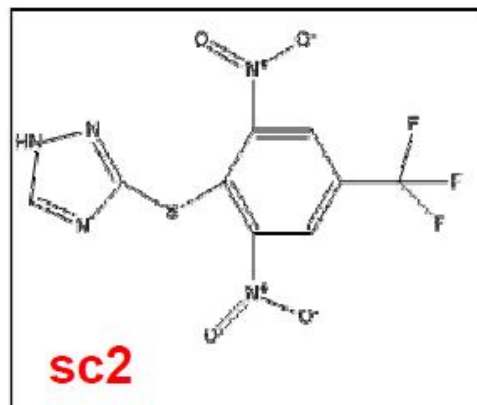
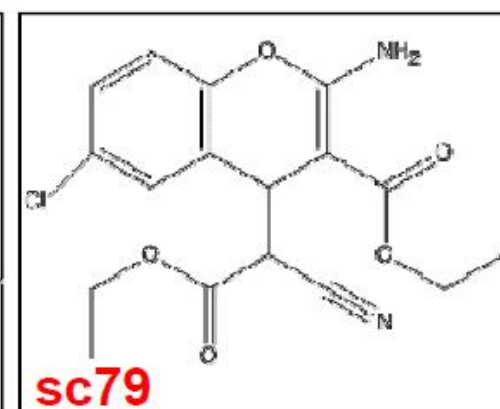
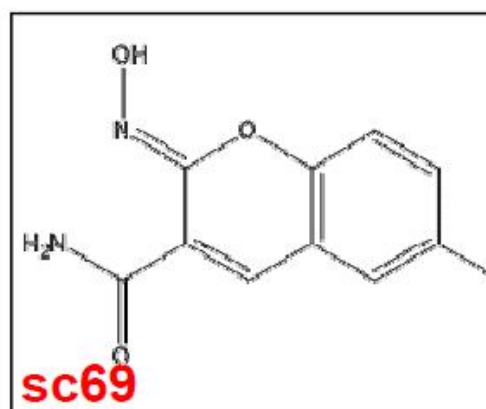
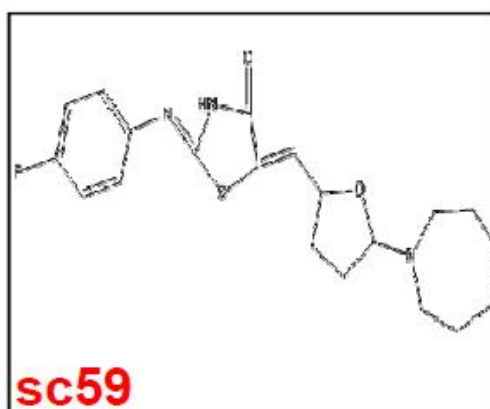
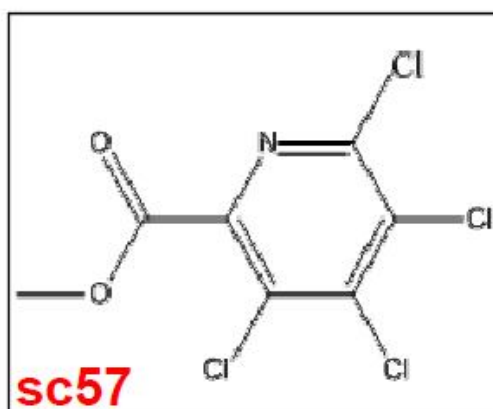
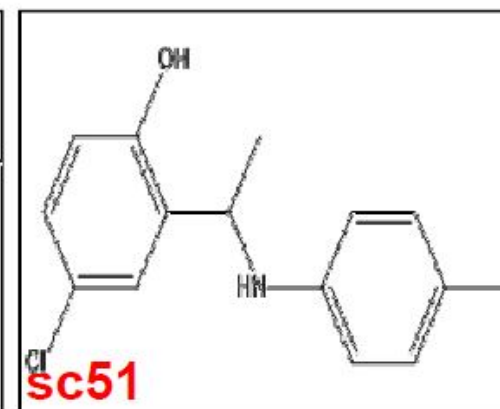
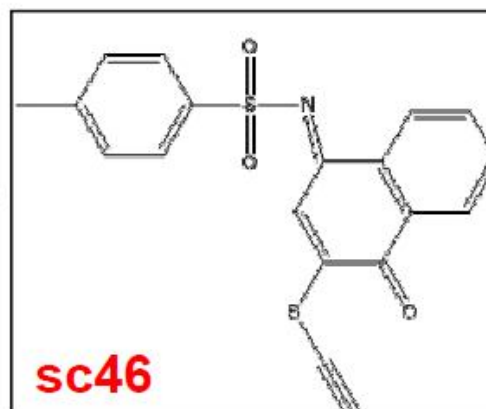
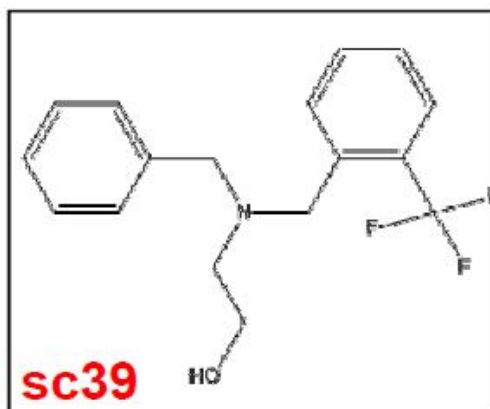
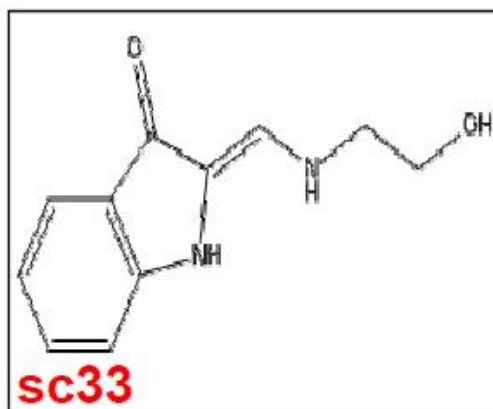
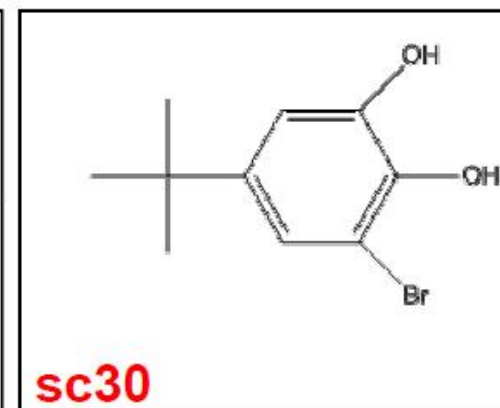
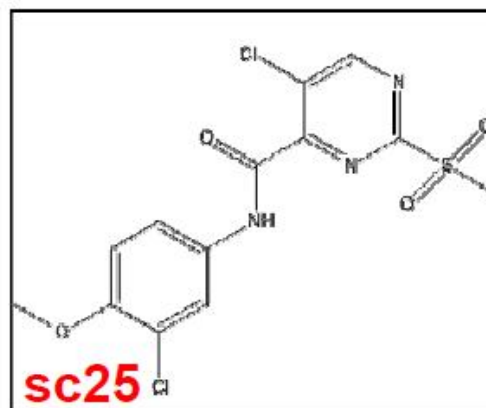
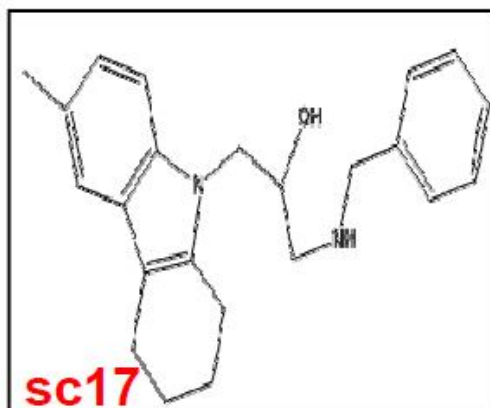
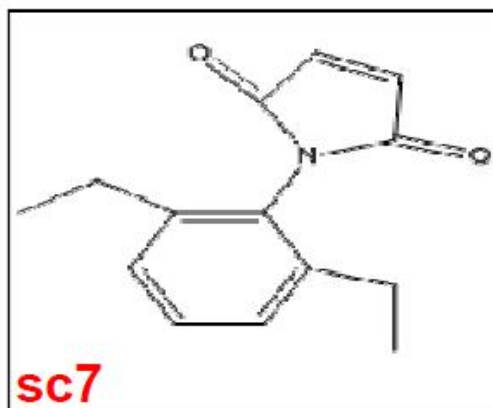
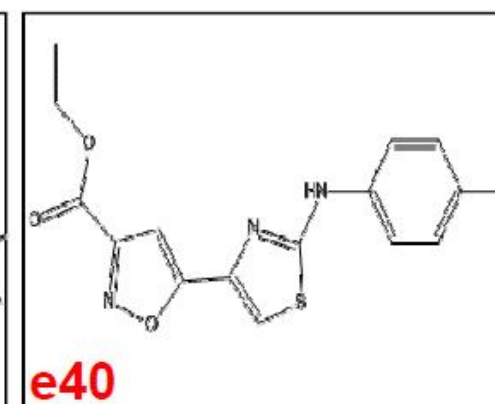
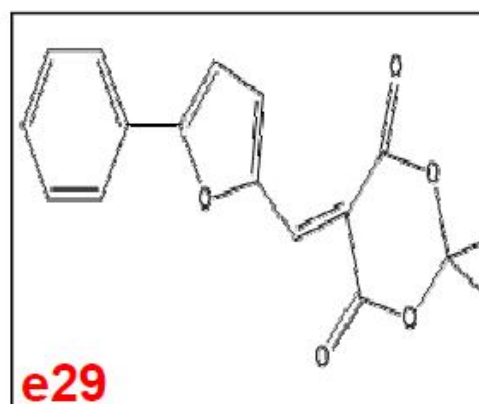
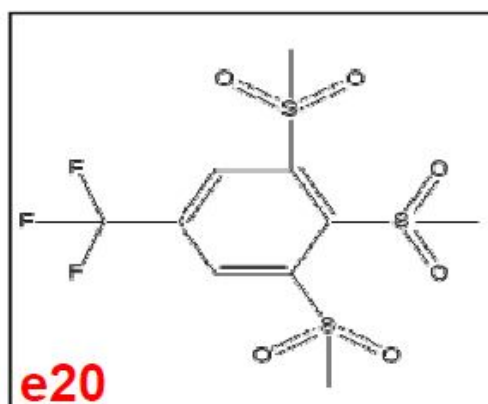
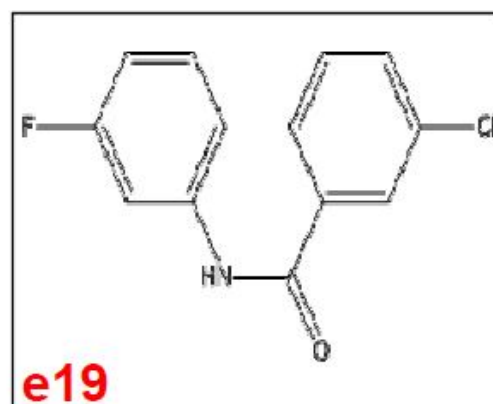
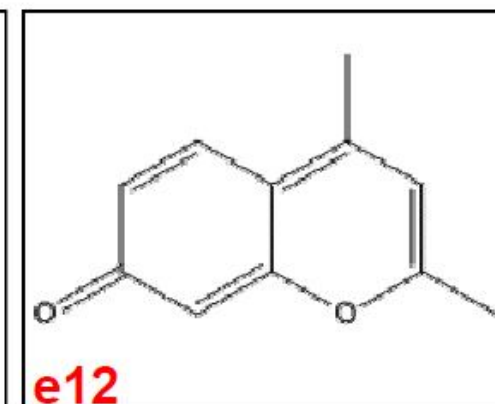
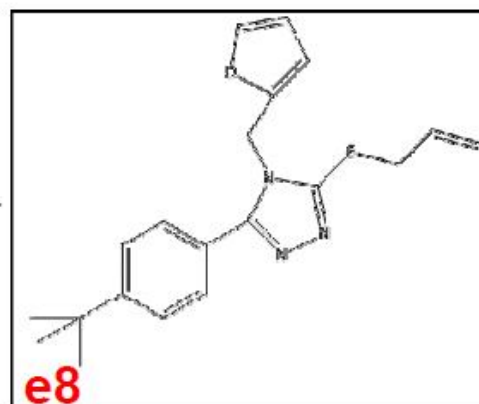
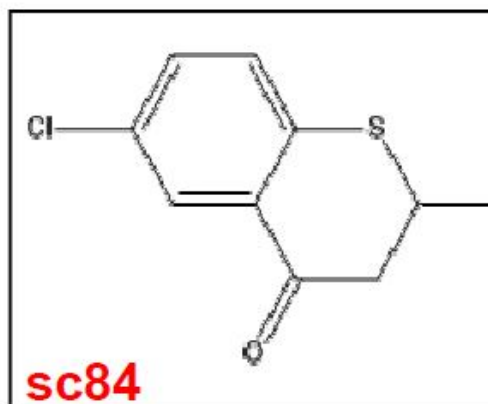
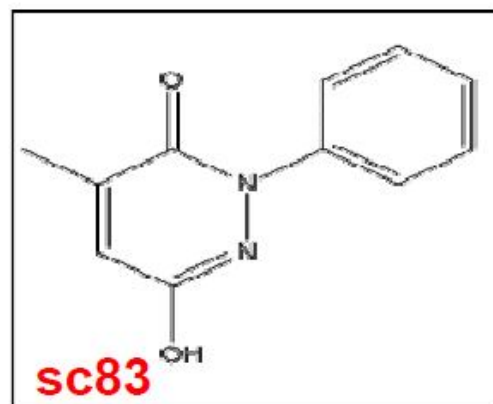


Figure S6. Positive hit compounds confirmed by live cell imaging.









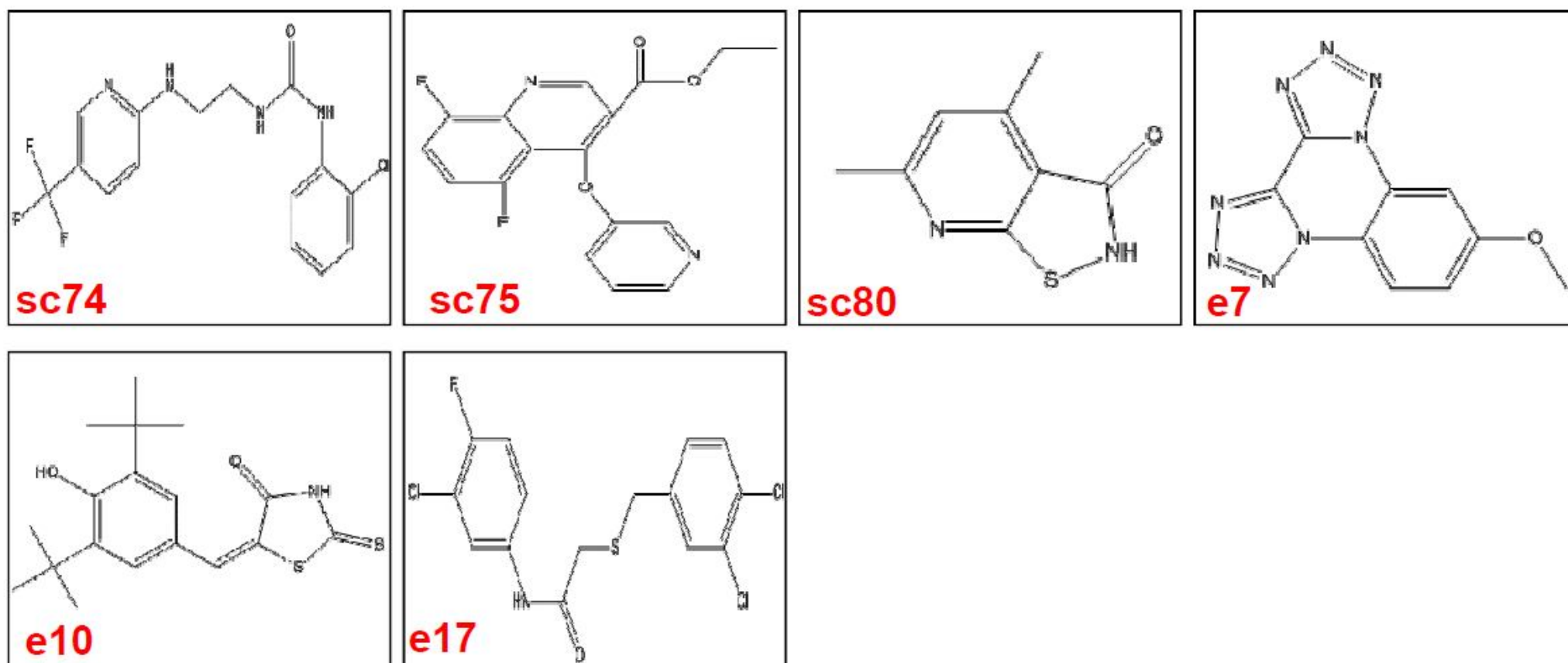
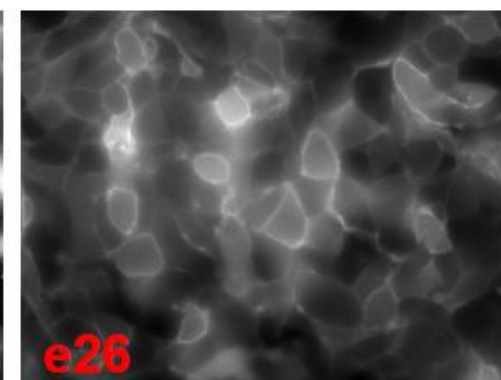
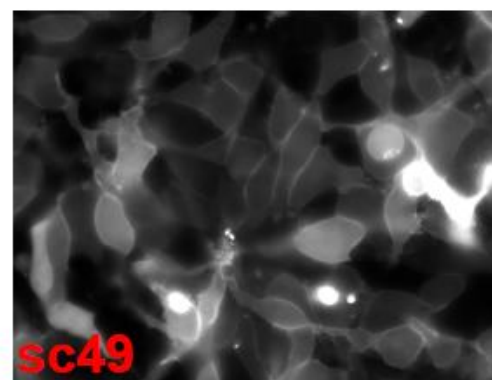
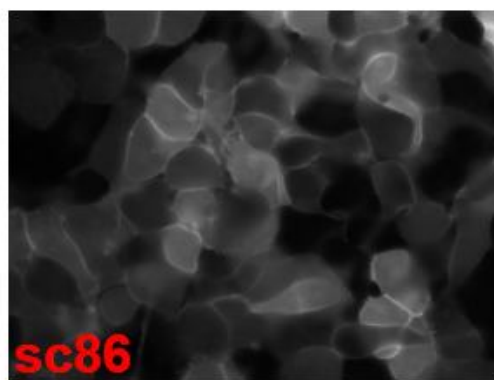
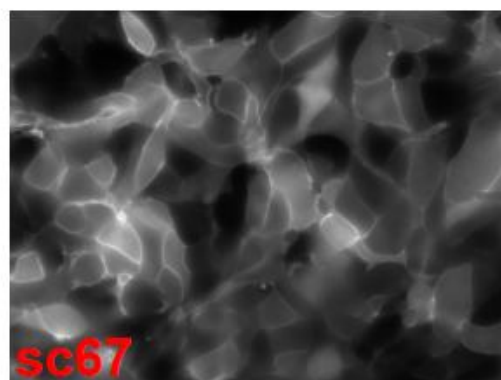
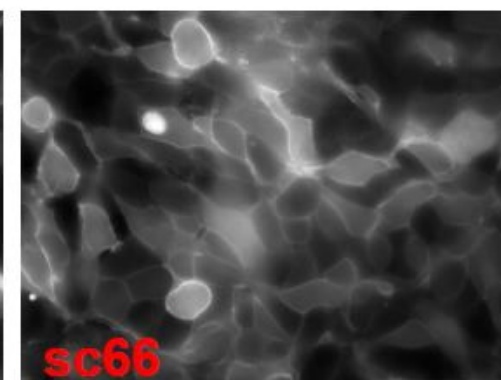
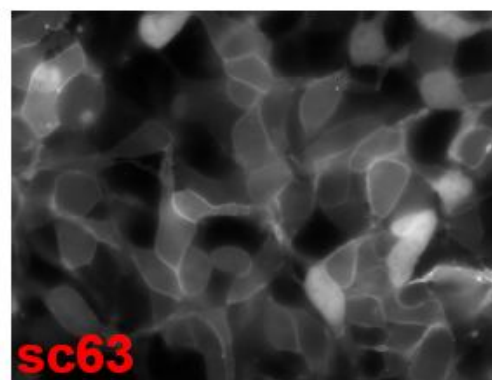
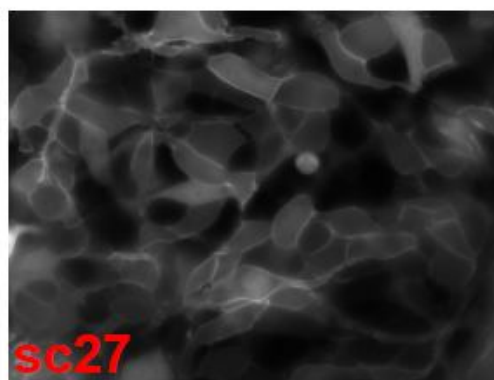
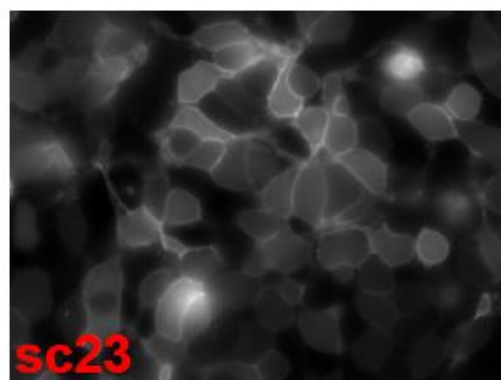
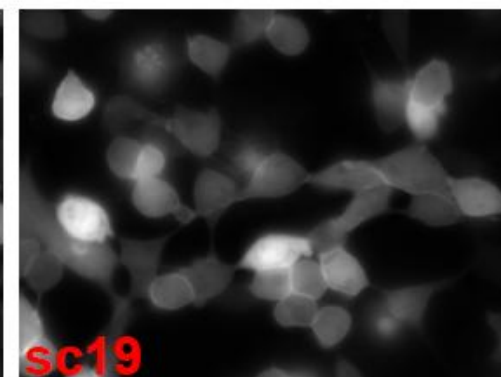
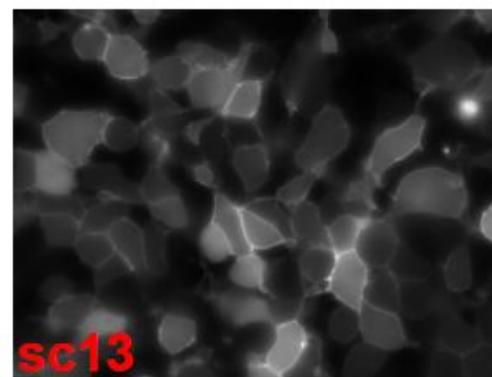
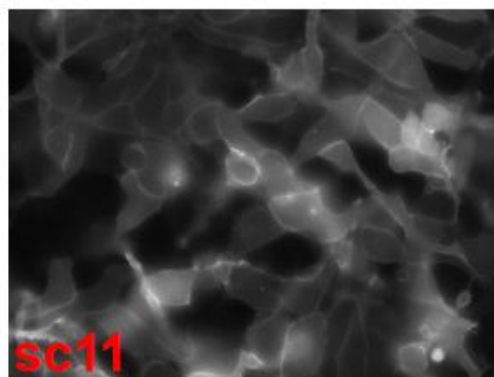
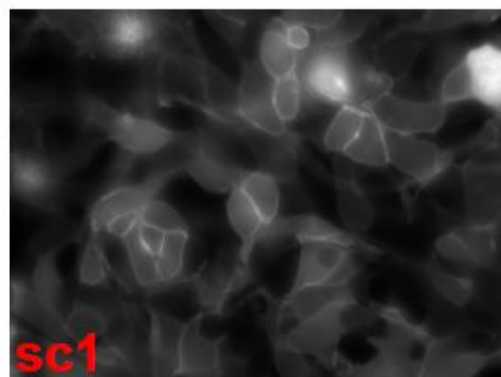
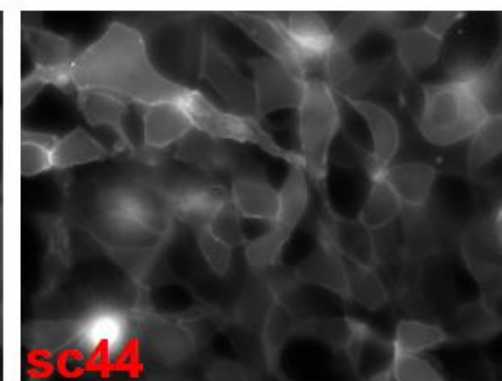
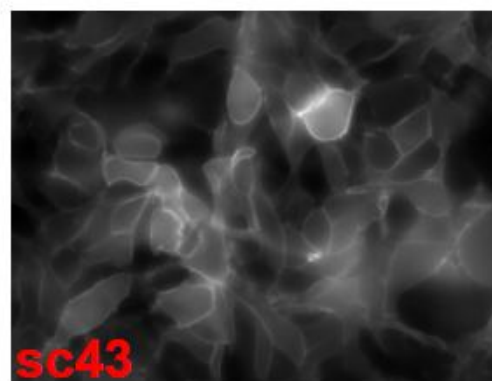
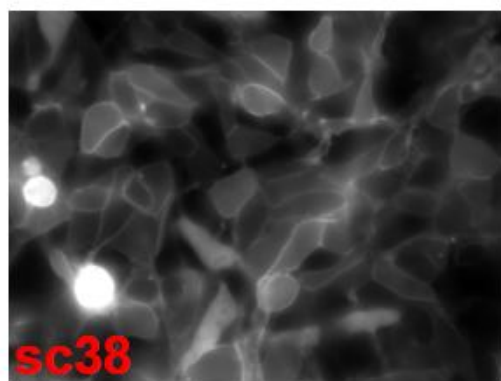
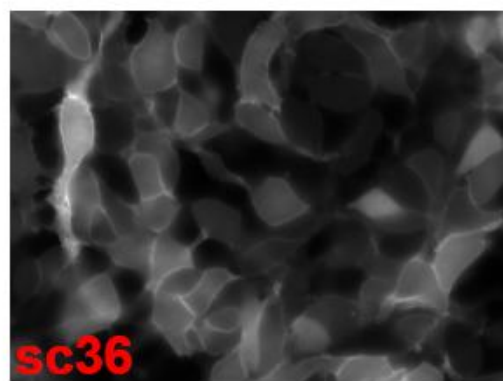
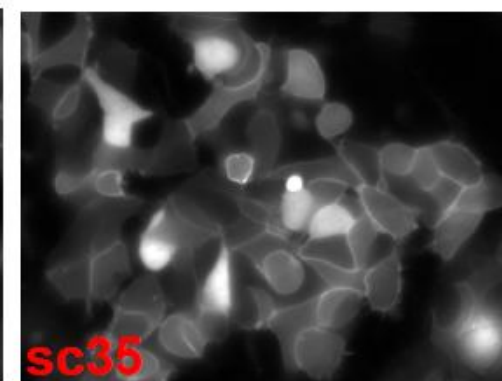
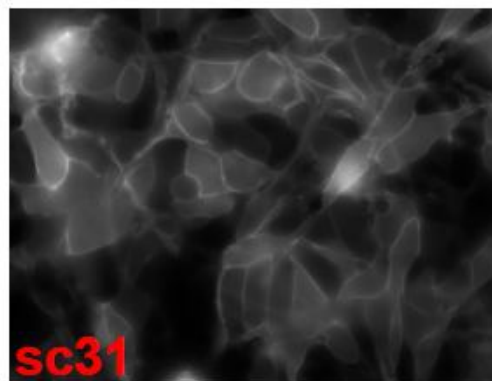
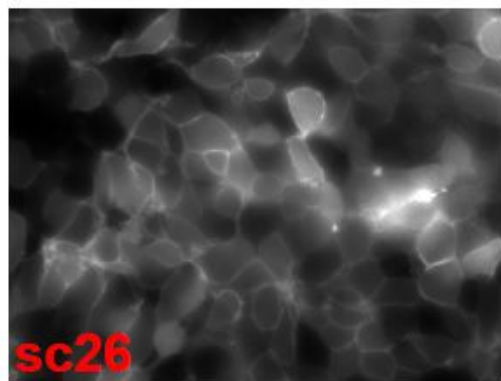
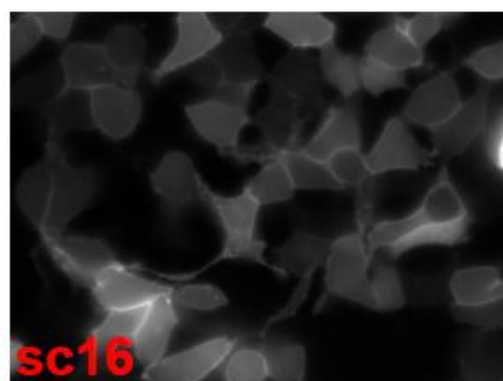
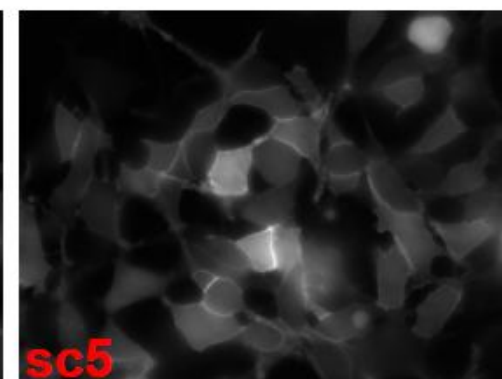
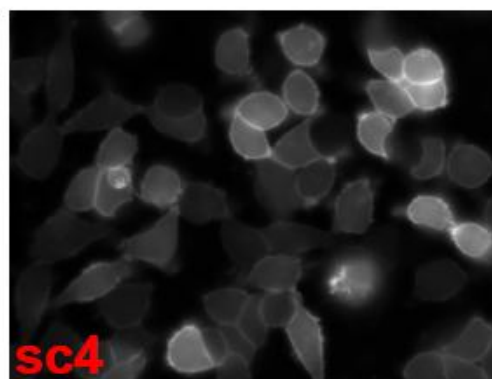
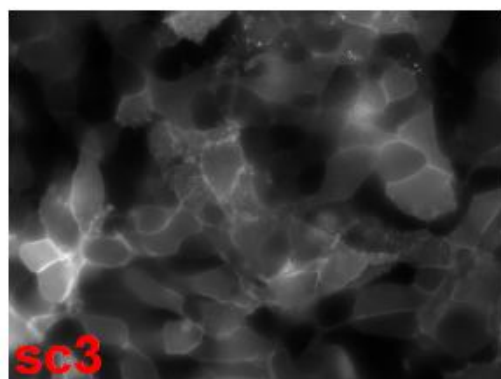
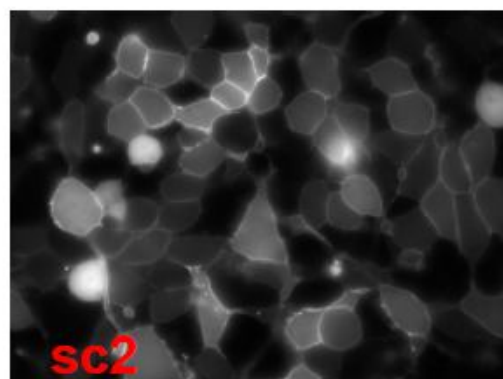
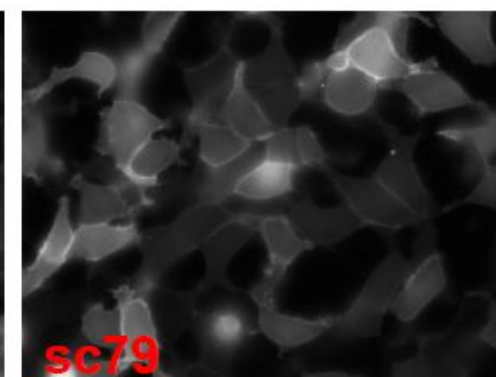
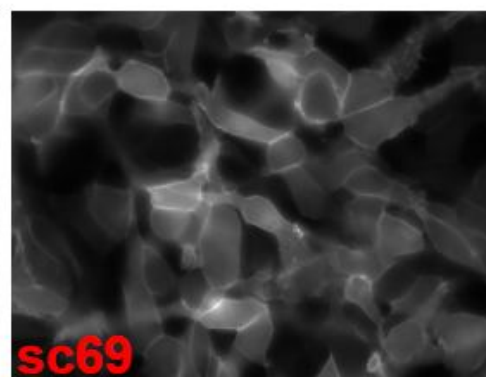
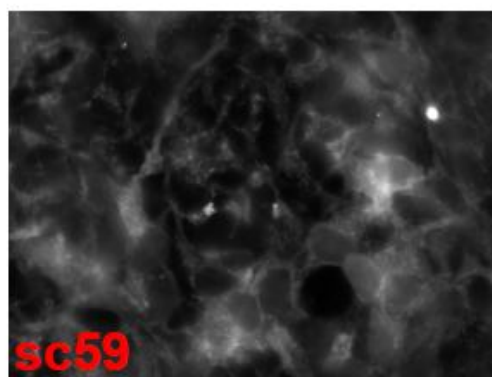
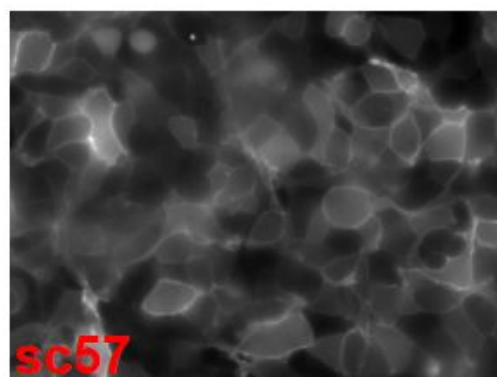
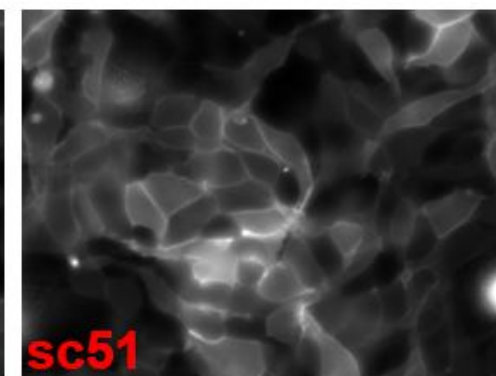
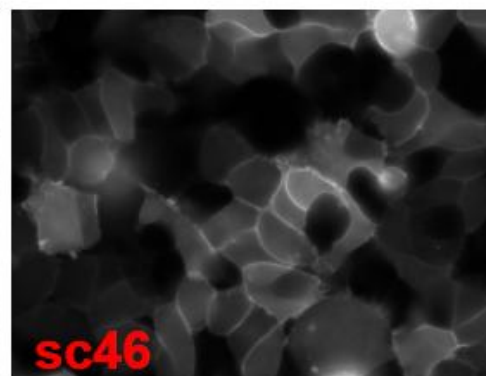
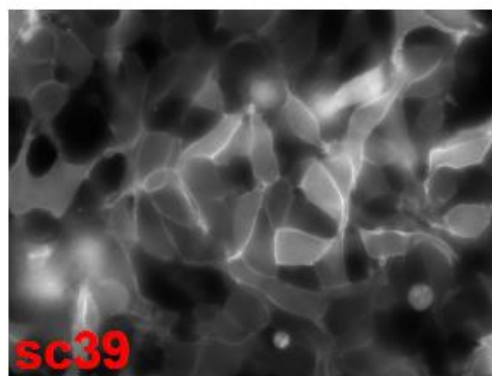
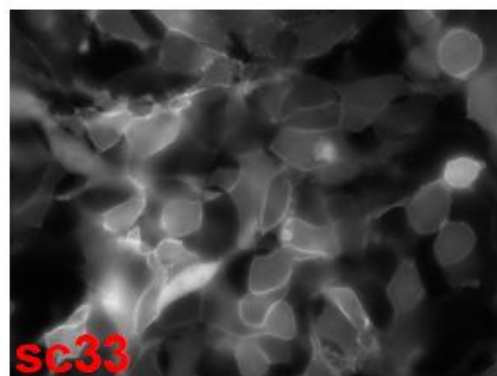
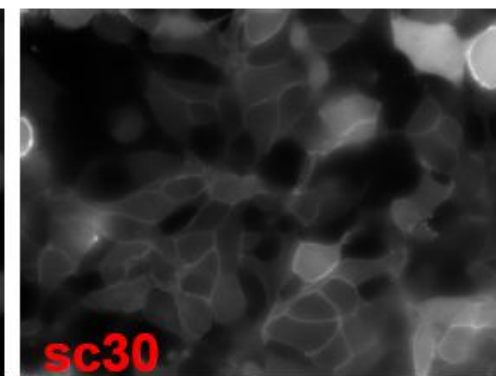
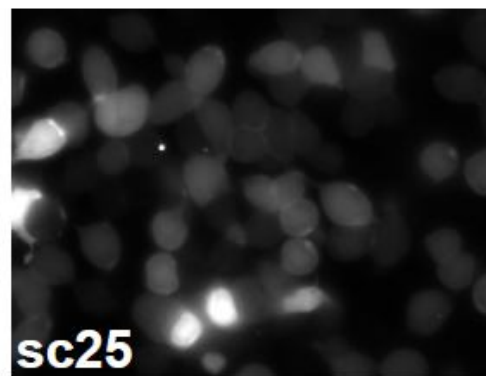
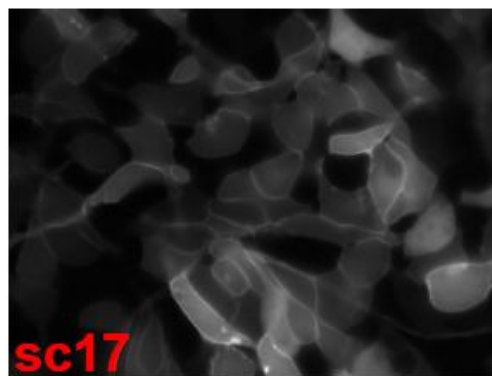
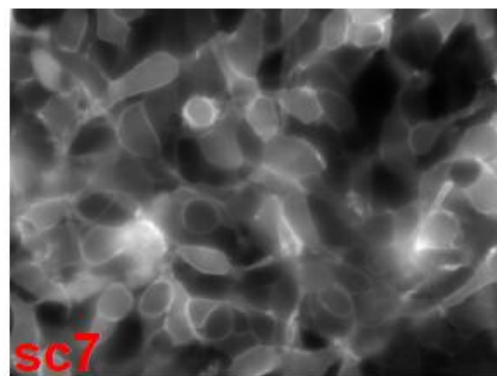
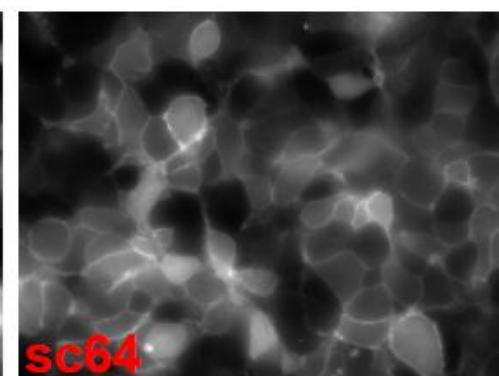
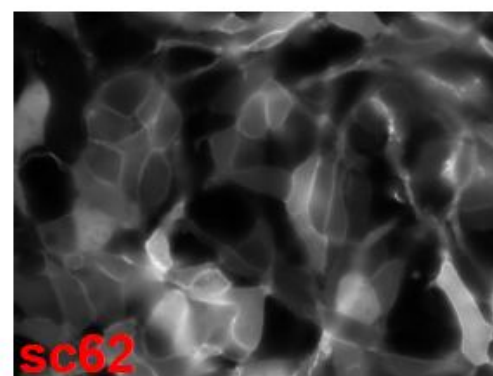
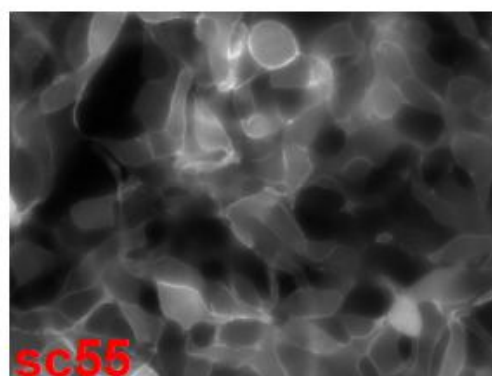
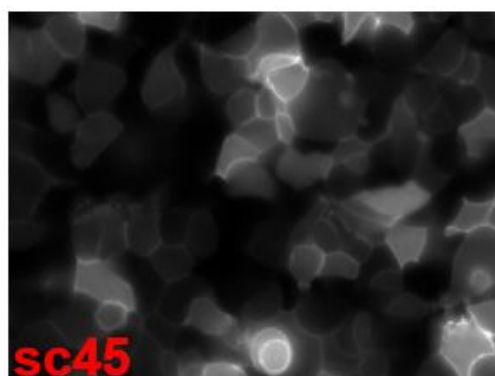
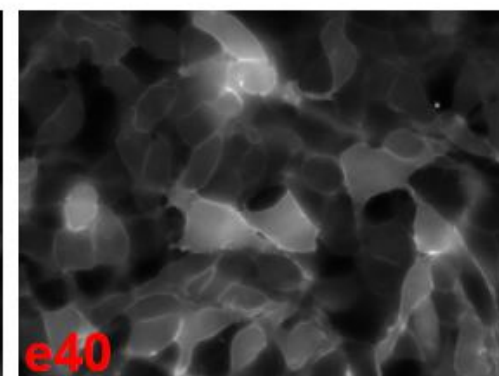
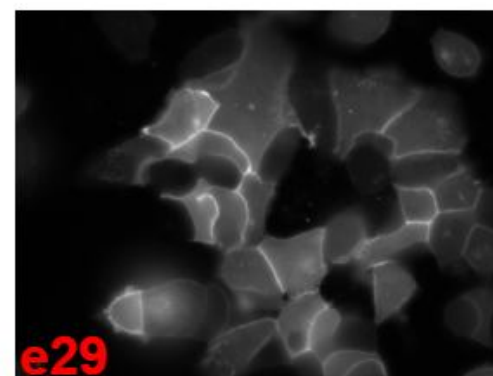
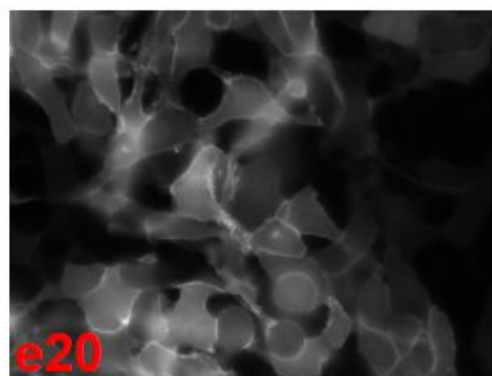
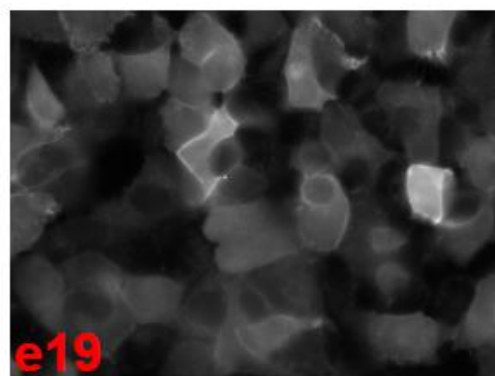
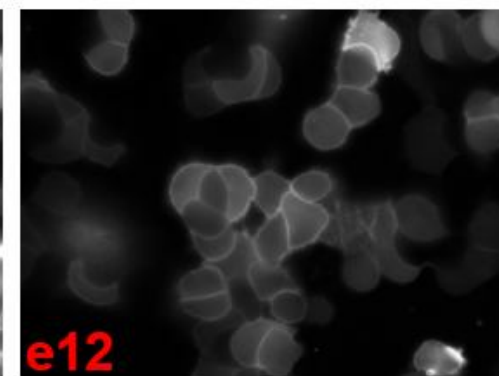
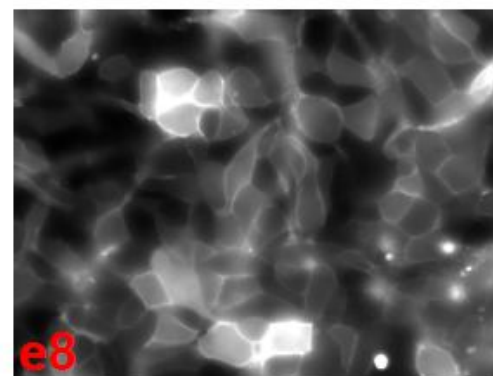
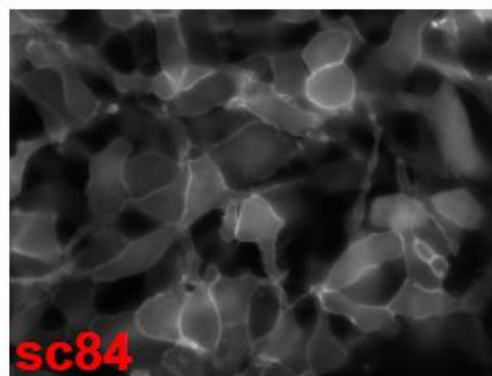
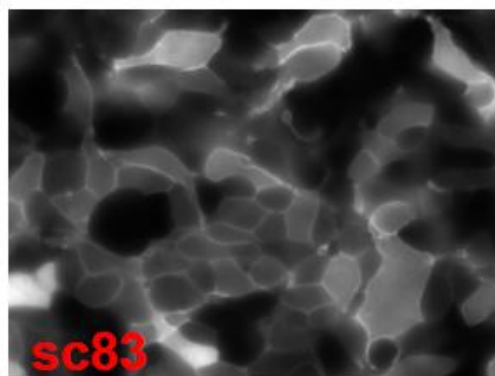


Figure S7. Chemical structure of confirmed positive hit compounds.









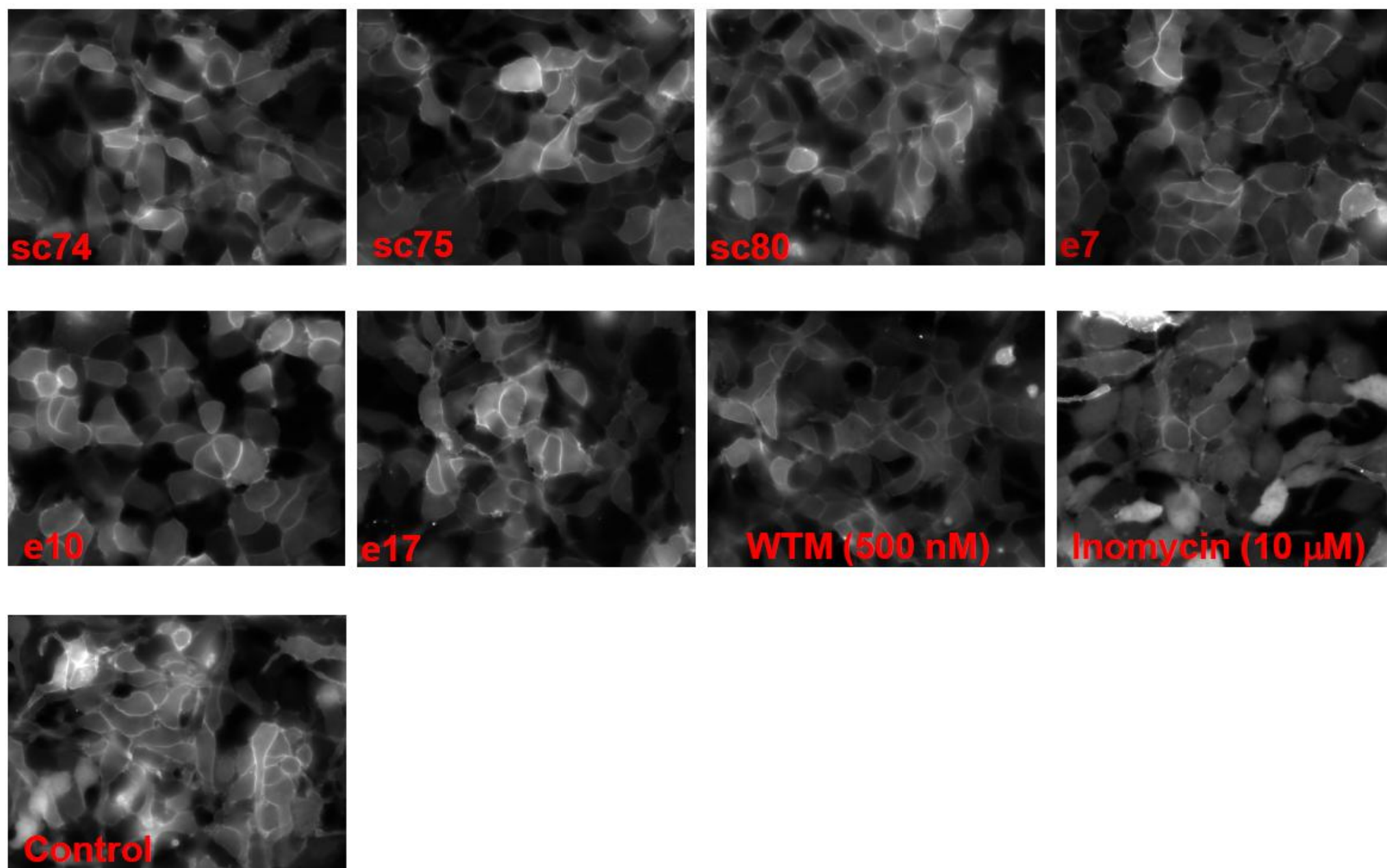
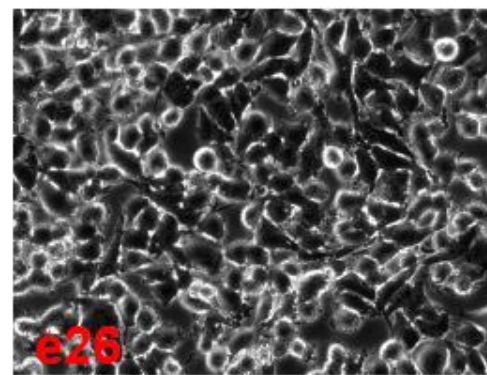
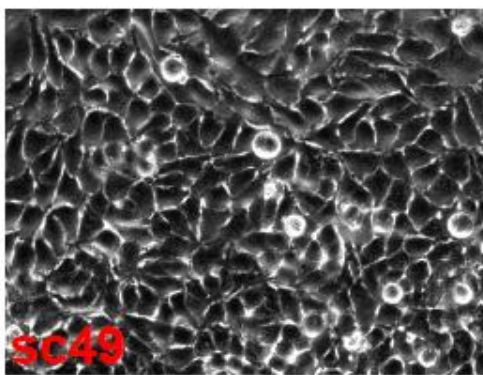
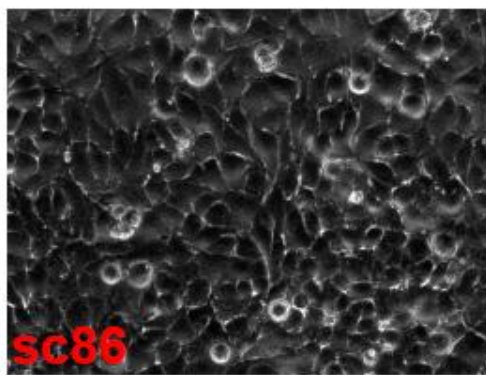
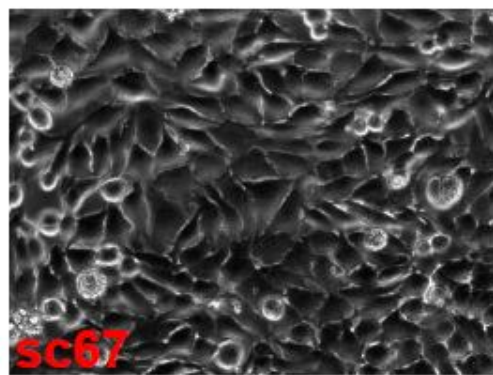
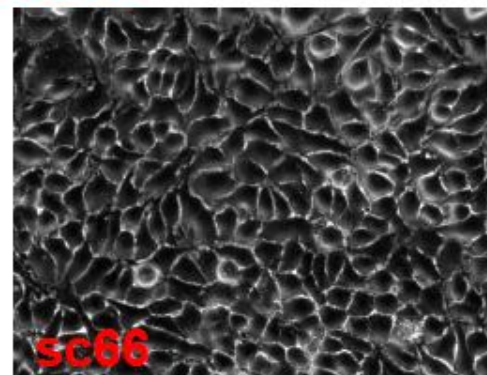
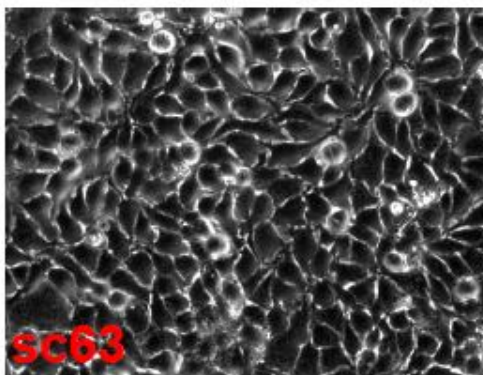
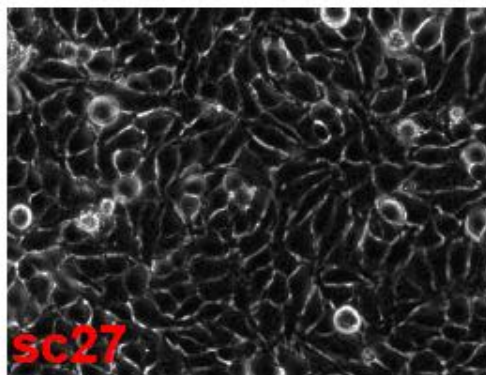
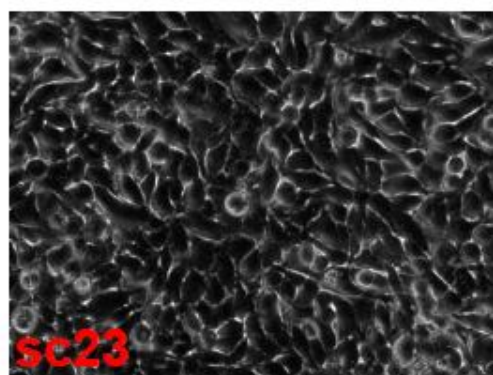
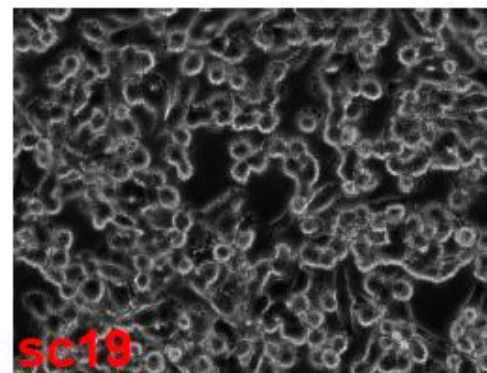
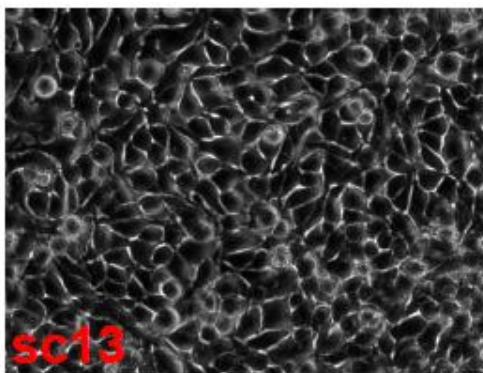
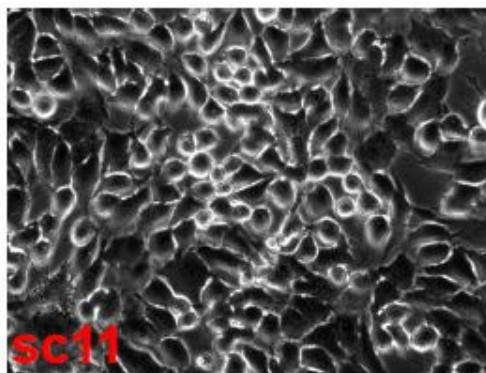
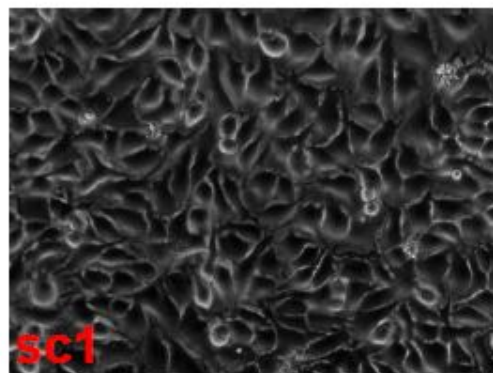


Figure S8. The effect of positive compounds on PtdIns(4,5)P₂-mediated membrane localization of EGFP-PLC-delta1-PH. HEK293 cells stably expressing EGFP-PLC-delta-PH were treated with each compound (8 μ g/ml) for 30 minutes before imaging.

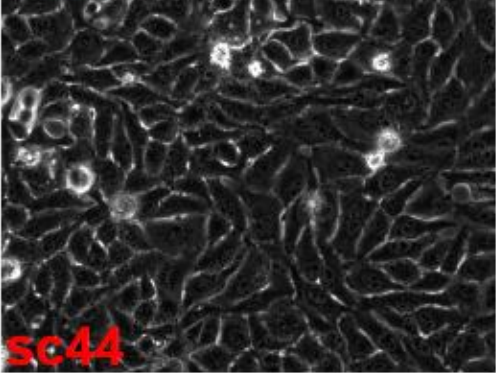
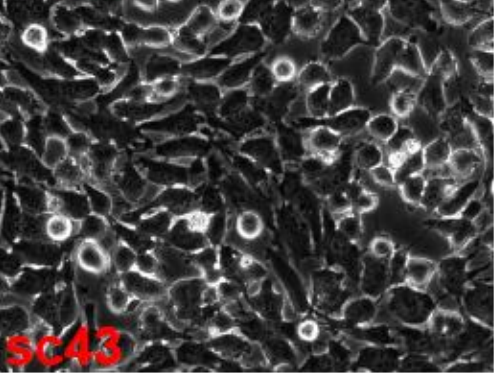
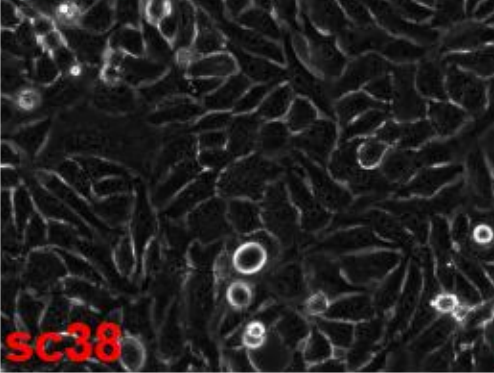
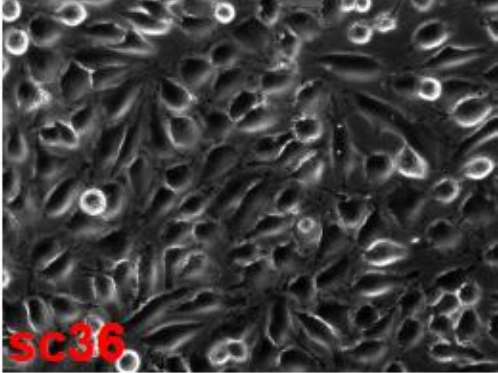
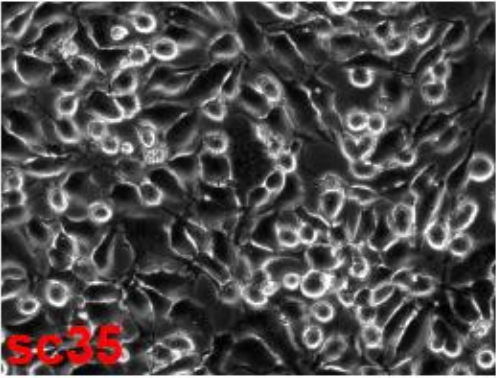
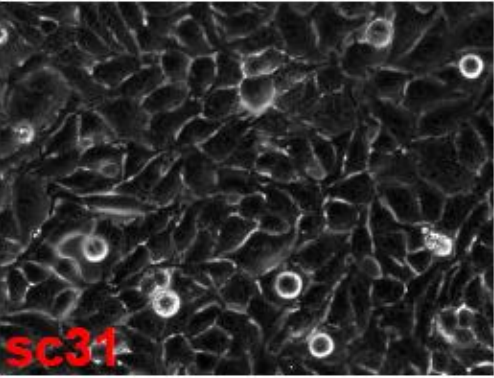
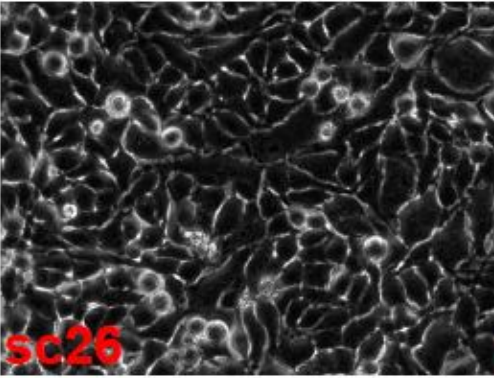
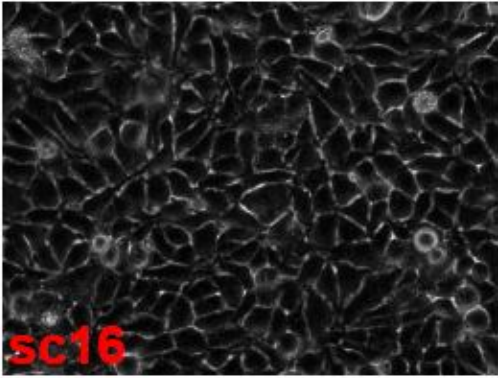
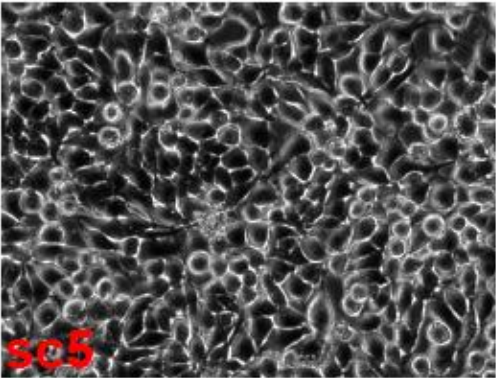
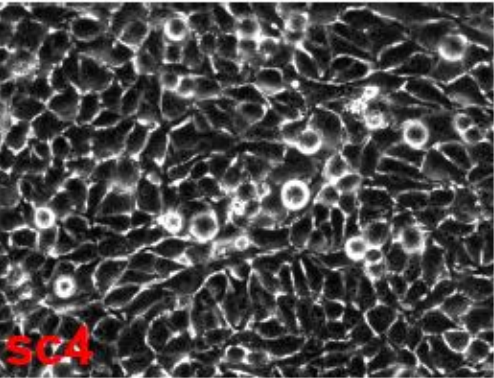
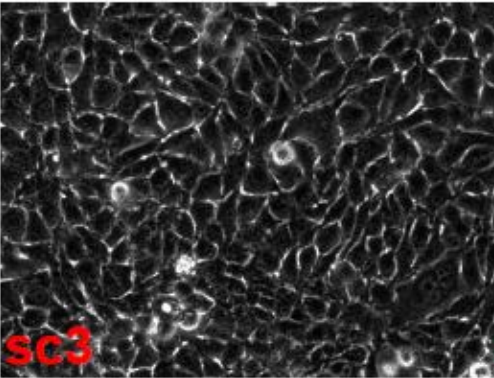
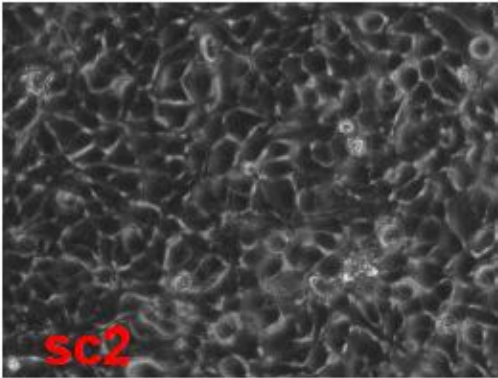
HeLa-30min

Figure S9-Page 1



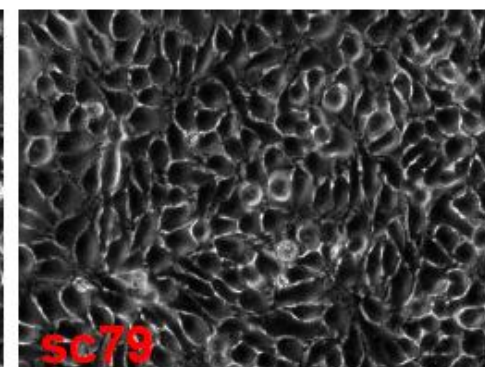
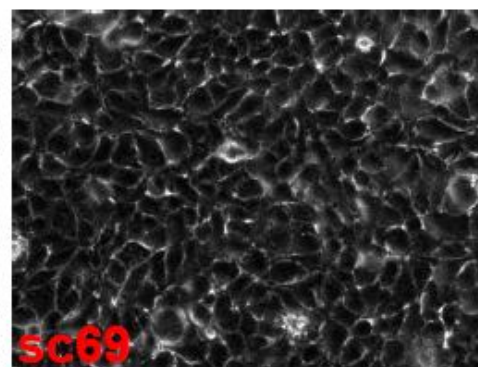
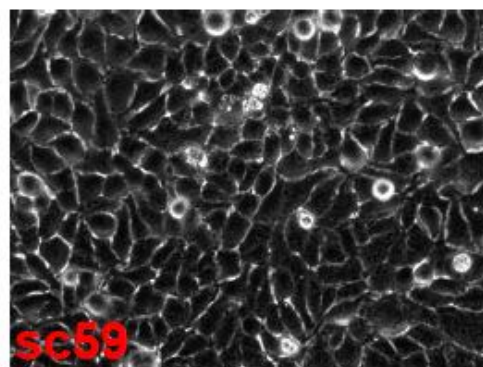
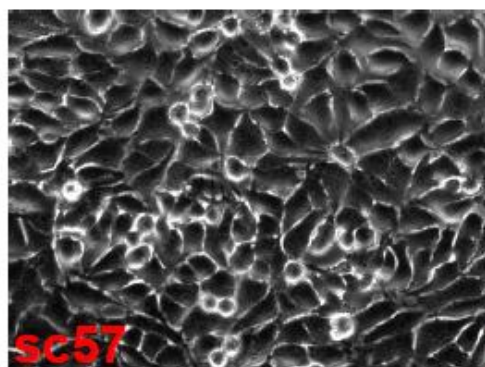
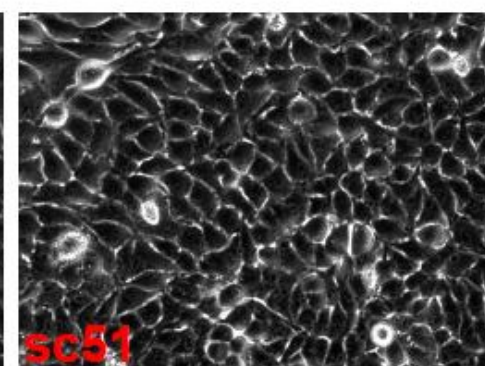
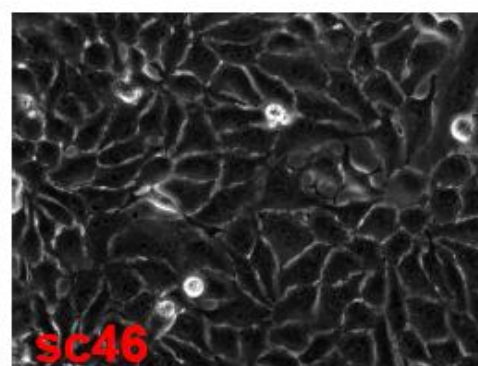
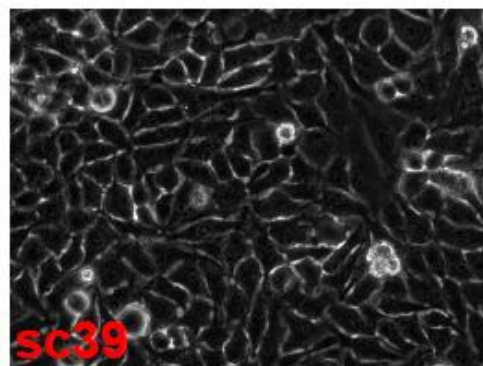
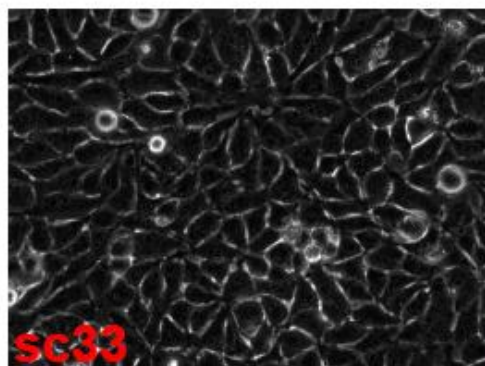
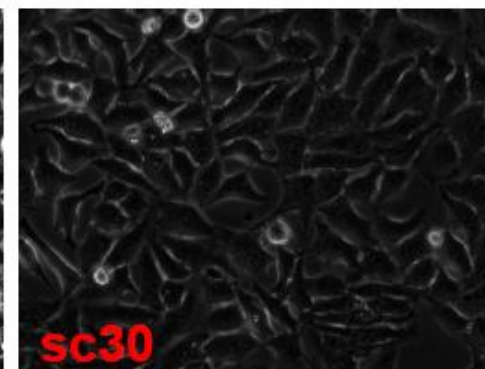
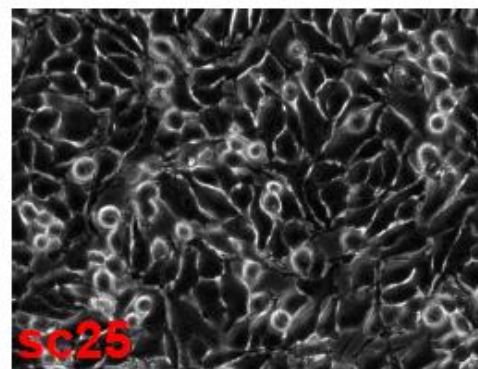
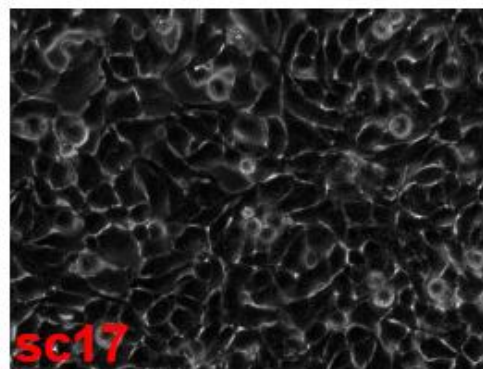
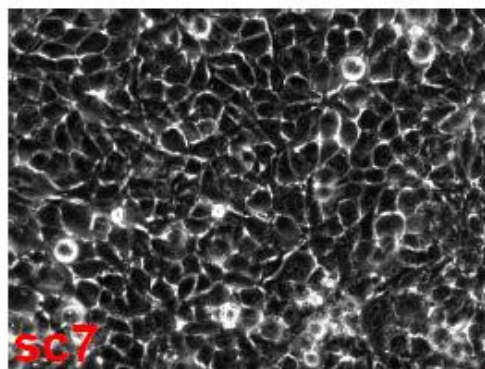
HeLa-30min

Figure S9-Page 2

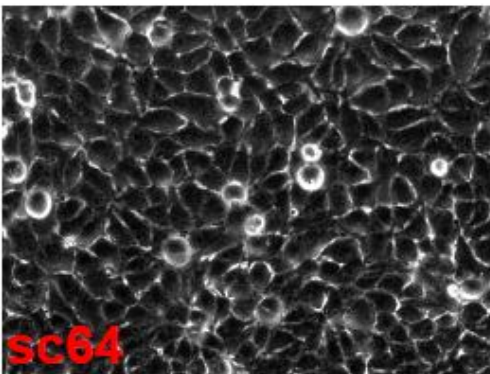
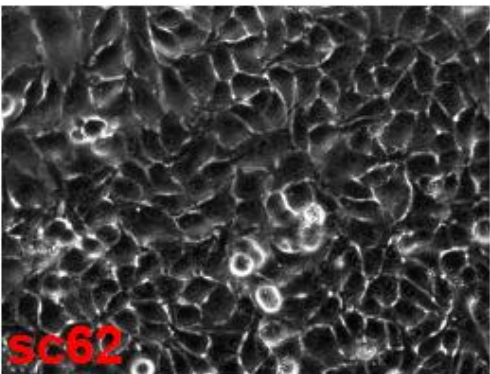
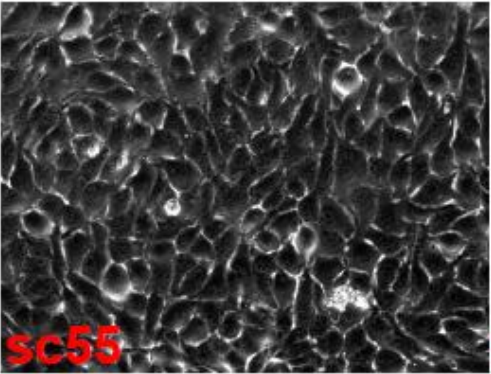
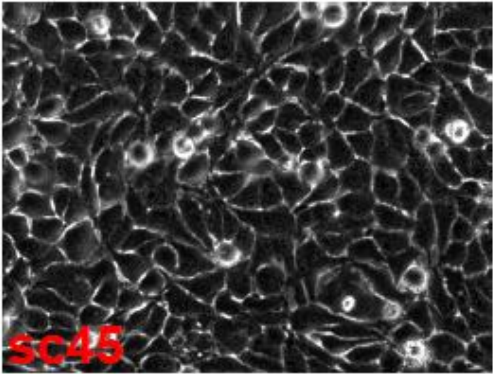
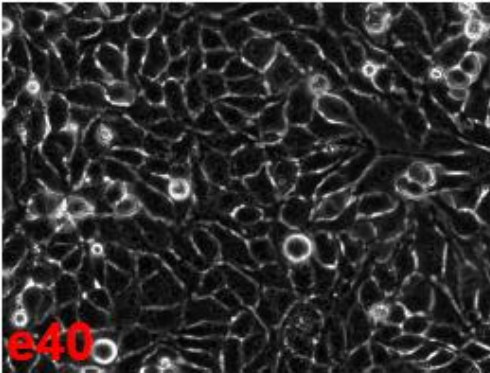
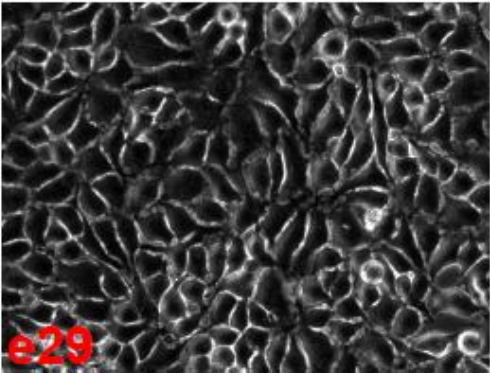
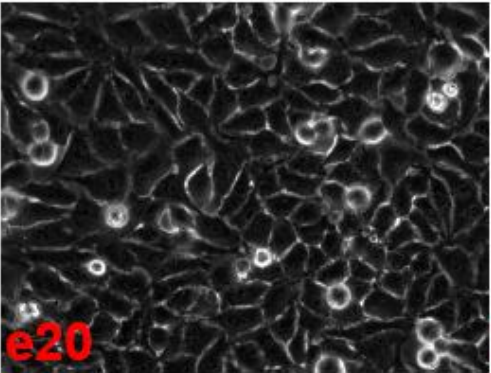
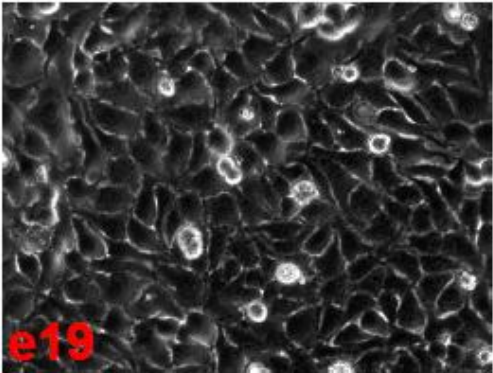
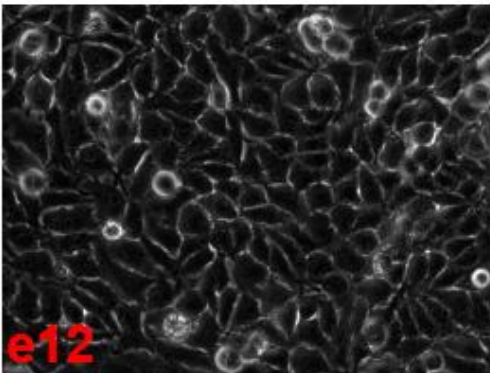
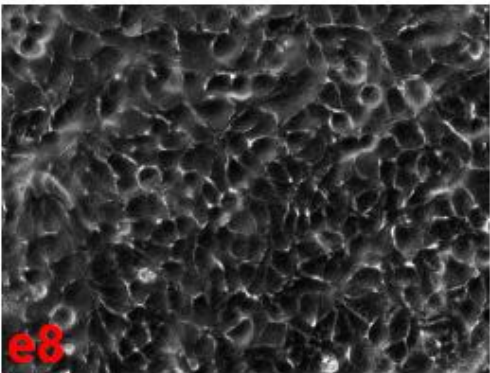
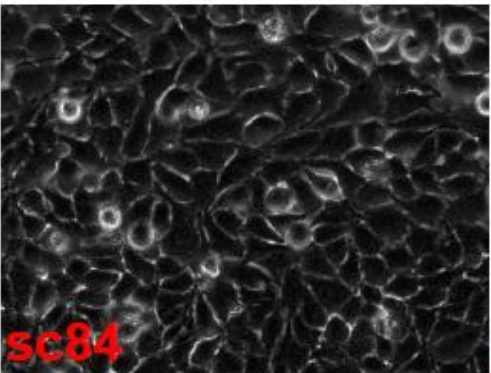
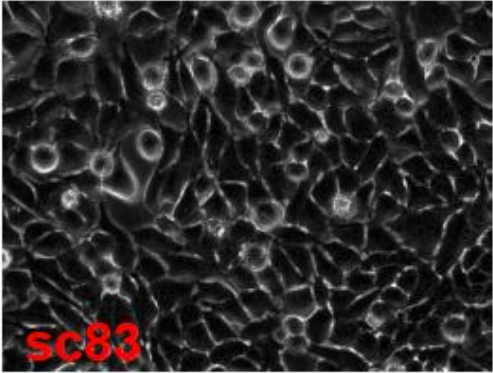


HeLa-30min

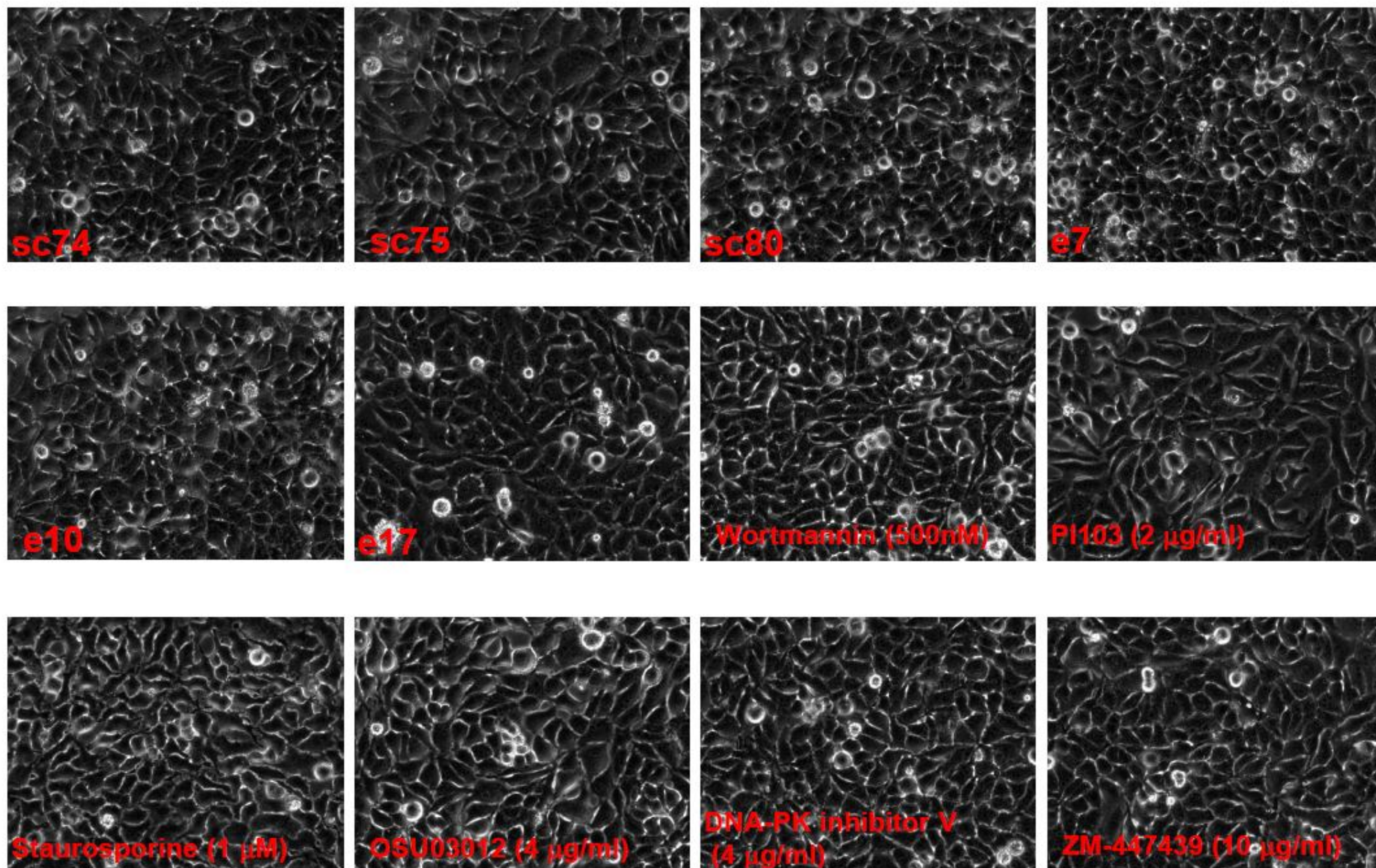
Figure S9-Page 3

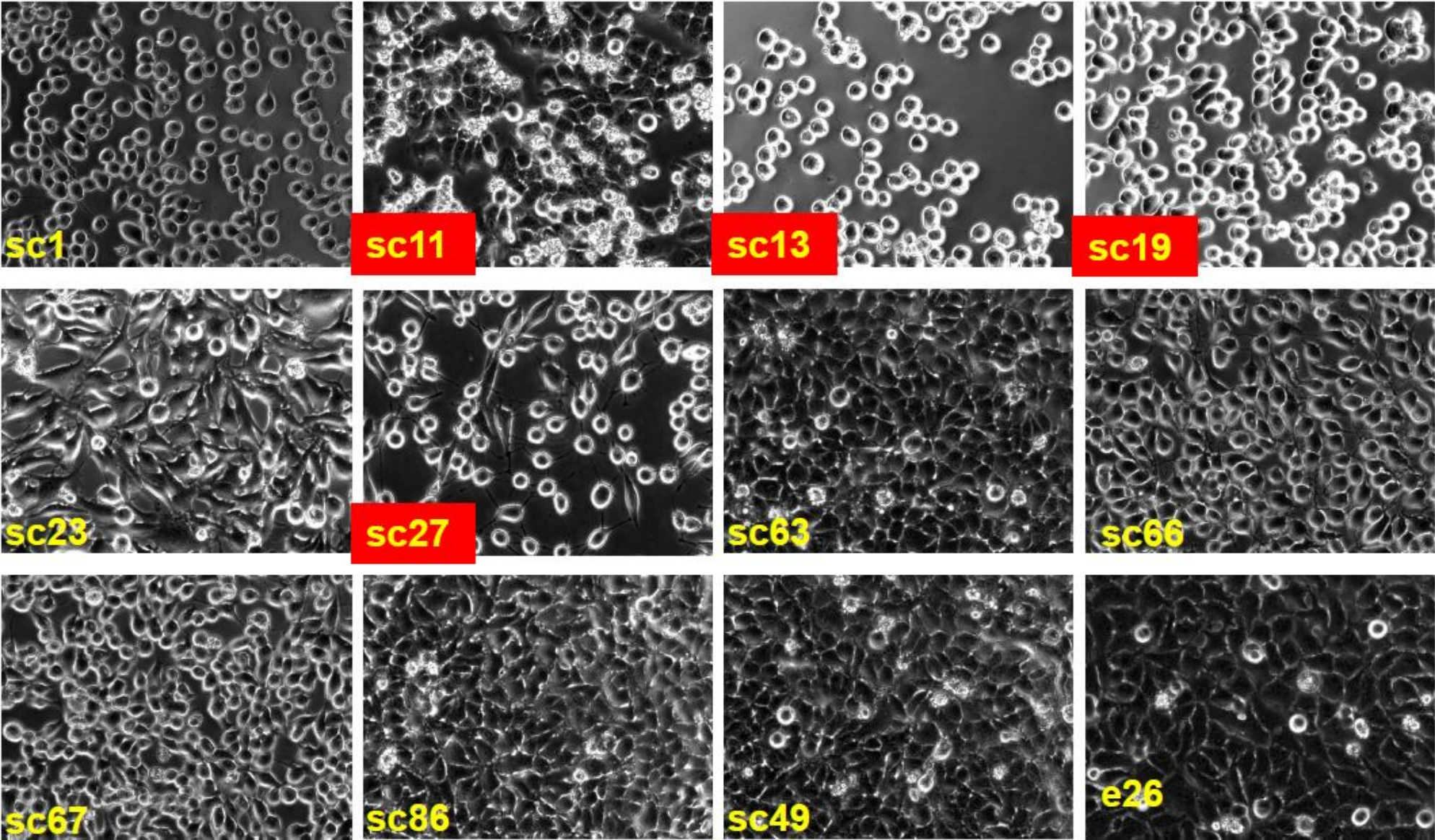


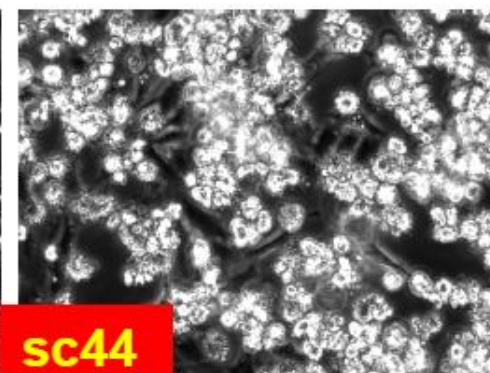
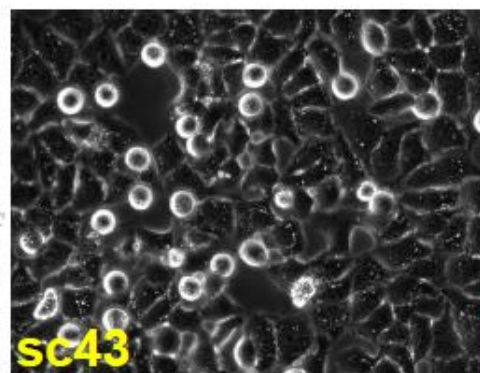
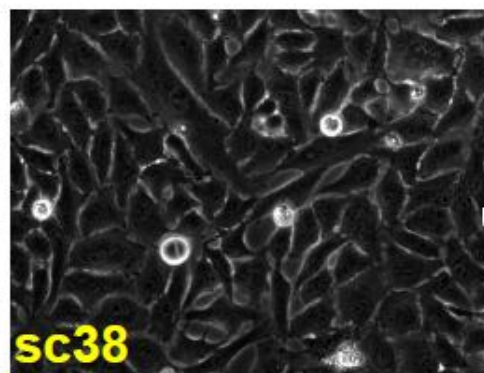
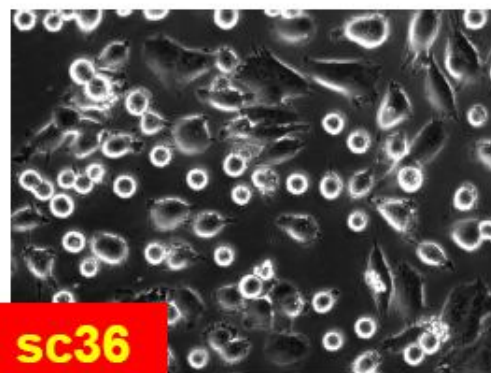
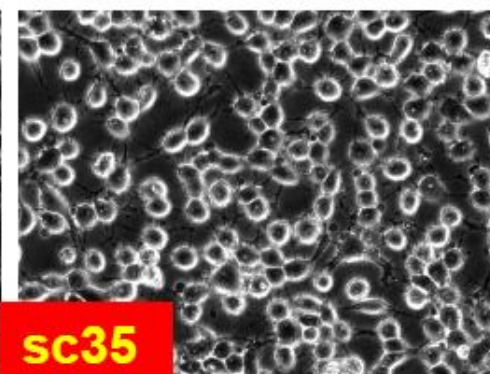
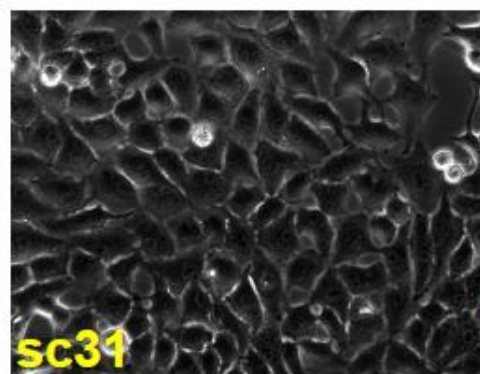
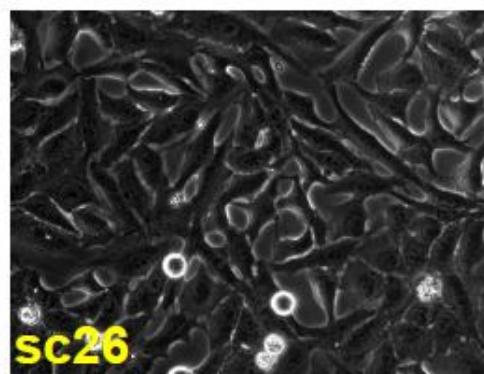
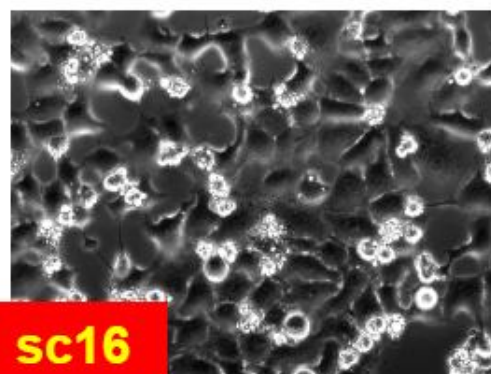
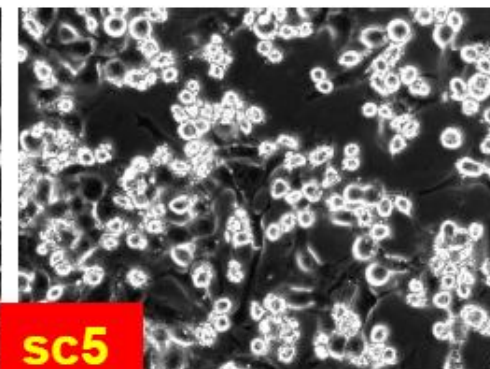
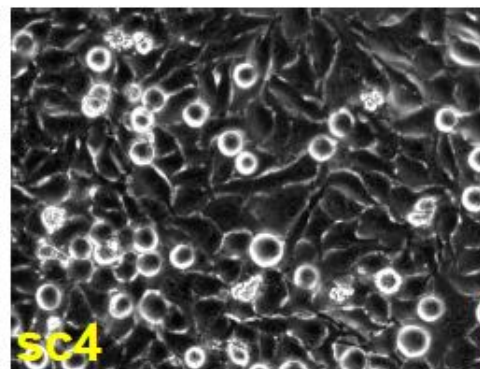
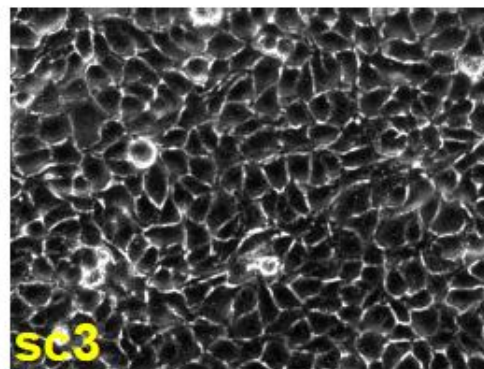
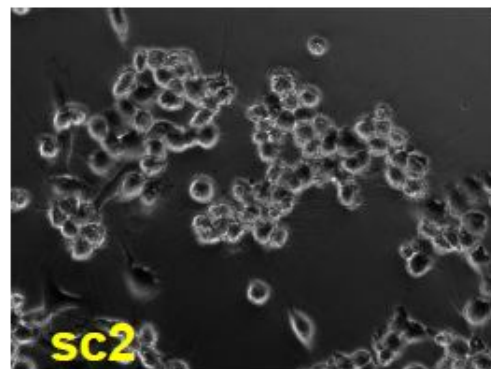
HeLa- 30min



HeLa- 30min

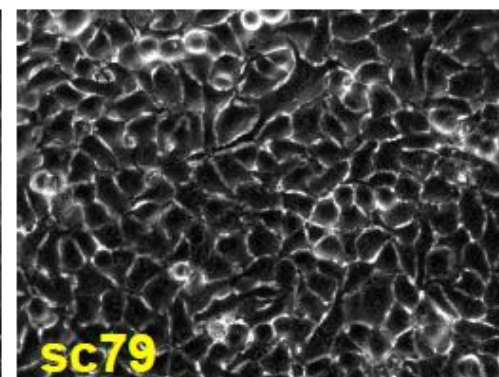
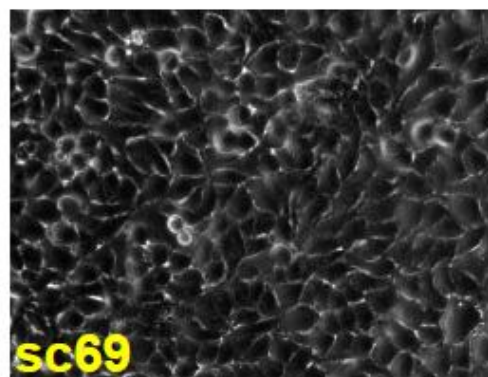
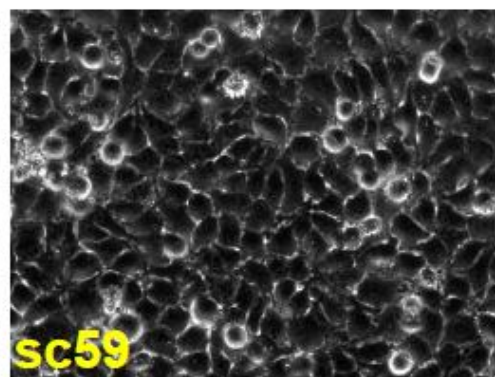
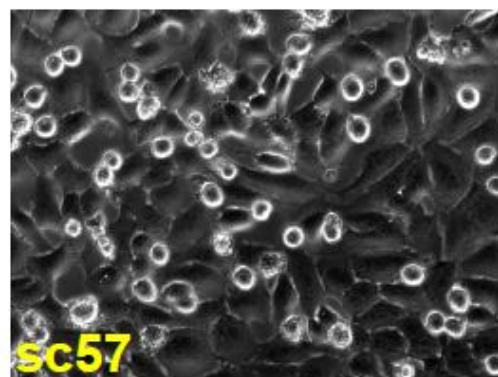
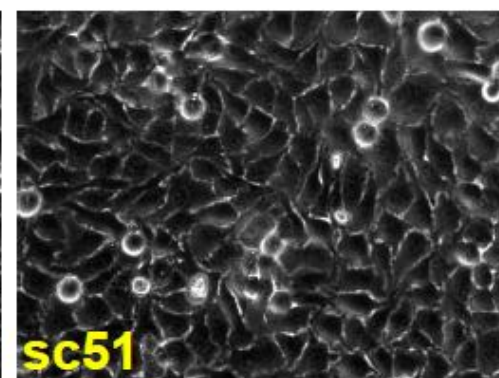
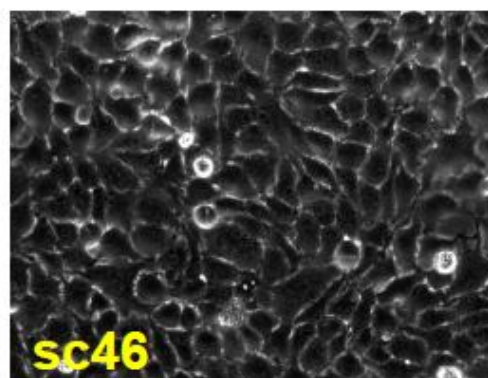
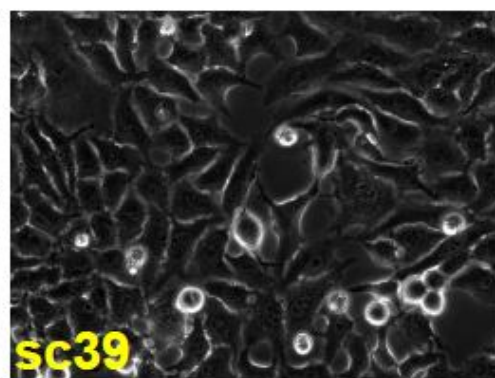
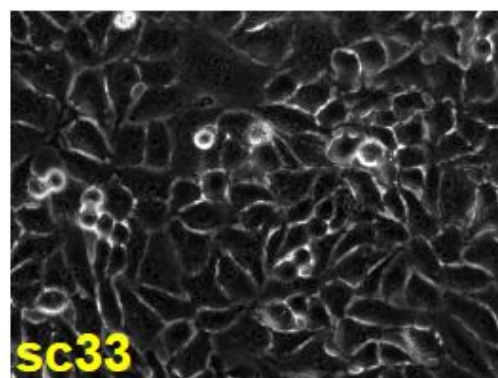
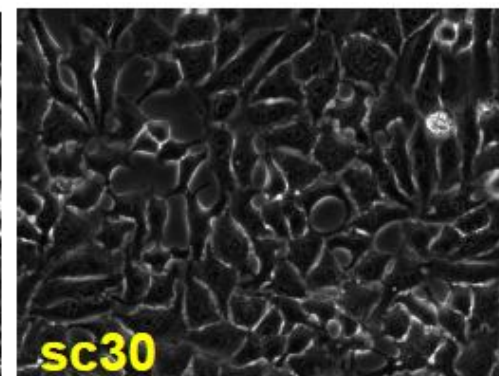
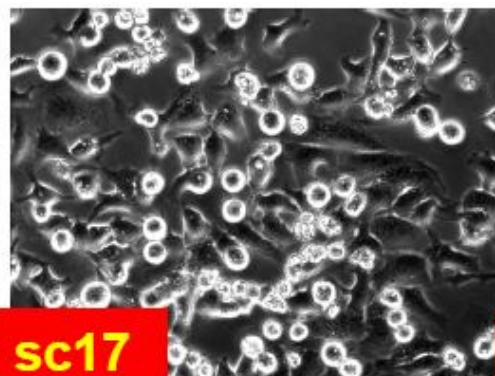
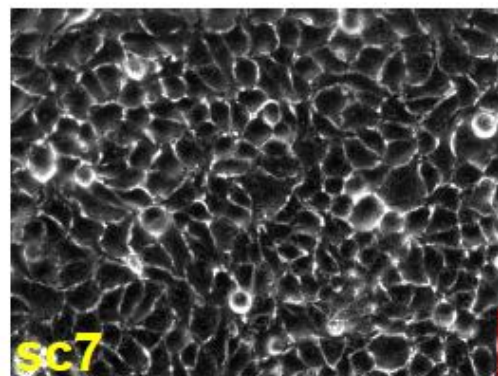






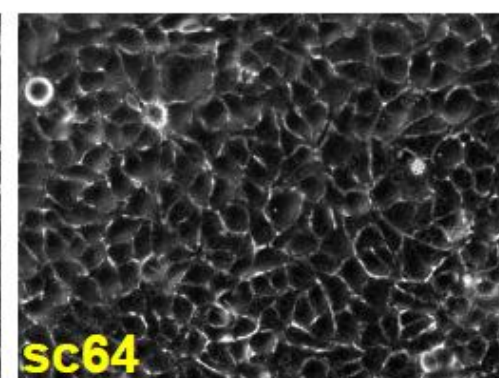
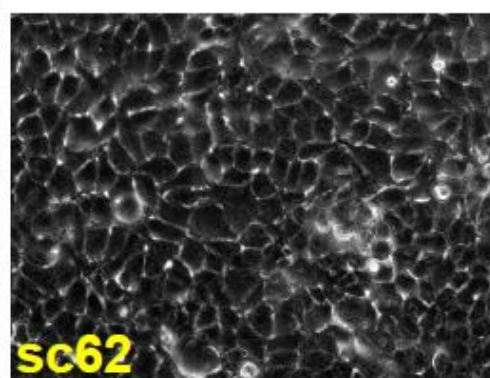
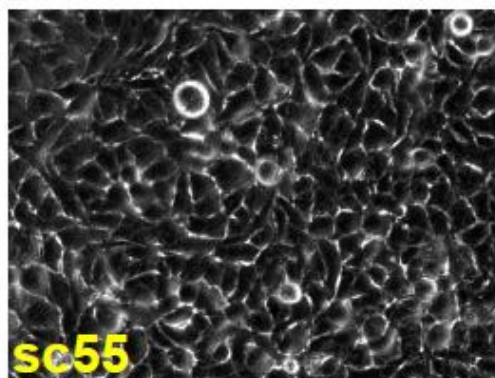
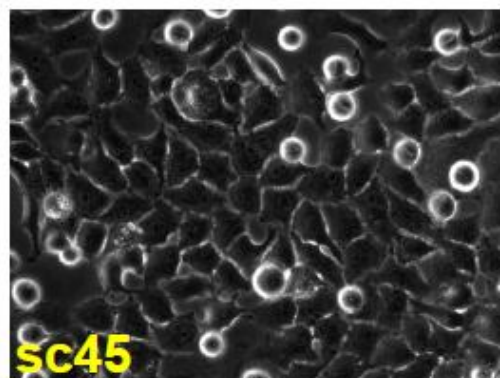
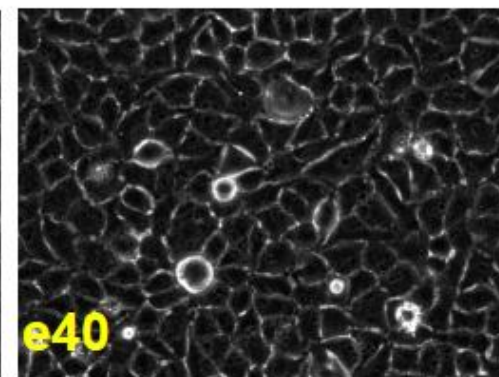
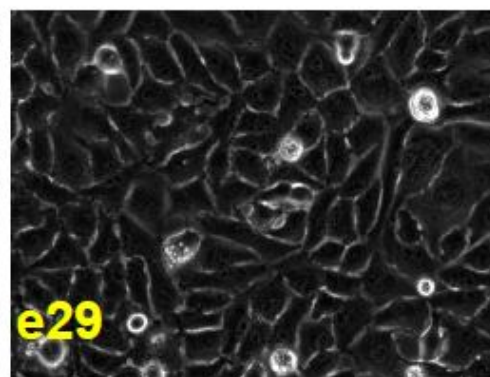
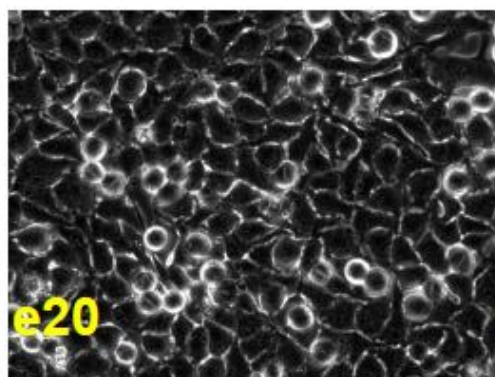
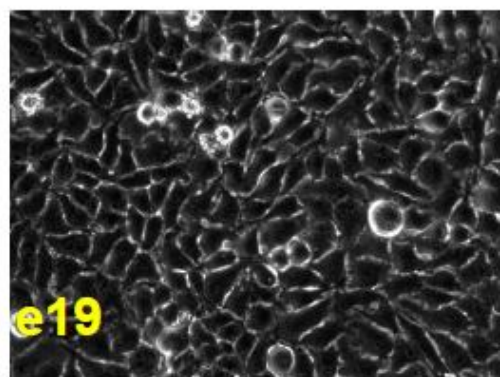
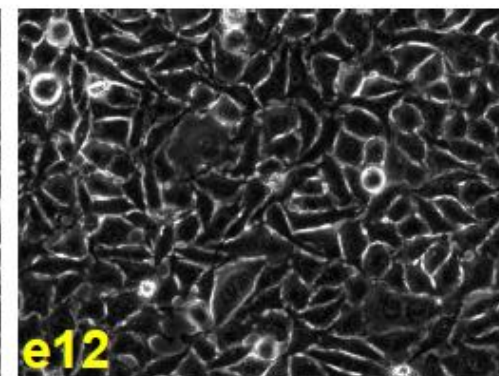
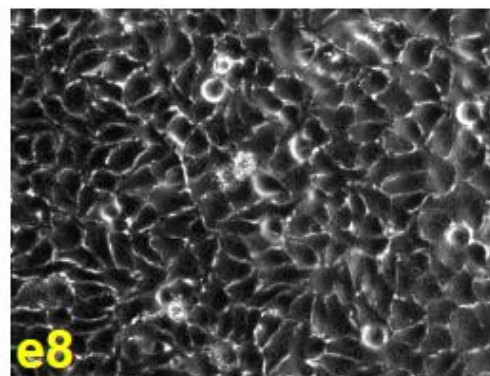
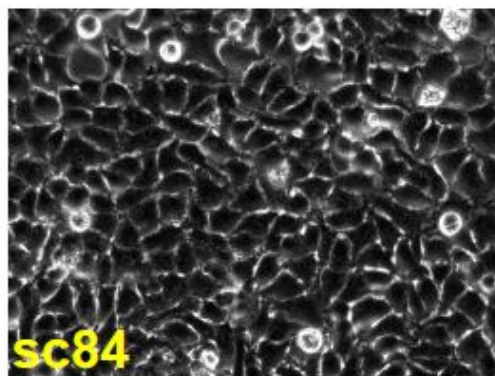
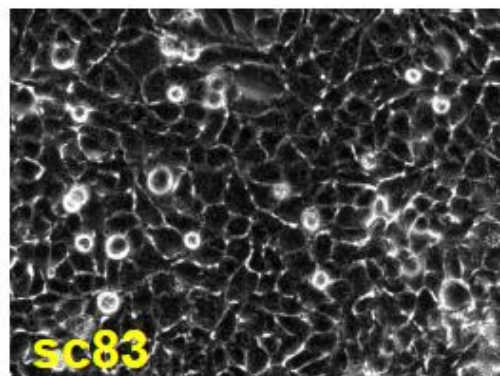
HeLa- 6 hr

Figure S9-Page 8



HeLa- 6 hr

Figure S9-Page 9



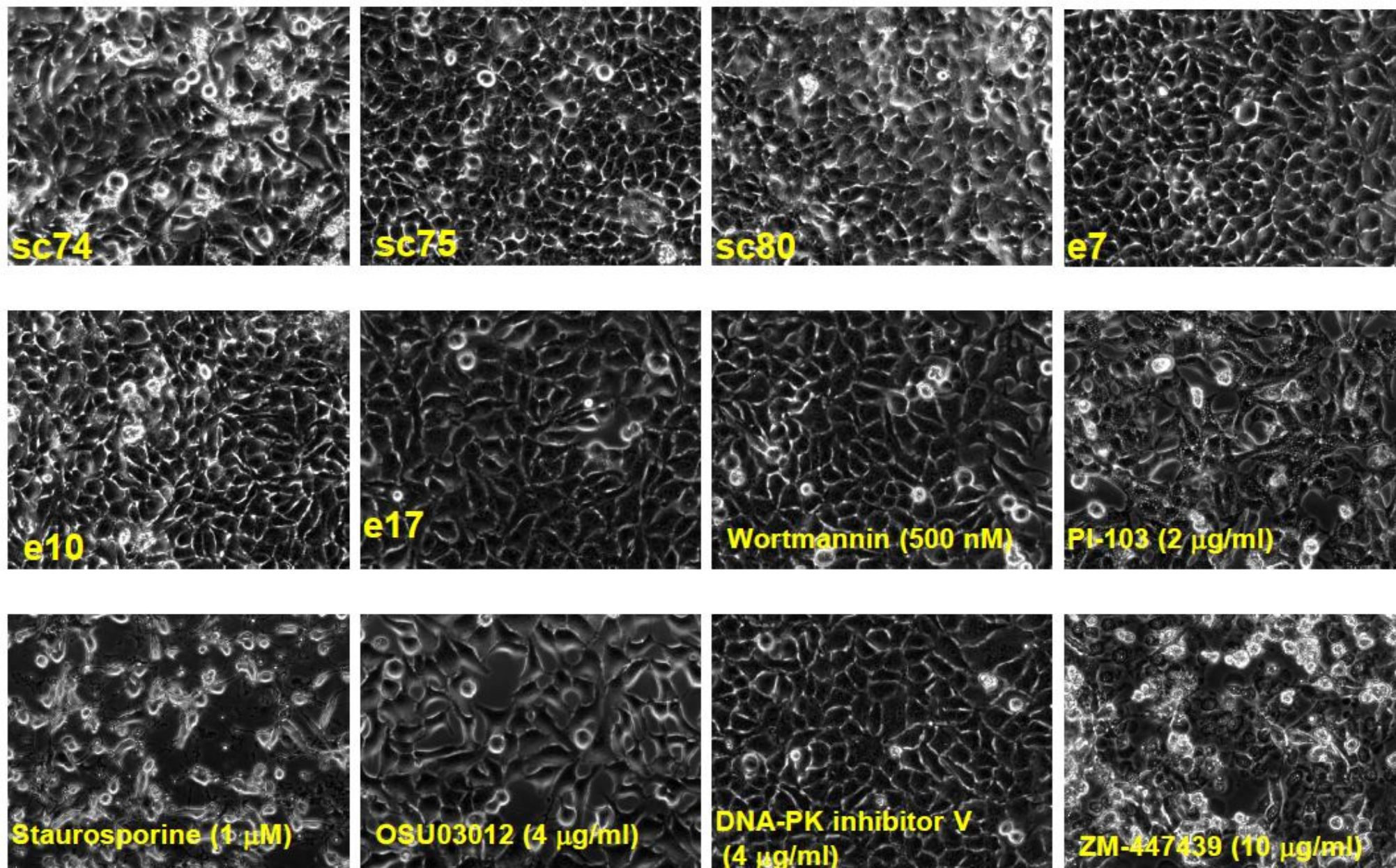


Figure S9. Morphological changes induced by identified positive hit compounds. HeLa cells were cultured in 24-well plate and treated with each compound (8 $\mu\text{g/ml}$) for indicated time. The bright field images were taken at each time points following chemical treatment. The compounds that induced significant morphological changes in 6 hrs are indicated in red. Cells were also treated with several known kinase inhibitors, including Wortmannin (PI3K inhibitor), PI-103 (PI3K and mTor kinase inhibitor), Staurosporine (broad-spectrum protein kinases inhibitor), OSU-0312 (Aurora kinase inhibitor), DNA-PK inhibitor V, and ZM447439 (PDK1 inhibitor) at the indicated concentrations.

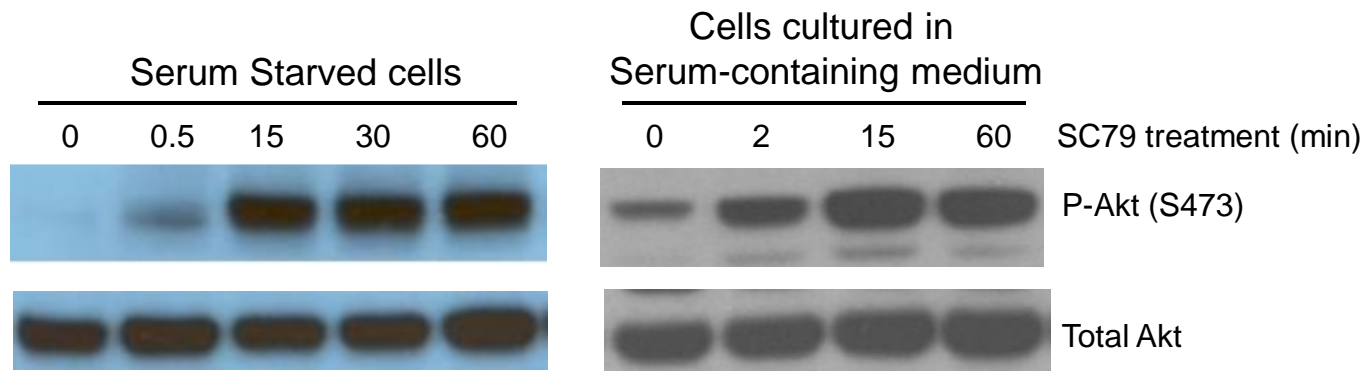


Figure S10. Kinetics of Akt phosphorylation by SC79. Serum-starved cells (overnight) or cells grown in serum-containing medium (1% FBS) were treated with SC79 (4mg/ml) for indicated time. Total and phosphorylated Akt were detected by Western blot using anti-Akt and anti-Phospho-Akt (Ser473) antibodies, respectively.

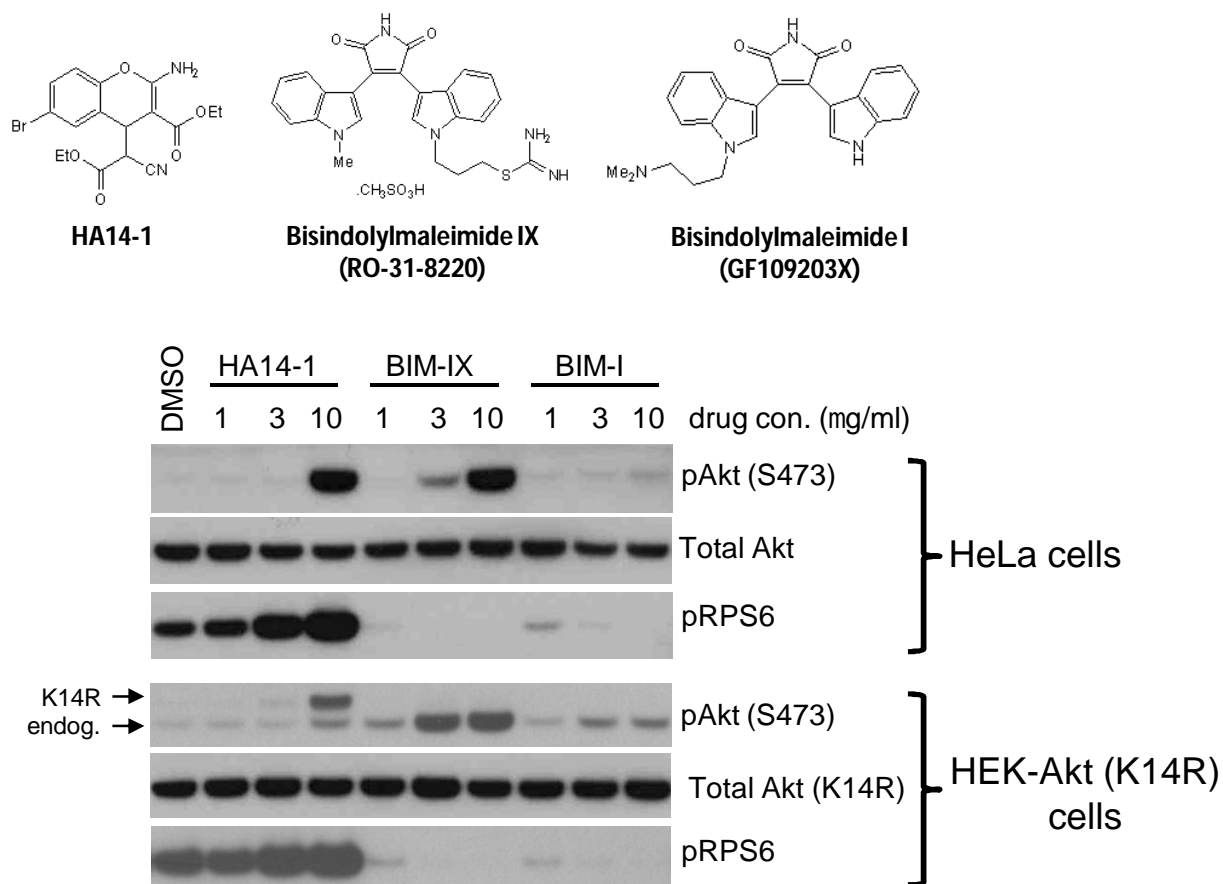


Figure S11. HA14-1, a structural analog of SC79, increases phosphorylation of both endogenous and mutant Akt (K14R) and enhances Akt signaling. In contrast, BIM-IX and BIM-I, two kinase inhibitors of PKC, enhance phosphorylation of endogenous Akt but inhibit its kinase activity. Both PKC and Akt belong to AGC family kinases with a similar kinase domain. HeLa or HEK-Akt (K14R) cells were treated with the indicated amounts of chemicals for 30 minutes. The levels of phosphorylation of Akt and RPS6 (ribosomal protein S6), a target of AGC family kinase, were analyzed by Western blot.

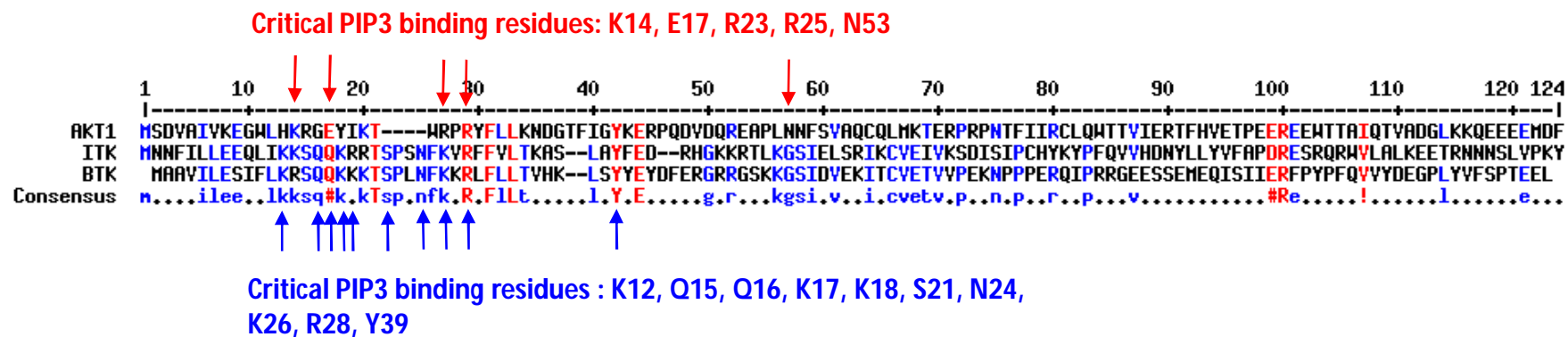


Figure S12. Alignment of PH domains of Akt and Tec family tyrosine kinase (Itk and Btk). The critical residues for PtdIns(3,4,5)P3 binding were indicated by arrows.

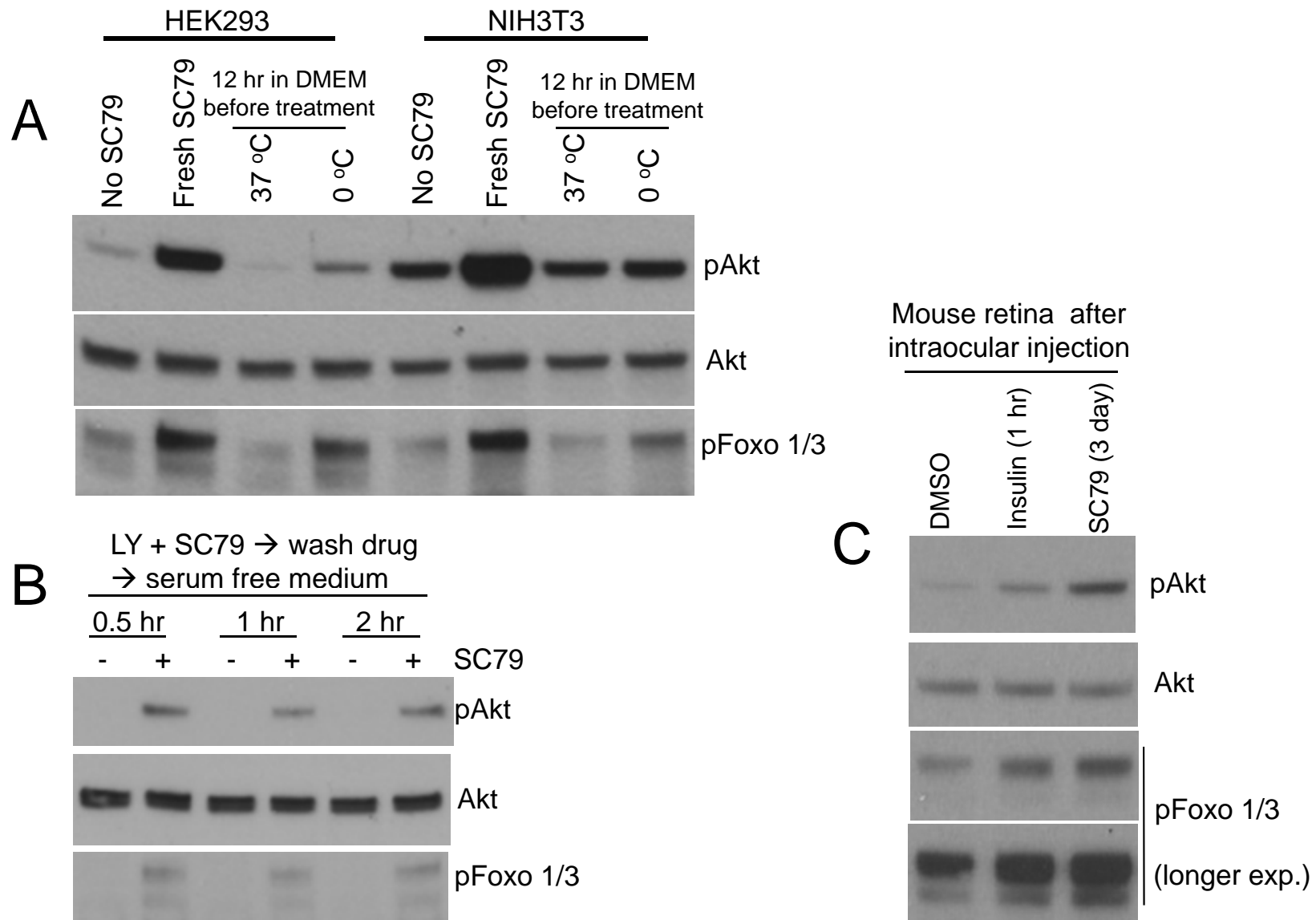


Figure S13. A sustained Akt activity after removal of SC79. (A) Serum-deprived HEK293 or NIH3T3 cells were treated with fresh SC79 (4 mg/ml) or SC79 pre-incubated in aqueous medium for 12 hr at 37°C or on ice. The levels of pAkt and pFoxo were analyzed after 30 min-drug treatment. (B) HeLa cells were treated with LY294002 (40 μ M) and SC79 (4 μ g/ml) for 30 min. After removal of drug, cells were left in serum free medium and the levels of pAkt and pFoxo were analyzed in time course. (C) SC79 (100ng) was intravitreally injected into mouse eyes and the level of pAkt and pFoxo was analyzed in the retina on day 3. The retina from 1 hour after insulin (100 ng) injection serves as a positive control for Akt activation.

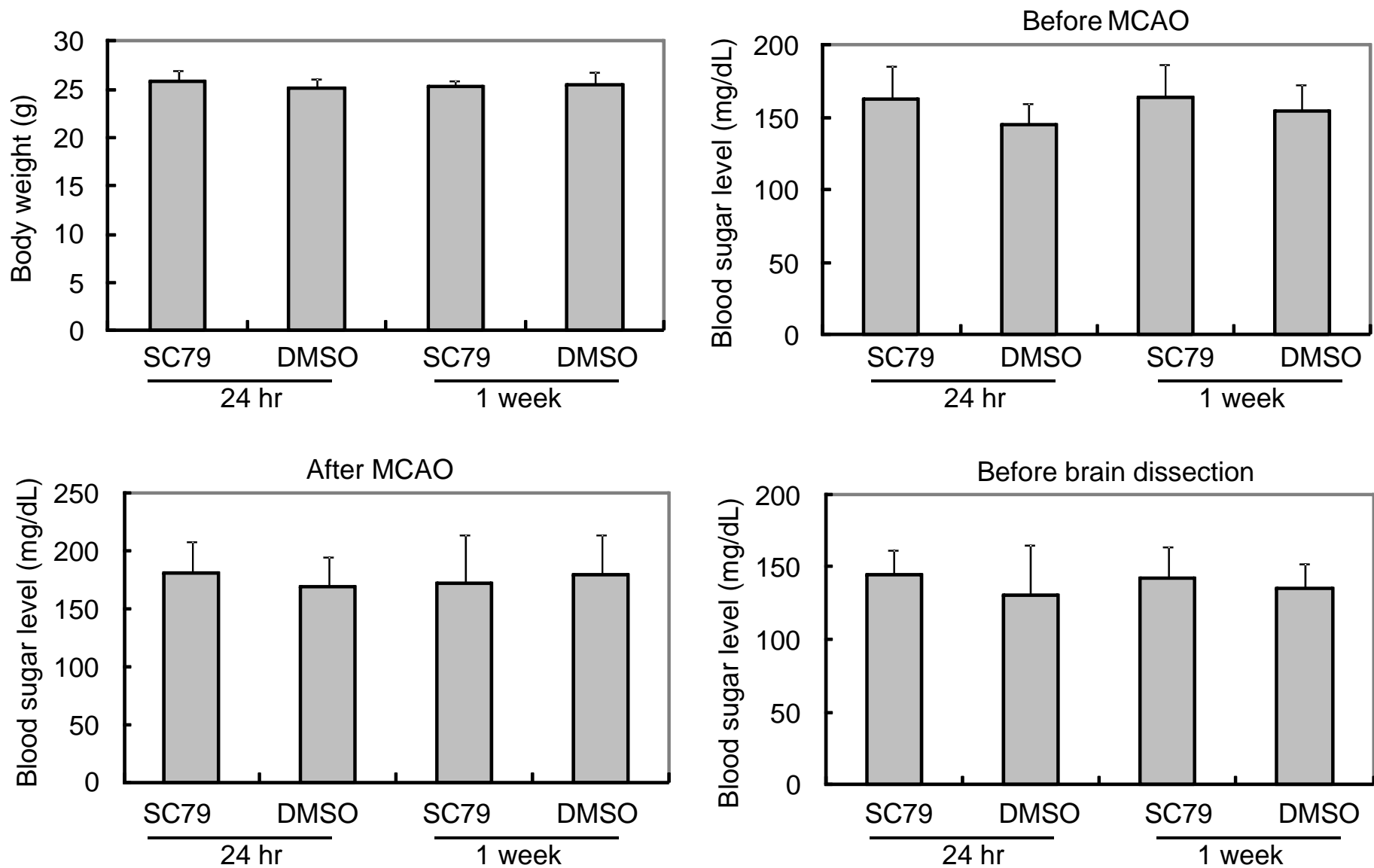


Figure S14. SC79 treatment does not alter the body weight and blood sugar level in experimental animals. SC79 was applied intravenously via tail vein injection at a concentration of 0.4 mg/g body weight. The body weight and blood sugar levels were measured at each indicated time points.